

0

Report No. BMI-1154
Physics
(TID-4500, 12th Ed.)

Contract No. W-7405-eng-92

STUDIES RELATING TO THE REACTION BETWEEN
ZIRCONIUM AND WATER AT HIGH TEMPERATURES

by

Alexis W. Lemmon, Jr.

January 3, 1957

BATTELLE MEMORIAL INSTITUTE
505 King Avenue
Columbus 1, Ohio

This document is
PUBLICLY RELEASABLE
Larry E. Williams

Authorizing Official
Date: 05/10/2006

DISCLAIMER

This report was prepared as an account of works sponsored by an agency of the United States Government. Neither the United States Government nor any agency thereof, nor any of their employees, makes any warranty, express or implied, or assumes any legal liability or responsibility for the accuracy, completeness, or usefulness of any information, apparatus, product, or process disclosed, or represents that its use would not infringe privately owned rights. Reference herein to any specific commercial product, process, or service by trade name, trademark, manufacturer, or otherwise does not necessarily constitute or imply its endorsement, recommendation, or favoring by the United States Government or any agency thereof. The views and opinions of authors expressed herein do not necessarily state or reflect those of the United States Government or any agency thereof.

DISCLAIMER

Portions of this document may be illegible in electronic image products. Images are produced from the best available original document.

1

TABLE OF CONTENTS

	<u>Page</u>
ABSTRACT	1
INTRODUCTION	1
SECTION A. EMISSIVITY MEASUREMENTS ON ZIRCALOY	A-1
PART 1. SPECTRAL AND TOTAL EMISSIVITIES OF ZIRCALOY 2 AND ZIRCALOY B IN THE SOLID STATE	A-1
Introduction	A-1
Methods and Apparatus	A-2
Results	A-5
PART 2. SPECTRAL AND TOTAL EMISSIVITY MEASUREMENTS ON ZIRCONIUM OXIDE AND MOLTEN ZIRCALOY 2	A-17
Introduction	A-17
Method and Apparatus	A-17
Results	A-19
REFERENCES	A-21
SECTION B. THE DIFFUSION OF OXYGEN IN ALPHA AND BETA ZIRCALOY 2 AND ZIRCALOY 3 AT HIGH TEMPERATURES	B-1
Introduction	B-1
Materials	B-2
Method and Experimental Procedure	B-3
Results and Discussion	B-6
References	B-13
SECTION C. MEASUREMENT OF STEAM-ZIRCALOY 2 REACTION RATES	C-1
PART 1. CONVENTIONAL EXPERIMENTS	C-2
Introduction	C-2
Experimental Methods	C-2
Results and Discussion	C-8
PART 2. DROP-TEST EXPERIMENTS	C-32
Introduction	C-32
Apparatus	C-32
Procedure	C-36
Results	C-36
Discussion	C-46
Conclusions	C-48
REFERENCES	C-48
SECTION D. COOLING MECHANISM OF ZIRCALOY 2 DROPLETS IN WATER	D-1
Introduction	D-1
Formulation of the Problem	D-1
Results of the Calculations	D-17
References	D-32

STUDIES RELATING TO THE REACTION BETWEEN ZIRCONIUM AND WATER AT HIGH TEMPERATURES

Alexis W. Lemmon, Jr.

Attempts to calculate the extent of reaction between molten or solid zirconium and water have been hampered by the scarcity of basic data necessary for the calculation. To increase the quantity of available data, experimental studies were made of (a) the rate of reaction between solid and molten Zircaloy and steam, (b) the spectral and total emissivity of Zircaloy and its oxide, and (c) the rate of diffusion of oxygen in Zircaloy. Data from these studies are reported.

In addition, both theoretical and experimental studies were made of the amount of reaction expected for a molten drop of Zircaloy falling through water. In the theoretical studies, a model was used in which temperature variations around the drop are considered. Unresolved discrepancies between theory and experiment were found.

Owing to the fact that all studies were made concurrently, the experimental data obtained in this study could not be used in the theoretical studies. The discrepancy just noted may arise from this fact, or from other causes.

INTRODUCTION

Previous analytical studies of the reaction between zirconium and water, such as that reported in WAPD-137*, were hampered by the paucity of basic data on which to base them. Consequently, a series of experimental programs was undertaken in support of WAPD to provide data needed to make possible a more refined evaluation of the problem.

Three experimental programs were designed to provide basic data on (1) the radiation emissivity of Zircaloy 2 and its oxide, (2) the reaction rates of water (steam) with solid and liquid Zircaloy 2, and (3) the diffusion rates of oxygen in solid Zircaloy 2 and Zircaloy 3. In addition to these programs, a mathematical study of the amount of chemical reaction and heat transfer encountered by an initially molten Zircaloy 2 droplet falling through steam and water also is reported. Each of these studies is reported separately in the sections of the following report.

*Lustman, B., "Zirconium-Water Reactions", WAPD-137, Westinghouse Electric Corporation, Atomic Power Division, Pittsburgh, Pennsylvania (December 1, 1955).

SECTION A

EMISSIVITY MEASUREMENTS ON ZIRCALOY

W. D. Wood, W. E. Nexsen, Jr., H. W. Deem,
G. B. Gaines, and C. F. Lucks

SECTION A

EMISSIVITY MEASUREMENTS ON ZIRCALOY

W. D. Wood, W. E. Nexsen, Jr., H. W. Deem,
G. B. Gaines, and C. F. Lucks

The total emissivities of both Zircaloy 2 and Zircaloy B in the solid state were found to increase with temperature and with oxygen content. The total emissivities of both alloys as received were about 0.22 at 1000 C and near 0.25 at 1750 C. With 5 a/o oxygen in solution, the total emissivities of both alloys were near 0.24 at 1000 C and 0.28 at 1750 C; with 20 a/o oxygen, both had total emissivities in the neighborhood of 0.33 for temperatures from 1200 to 1600 C. Near 800 C, the total emissivity for Zircaloy 2 with a surface oxide coating was 0.67.

The spectral emissivity ($\lambda=0.65 \mu$) of Zircaloy 2 is nearly constant at 0.45 from 1000 to 1750 C, while that of Zircaloy B decreases from 0.47 at 1000 C to 0.42 at 1600 C. With 5 a/o oxygen in solution, approximate values for Zircaloy 2 and Zircaloy B are 0.43 and 0.39 respectively for the temperature range 1000 to 1700 C. For Zircaloy 2 only, with 10 a/o oxygen, the spectral emissivity is approximately 0.39 over the same temperature range. Spectral-emissivity evaluations were not attempted for higher oxygen concentrations.

Total-emissivity measurements on zirconia (stabilized) and on molten Zircaloy 2 were not successful owing to changes in the materials when heated in a graphite crucible in vacuum. Values might be extrapolated for the molten Zircaloy 2 from the data for the solid material. However, these values could be in error by ± 50 per cent or more.

PART 1SPECTRAL AND TOTAL EMISSIVITIES OF ZIRCALOY 2
AND ZIRCALOY B IN THE SOLID STATEIntroduction

Spectral- and total-emissivity measurements were carried out for both Zircaloy 2 and Zircaloy B with the unoxidized material and with various percentages of oxygen added. Two methods of obtaining emissivities were employed. The hole-in-tube method was adapted for all spectral-emissivity and most of the total-emissivity measurements. This method

was used successfully by Worthing and Halliday^{(A-1)*} in their studies of the spectral emissivity of tungsten, and by Jain and Krishman^(A-2) in their studies of graphite.

The wire-loop method of Worthing^(A-3) was used with Zircaloy 2 to determine whether the hole-in-tube method would give accurate total emissivity values or if it might be necessary to form the hard-to-work Zircaloy B into wire. The results of the two methods were in close agreement and the hole-in-tube method was used for all other measurements.

Methods and Apparatus

Hole-In-Tube Method

The apparatus for the measurement of emissivities by the hole-in-tube method is shown schematically in Figure A-1. A sheet of 5-mil-thick material was rolled into a 1/2-in.-diameter tube, A, 11 in. long and annealed to shape in a vacuum. A 3/64-in. hole, O, was drilled through one wall near the center of the tube, and two 5-mil-diameter zirconium wire potential leads, V, were resistance welded to the tube about 1-1/2 in. above and below the hole. Water-cooled current leads, I, were affixed to each end of the tube and the assembly placed in an evacuated, water-cooled chamber, F. Measurements were taken of the current and the voltage across the measured length, V. Optical-pyrometer readings were taken through the Vycor window, W, of the black-body temperature through the hole, O, and the surface temperature beside the hole. The spectral emissivity was determined from the following relationship:

$$\ln E\lambda' = \frac{-C_2}{\lambda} \frac{(T-S)}{(ST)}, \quad (A-1)$$

where

$E\lambda'$ = spectral emissivity

λ = observed wavelength = 0.65μ

C_2 = radiation constant = 1.438 cm-K

S = surface temperature, K

T = true (black body) temperature, K.

*References are at end of Section A.

The total emissivities were determined by using the following equation:

$$E_{T'} = \frac{IV}{2\pi r \ell \sigma T^4} \quad , \quad (A-2)$$

where

$E_{T'}$ = total hemispherical emissivity

I = current through specimen, amp

V = potential drop across measured section, v

r = radius of the specimen, cm

ℓ = length of measured section, cm

σ = Boltzmann's constant = 5.673×10^{-12}
watts/(cm²)(K⁴)

T = true (black body) temperature, K.

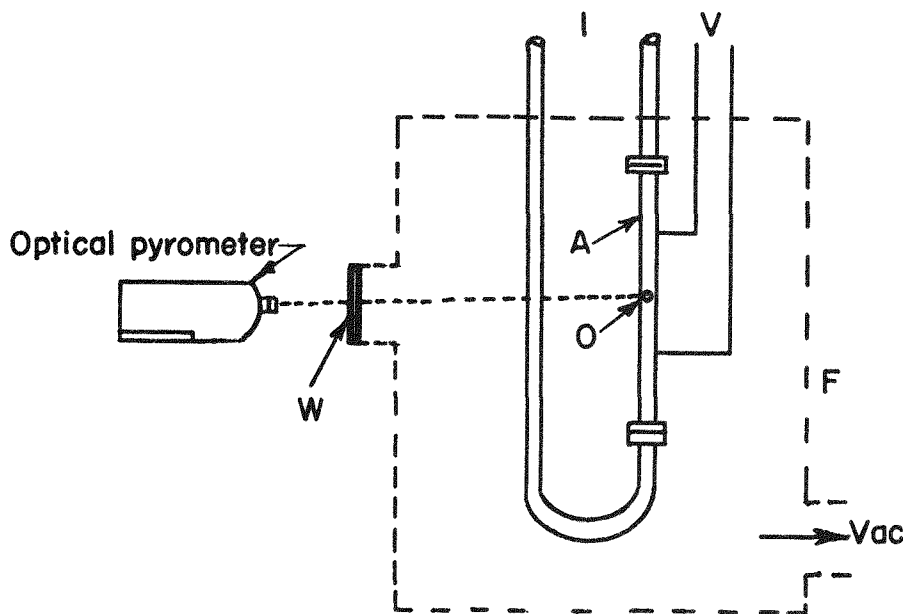


FIGURE A-1. SCHEMATIC DIAGRAM OF THE APPARATUS FOR MEASURING EMISSIVITIES BY THE HOLE-IN-TUBE METHOD

Samples containing 5 and 10 a/o oxygen were prepared in a modified Sieverts apparatus by adding oxygen in measured amounts to the surface of a formed metallic tube at a temperature below the alpha-beta transition temperature. The tube was then transferred to the emissivity apparatus. Higher oxygen concentration was obtained within the emissivity apparatus by adding individual charges of oxygen (2.5 cm^3 per charge) to the tube while the tube was kept at a nearly constant temperature between 1175 and 1275 C. The system was evacuated between charges, and whatever oxygen remained in the system was removed. Therefore, it was impossible to tell, during the test, exactly what percentage of each charge had combined with the tube. The actual percentage of combined oxygen was determined by analysis after the test was completed.

As each oxygen charge was added, the surface of the tube "flashed" instantaneously to a higher temperature because of the heat of reaction, then dropped immediately to a lower temperature because of the high emissivity of the oxide coating, and finally increased to an equilibrium value as the oxygen diffused into the metal.

After about 20 a/o oxygen had been added (115 charges), the temperature of the tube was increased to obtain the relation of emissivity to temperature at that percentage of oxygen.

One other oxygen-addition run was made on Zircaloy 2 in which oxygen was added at a temperature below the alpha-beta transition temperature (between 750 and 850 C) in order to obtain total-emissivity values with a surface oxide present.

Wire-Loop Method

The apparatus for the wire-loop method is shown schematically in Figure A-2. The system was essentially the same except that two 33-mil-diameter wire filaments instead of a tube were used as the specimen. The short filament, L_s , was approximately 10 in. long and the long filament, L_l , was approximately 15 in. long. The central portion of the long filament was used for the measurement, and its active length was the difference between the lengths of the two filaments. The potential drop used was the difference between the two potential drops for the filaments taken separately. The filaments were long enough to insure that the temperature of the central portion of the longer filament would be uniform.

The total-emissivity relationship (Equation A-2) was used in this determination. The temperature was determined by using the hole-in-tube emissivity data and the surface temperature of the wire.

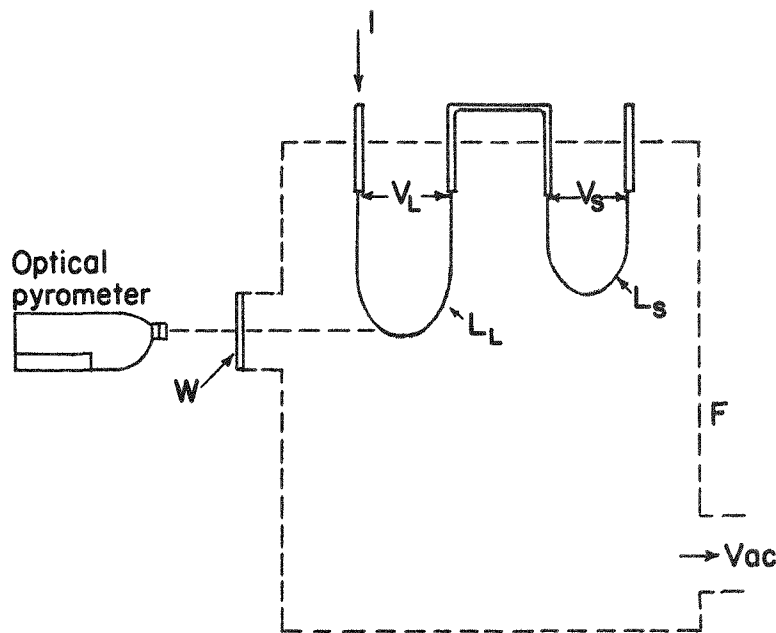


FIGURE A-2. SCHEMATIC DIAGRAM OF THE APPARATUS FOR MEASURING EMISSIVITIES BY THE WIRE-LOOP METHOD

Discussion of Errors

Some difficulty was encountered in measuring the spectral emissivity of specimens to which oxygen had been added. The surface of such specimens became mottled and uneven in apparent temperature to the extent of spreading the calculated values by as much as ± 15 per cent.

Errors inherent in meter accuracy and calculations plus the human factors of reproducibility and readability of instruments, particularly the optical pyrometer readings, indicate a probable error of ± 5 per cent in the spectral emissivities of the as-received materials and ± 3 per cent in all total emissivities.

Results

Zircaloy 2

The experimental values of the total emissivity of Zircaloy 2, as received, and with about 5, 10, and 22 a/o oxygen in solution are shown plotted versus temperature in Figure A-3. The values for the material, as received, are shown for both the wire-loop and hole-in-tube methods,

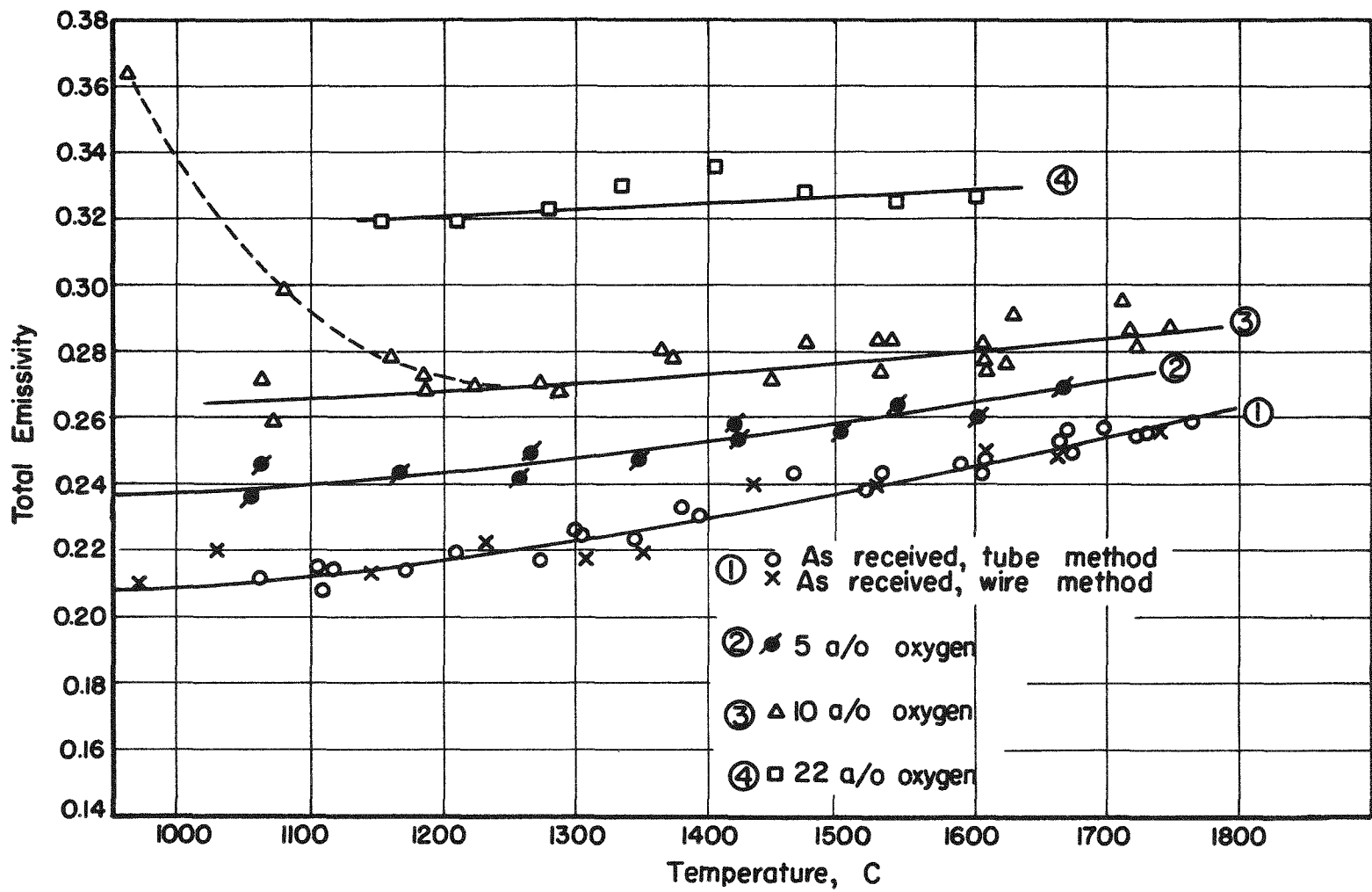


FIGURE A-3. TOTAL EMISSIVITY OF ZIRCALOY 2 VERSUS TEMPERATURE FOR VARYING OXYGEN CONTENTS

showing the close agreement between the two. The dotted portion of the curve for the 10 a/o oxygen in Figure A-3 represents the nonequilibrium values as the surface-applied oxygen is being diffused into the metal. Interpolated values for the total emissivities are given in Table A-1.

TABLE A-1. TOTAL EMISSIVITY OF ZIRCALOY 2

Temperature, C	Total Emissivity			
	As Received	Approx. 5 a/o Oxygen	Approx. 10 a/o Oxygen	Approx. 22 a/o Oxygen
1000	0.21	0.24	0.26	--
1100	0.21	0.24	0.26	0.32
1200	0.22	0.24	0.26	0.32
1300	0.23	0.25	0.27	0.33
1400	0.23	0.25	0.27	0.33
1500	0.24	0.26	0.28	0.33
1600	0.25	0.26	0.28	0.33
1700	0.25	0.27	0.29	--
1750	0.26	0.27	0.29	--

A plot of the total emissivity versus oxygen addition is shown in Figure A-4 for a temperature range of 1175 to 1275 C. Time was allowed between charges for diffusion of the oxygen into the specimen. One hundred fifteen charges (2.5 cm³ each) of oxygen resulted in an oxygen content of about 22 a/o.

The uppermost points in Figure A-4 are for readings immediately following each oxygen addition. The succeeding lower points were obtained at later times; the lowest point of each group indicates nearly complete diffusion of the oxygen into the metal.

Figure A-5 shows the total emissivity of Zircaloy 2 with an oxide coating built up by oxygen addition below the transition temperature (775 to 875 C). The photomicrograph of this oxidized specimen in Figure A-6 clearly shows an oxide coating plus an oxygen-metal layer and the base material beneath. The maximum observed total emissivity for the oxide coating was 0.67.

Experimental values for the spectral emissivity of the as-received material are shown plotted as emissivity versus temperature in Figure A-7. Because of the large experimental deviations (± 15 per cent) in the oxygen addition runs, the values were not plotted but are shown only as averages in Table A-2 with the interpolated values for the as-received material.

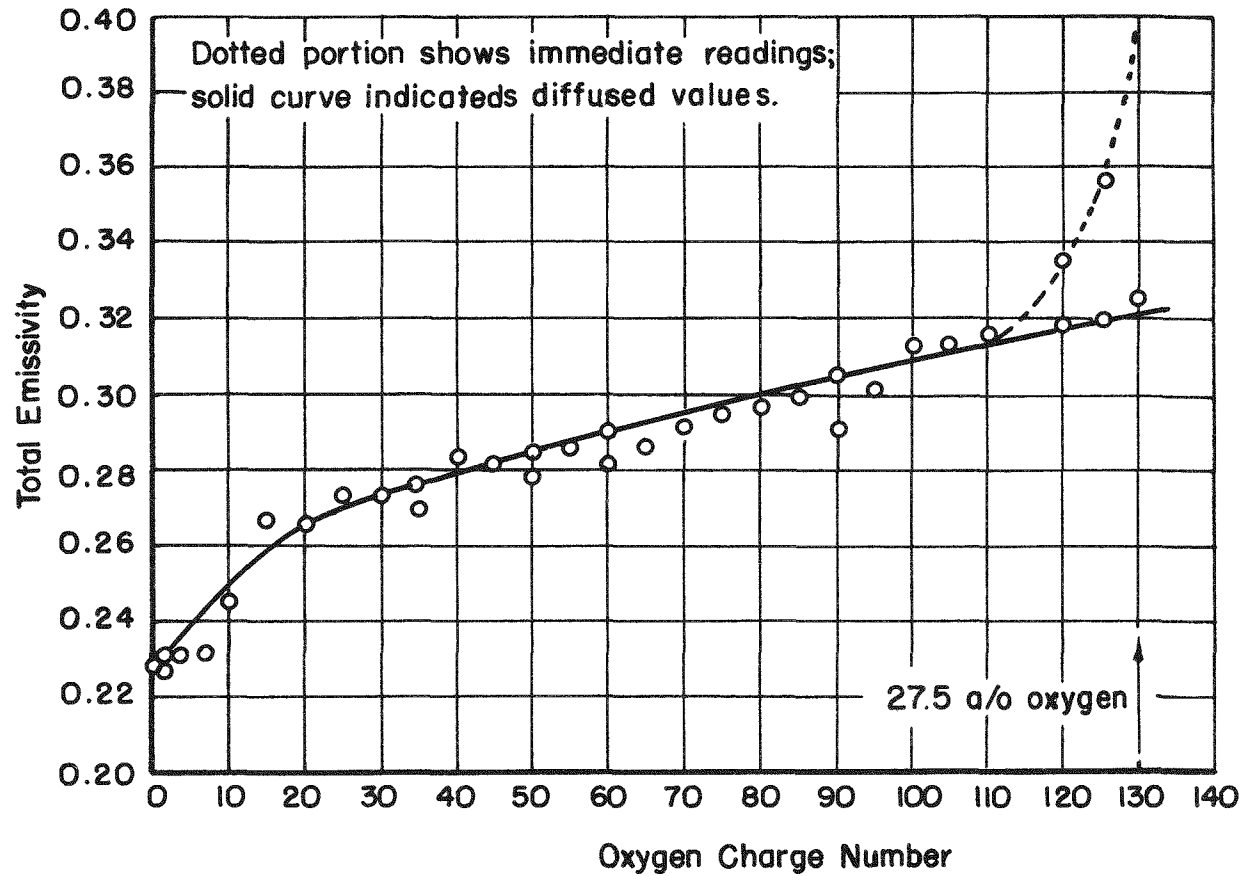


FIGURE A-4. TOTAL EMISSIVITY OF ZIRCALOY 2 VERSUS OXYGEN ADDITION AT TEMPERATURES BETWEEN 1175 AND 1275 C

12

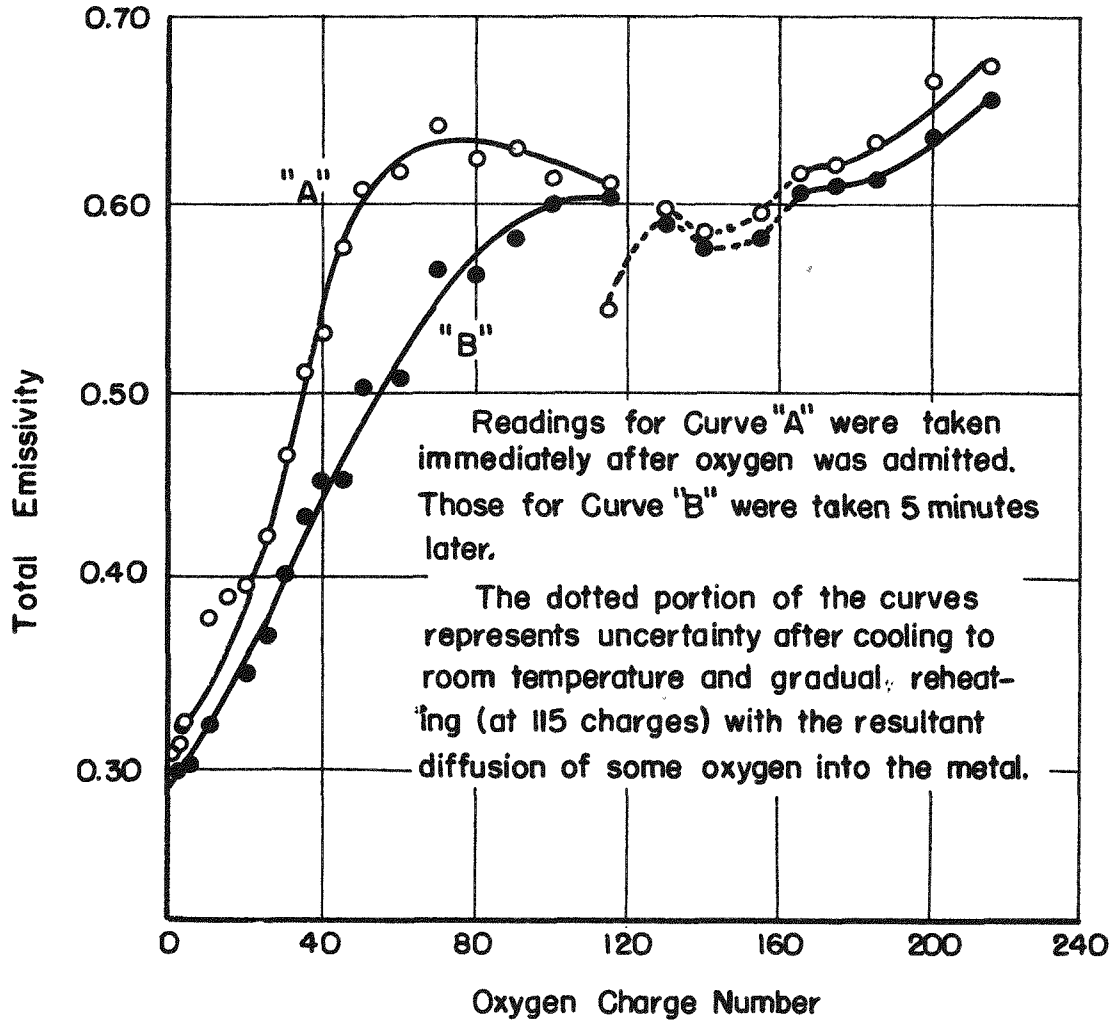
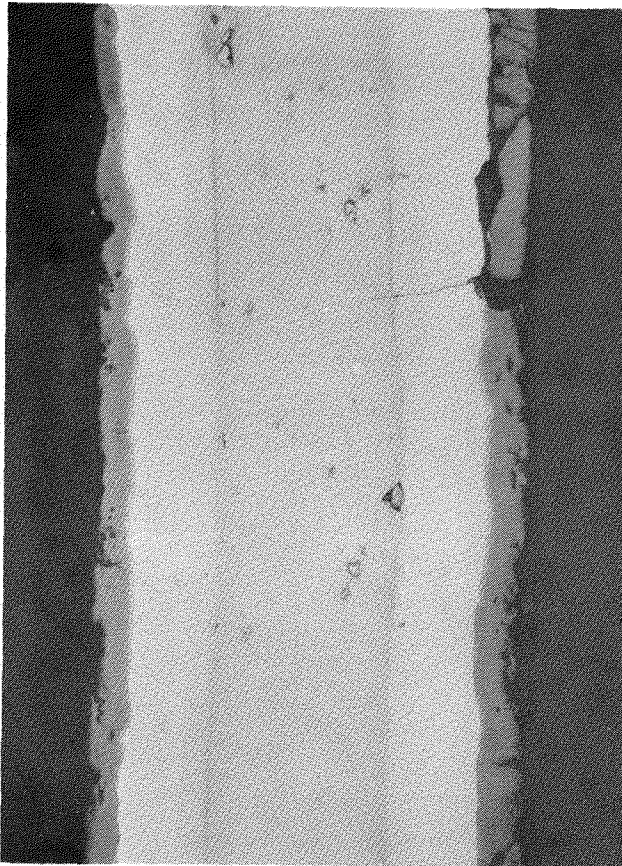


FIGURE A-5. TOTAL EMISSIVITY OF ZIRCALOY 2 VERSUS OXYGEN ADDITION FOR A SURFACE OXIDE AT TEMPERATURES BETWEEN 775 AND 875 C

13



N32129

FIGURE A-6. PHOTOMICROGRAPH OF SECTION OF SPECIMEN OF ZIRCALOY 2 WITH OXIDE COATING

14

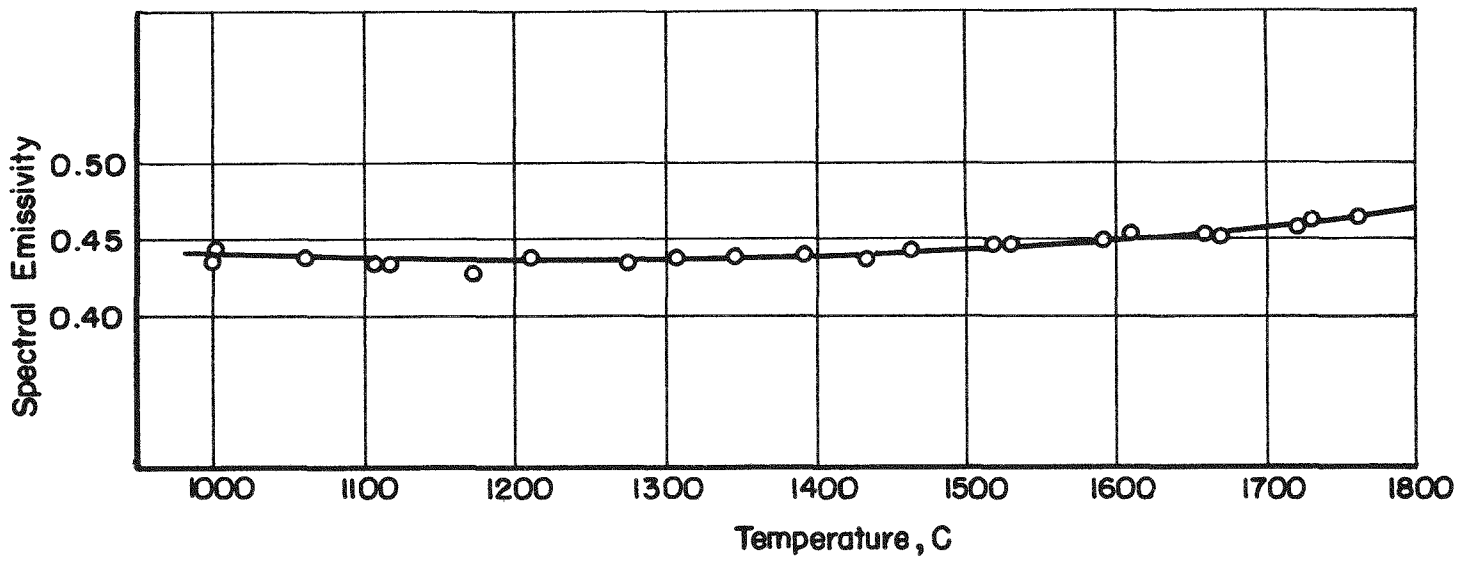


FIGURE A-7. SPECTRAL EMISSIVITY OF ZIRCALOY 2

$\lambda = 0.65 \mu$

A-11

TABLE A-2. SPECTRAL EMISSIVITY OF ZIRCALOY 2

Temperature, C	Spectral Emissivity ($\lambda = 0.65 \mu$)		
	As Received	Approx. 5 a/o Oxygen	Approx. 10 a/o Oxygen
1100	0.43		
1200	0.43		
1300	0.44	0.43(a)	0.39(a)
1400	0.44		
1500	0.44		
1600	0.45		
1700	0.46		

(a) Average values.

Molten Zircaloy 2

Since no experimental values were obtained for the total emissivity of molten Zircaloy 2, values might be extrapolated from the high-temperature data for the solid material. However, since there seems to be some correlation between electrical resistivity and total emissivity and since, with many metals, resistivity changes radically through the melting point, it would seem that extrapolated total emissivity values might be in error by as much as ± 50 per cent or more.

Zircaloy B

Figure A-8 shows the experimental values of total emissivities of Zircaloy B plotted against temperature for the material, as received and with 5 and 20 a/o oxygen added. Interpolated values for the above are given in Table A-3. The increase of total emissivity with oxygen addition is shown in Figure A-9 in the same manner as previously shown in Figure A-5 for Zircaloy 2. No attempt was made to obtain an oxide layer on Zircaloy B.

Figure A-10 shows the spectral emissivity for the Zircaloy B as received. Interpolated values for the as-received material and the average value for the 5 and 10 a/o oxygen additions are given in Table A-4.

Comparison of Spectral Emissivities

Table A-5 shows a comparison of the spectral emissivities of Zircaloy 2 and Zircaloy B as determined in this study with those for zirconium as determined by Cubicciotti(A-4).

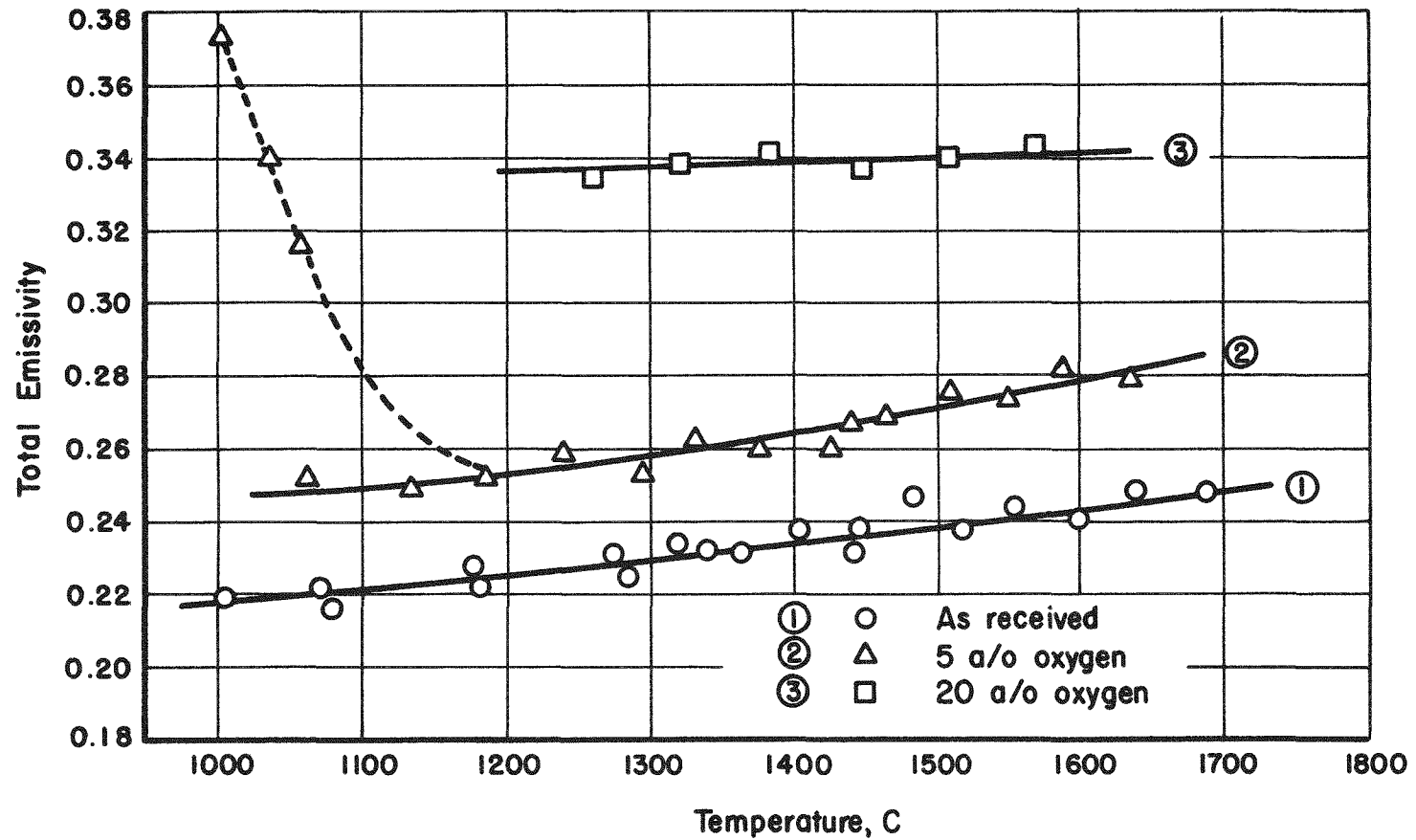


FIGURE A-8. TOTAL EMISSIVITY OF ZIRCALOY B FOR VARYING OXYGEN CONTENTS

17

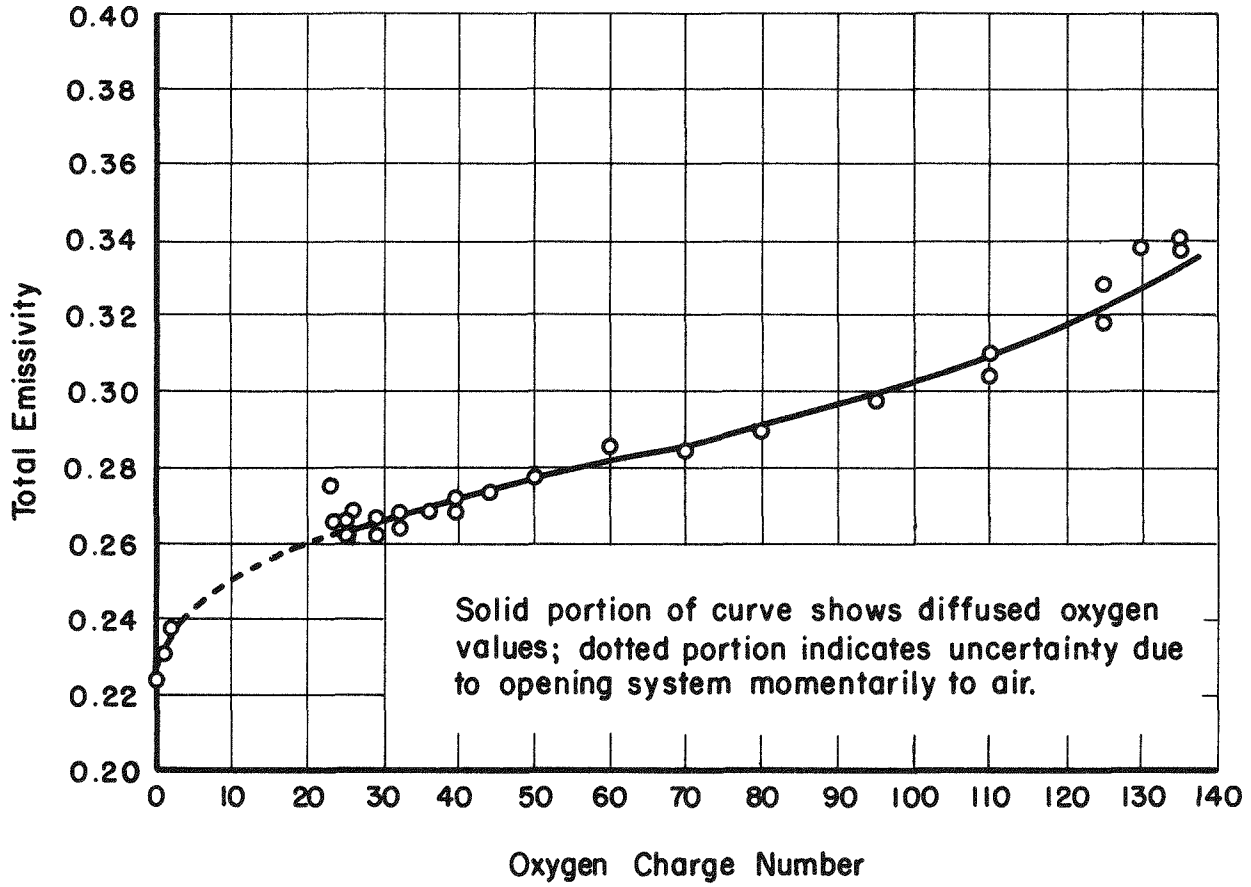


FIGURE A-9. TOTAL EMISSIVITY OF ZIRCALOY B VERSUS OXYGEN ADDITION AT TEMPERATURES BETWEEN 1175 AND 1275 C

18

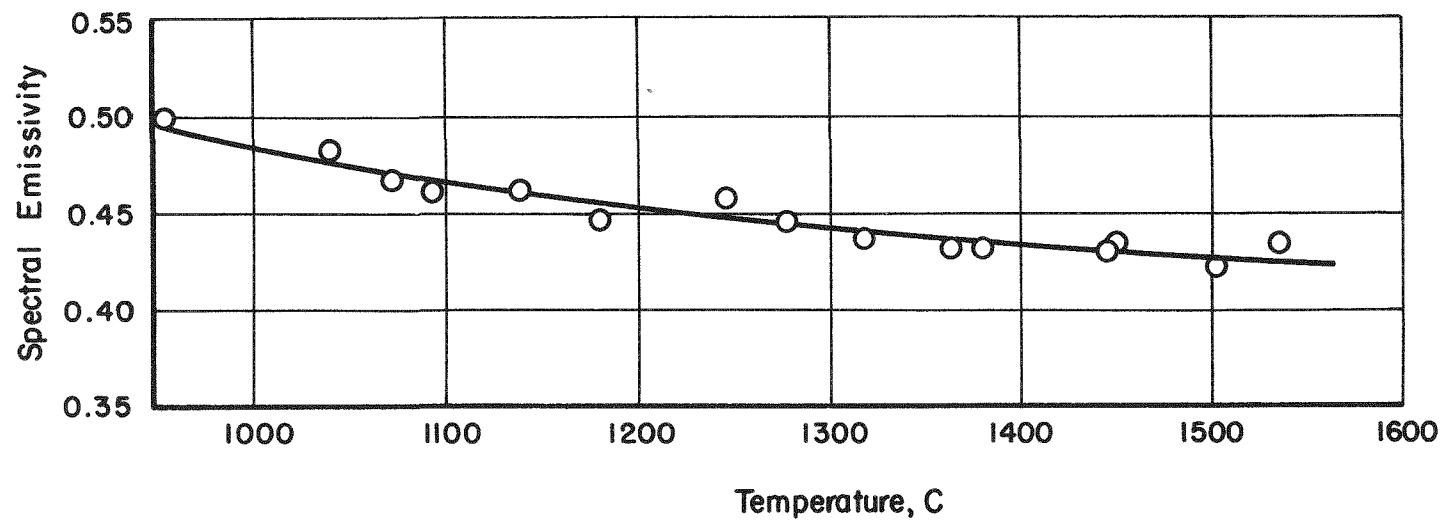


FIGURE A-10. SPECTRAL EMISSIVITY OF ZIRCALOY B

$\lambda=0.65$

TABLE A-3. TOTAL EMISSIVITY OF ZIRCALOY B

Temperature, C	Total Emissivity		
	As Received	Approx. 5 a/o Oxygen	Approx. 20 a/o Oxygen
1000	0.22	0.25	--
1100	0.22	0.25	--
1200	0.23	0.25	0.34
1300	0.23	0.26	0.34
1400	0.24	0.26	0.34
1500	0.24	0.27	0.34
1600	0.25	0.28	0.34
1700	0.25	0.29	--

TABLE A-4. SPECTRAL EMISSIVITY OF ZIRCALOY B

Temperature, C	Spectral Emissivity ($\lambda = 0.65 \mu$)		
	As Received	Approx. 5 a/o Oxygen	Approx. 10 a/o Oxygen
1100	0.43		
1200	0.43		
1300	0.44	0.43(a)	0.39(a)
1400	0.44		
1500	0.44		
1600	0.45		
1700	0.46		

(a) Average values.

TABLE A-5. COMPARISON OF SPECTRAL EMISSIVITY VALUES FOR ZIRCONIUM AS OBTAINED BY CUBICCIOTTI^(A-4) WITH THOSE FOR ZIRCALOY OBTAINED IN THIS RESEARCH

Oxygen in Solution, a/o	Temperature, C	Spectral Emissivity ($\lambda = 0.65 \mu$)		
		Cubicciotti Zirconium	Observed	
			Zircaloy 2	Zircaloy B
0 (pure metal)	982	0.51	--	--
	1025	0.49	0.43	0.43
10	983	0.44	0.37	--
	1012	0.50	0.39	0.39
22	978	0.42	--	--
	1002	0.50	0.54	0.50

PART 2
SPECTRAL AND TOTAL EMISSIVITY MEASUREMENTS
ON ZIRCONIUM OXIDE AND MOLTEN ZIRCALOY 2

Introduction

The hole-in-tube and wire-loop methods described in Part 1 for emissivity depend upon the test material being a self-supporting electrical conductor. Therefore, neither of the two methods was suitable for emissivity measurements on zirconium oxide and molten Zircaloy 2. The method used for these two materials involved the comparison of the radiation from the specimen to that from a black body at the same temperature. The results obtained, however, were not satisfactory owing to changes which occurred in the specimen materials when they were heated in a graphite crucible in a vacuum.

Method and Apparatus

The total emissivity was determined by comparing the radiation from the specimen with that from a surface of graphite at the same temperature. The spectral and total emissivity of Acheson graphite has been measured as a function of temperature as far as 2100 K. (A-2) The total emissivity of the specimen was obtained by taking a ratio of the voltage output of the thermopile when "looking" at the specimen to the voltage output when looking at the adjacent graphite surface and multiplying this ratio by the emissivity of the graphite at that temperature. True temperature was obtained by measuring the brightness temperature of the graphite and using the relationship

$$\frac{1}{T} - \frac{1}{T'} = \frac{\lambda}{14380} \ln \epsilon_{\lambda} ,$$

where T is the true temperature, T' the brightness temperature, λ the wavelength passed by the optical pyrometer (0.65μ), and ϵ_{λ} is the spectral emissivity.

The measurements were performed in a water-cooled vacuum chamber made from a 14-in.-diameter brass tube as shown in Figure A-11. The sample (A), approximately 1/2 in. in diameter and 1-in. long, was placed in a hole in a graphite crucible (B) which was 2 in. in diameter and 2 in. long. This crucible was insulated from the Vycor cup (D) by powdered graphite (C). The Vycor cup was supported in the center of the chamber by three graphite rods. The graphite crucible was heated inductively by the coil (E) powered from a 50-kw heater operating at a frequency of approximately 500 kc. (F) is a water-cooled collimator for the thermopile (G). By means of a worm-gear-driven arm, the thermopile collimator could be

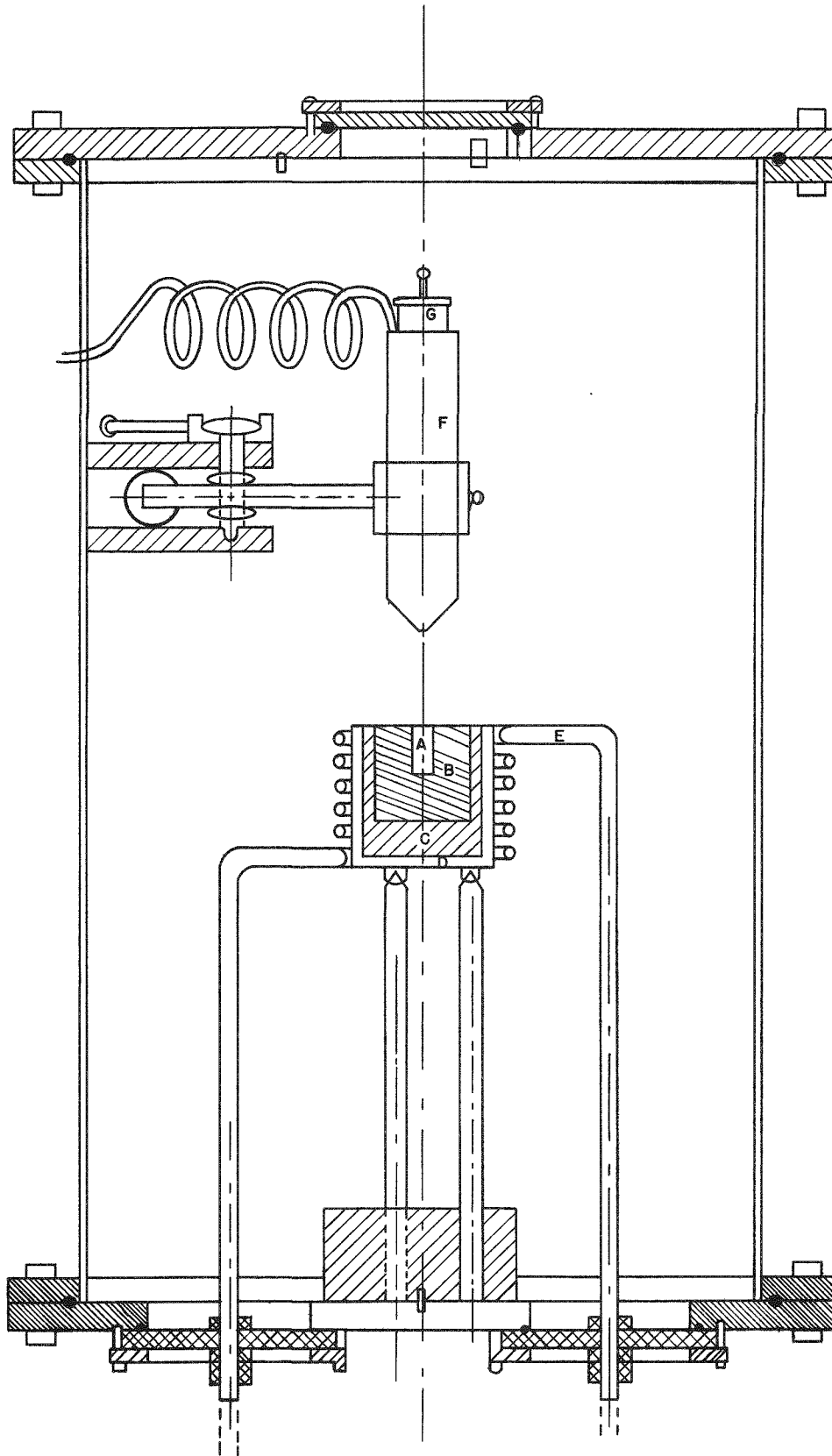


FIGURE A-11. TOTAL-EMISSIVITY APPARATUS

rotated around an axis parallel to the axis of the crucible so that it was possible to measure the radiation from different sections of the end of the crucible containing the specimen.

Results

Six runs were made in an effort to determine the total emissivity of zirconia and Zircaloy 2. Of these runs, three were made on zirconia and three on Zircaloy 2. In each of the six runs a fresh specimen was used, but in some cases the graphite cylinder was used for more than one run.

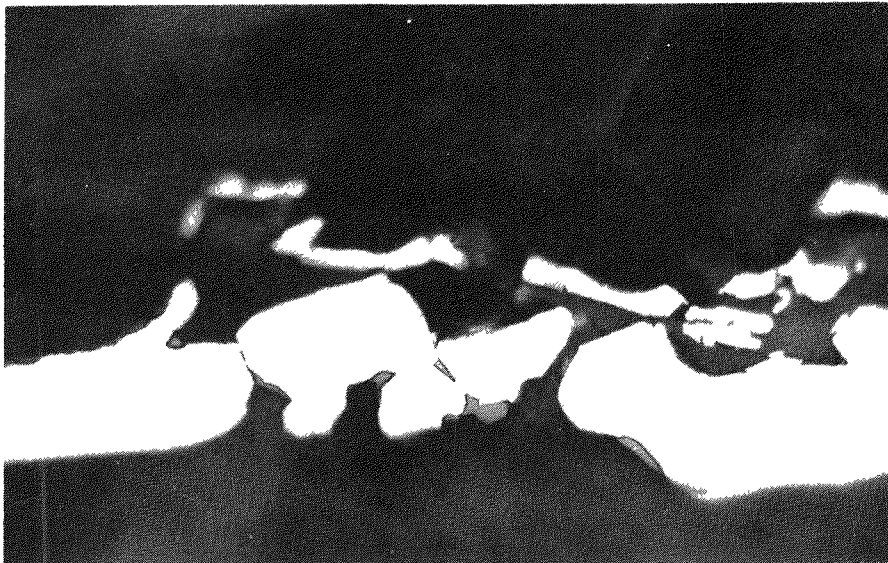
Zirconia

In all three specimens of the zirconia, a pronounced change in appearance of the surface occurred after heating in a vacuum. Before heating, the "stabilized" zirconia was a cream-colored ceramic, but after heating it was a dark gray. The surfaces of the specimens that were smooth (originally), Specimens 1 and 2, had, in addition, a metallic luster. Originally it was thought that the change in surface was due to a reaction between the graphite and the zirconia. Enclosing the zirconia in a 5-mil tantalum cup (Specimen 2) did not eliminate the change in surface appearance, so it is probable that the change is due directly to heating in vacuum.

A third zirconia specimen, which was roughened by sandblasting, did not give any better values for emissivity, so this technique was abandoned. It is believed that the values given for an oxide coating on Zircaloy are the best choice for the emissivity of zirconia.

Zircaloy 2

Total-emissivity measurements were attempted for three specimens of Zircaloy 2. In every case, the material permeated the graphite crucible. In the original attempt, the material also crept out over the surface of the graphite crucible. The surface creeping was eliminated in Specimen 3 by using a new graphite crucible which had a lip, 1/4 in. high and 1/16 in. thick, projecting above the surface around the hole which contained the specimen. At the end of the measurements on Specimen 3, it was found that what appeared to be the remains of the original surface of the specimen was actually a very thin skull and that most of the Zircaloy 2 had flowed into the graphite, leaving a large void under the skull. The surface, cooled by radiation, stayed slightly below the melting point while the material below the surface was molten. A photomicrograph of a section through the skull is shown in Figure A-12. The skull appears to be mostly Zircaloy 2 with small patches of oxide on the surface and some evidence of patches of zirconium nitride.



N32130

FIGURE A-12. PHOTOMICROGRAPH OF SECTION THROUGH SKULL OF ZIRCALOY 2 SPECIMEN

The values obtained for Specimen 3, as described above, are listed in Table A-6. It is probable that the values are too high because the temperature of the specimen surface could have been higher than the surface of the graphite and because patches of oxide were present.

TABLE A-6. THE TOTAL AND SPECTRAL EMISSIVITIES OF A SURFACE OBTAINED BY HEATING A ZIRCALOY 2 SURFACE IN A GRAPHITE CRUCIBLE IN VACUUM

True Temperature, C	Spectral Emissivity ($\lambda = 0.65 \mu$)	Total Emissivity
1112	0.77	0.68
1737	0.59	0.52
1742	0.59	0.61
1700	--	0.61

The results of the emissivity measurements on both zirconium oxide and molten Zircaloy 2 were unsatisfactory owing to changes occurring in the specimens as the result of their being heated in graphite in a vacuum.

REFERENCES

- (A-1) Worthing and Halliday, Heat, John Wiley and Sons, Inc., New York (1948), Chapter XIII, p 461.
- (A-2) Jain and Krishman, Proc. Roy. Soc. (London), 225, 7 (1954).
- (A-3) Temperature - Its Measurement and Control in Science and Industry, Reinhold Publishing Co., New York (1941), "Temperature Radiation Emissivities and Emittances", Worthing, A. G., pp 1176-1178.
- (A-4) Cubicciotti, D., J. Am. Chem. Soc., 73, 2032 (1951).

SECTION B

THE DIFFUSION OF OXYGEN IN ALPHA AND BETA
ZIRCALOY 2 AND ZIRCALOY 3 AT HIGH TEMPERATURES

M. W. Mallett, W. M. Albrecht, and P. R. Wilson

SECTION B

THE DIFFUSION OF OXYGEN IN ALPHA AND BETA
ZIRCALOY 2 AND ZIRCALOY 3 AT HIGH TEMPERATURES

M. W. Mallett, W. M. Albrecht, and P. R. Wilson

The diffusion rates of oxygen in alpha and beta Zircaloy 2 and Zircaloy 3 were determined in the range 1000 to 1500 C. For alpha Zircaloy 2, the variation of the diffusion coefficient, D_α , in cm^2 per sec, with temperature is given by the equation

$$D_\alpha = 0.196 \exp [(41,000 \pm 1500)/RT].$$

For beta Zircaloy 2,

$$D_\beta = 0.0453 \exp [(28,200 \pm 2400)/RT].$$

Spot checks of the diffusion of oxygen in alpha and beta Zircaloy 3 at 1100 and 1400 C show that the rates are in close agreement with those for oxygen in Zircaloy 2.

The diffusion coefficients for oxygen in beta Zircaloy 2 and Zircaloy 3 are about 10 times greater than those for nitrogen in high-purity beta zirconium.

Introduction

One of the processes that occurs during the reaction of Zircaloy 2 or Zircaloy 3 with water or water vapor is the diffusion of oxygen in the metal. In making calculations to estimate the high-temperature performance of these alloys in the presence of water, Lustman^(B-1) used the diffusion coefficients for nitrogen in high-purity iodide zirconium^(B-2) as an approximation of the diffusion rates for oxygen. This was done since oxygen-diffusion information was not available. It was realized that the rate of oxygen diffusion would be somewhat different than that of nitrogen at the same temperatures. As part of a program to determine the actual performance of the alloys in the presence of water at high temperatures, the rates of diffusion of oxygen in alpha and beta Zircaloy 2 and Zircaloy 3 were studied for the range 1000 to 1800 C. However, because of the rapidity of oxygen diffusion in both phases of the alloys, no diffusion measurements could be made above 1500 C. Rather complete data were obtained for alpha and beta Zircaloy 2, but the behavior of Zircaloy 3 was spot checked only to confirm that the rates agree with those for oxygen in Zircaloy 2.

Materials

The Zircaloy 2 and Zircaloy 3 for this work were fabricated into 5/8-in.-diameter rods. Specimens for the experiments were machined from these rods. Analyses of both alloys were obtained by spectrographic, chemical, and vacuum-fusion techniques. Results are given in Table B-1.

Oxygen was prepared by the thermal decomposition of degassed potassium permanganate as described by Hoge (B-3). It was dried with a dry ice-acetone cold trap.

TABLE B-1. ANALYSES OF ZIRCALOY 2
AND ZIRCALOY 3

Element	Amount Present (Balance Zirconium), w/o	
	Zircaloy 2	Zircaloy 3
Tin	1.5	0.22
Iron	0.20	0.34
Chromium	0.05	0.03
Nickel	0.03	0.005
Silicon	0.007	0.05
Aluminum	0.006	0.005
Manganese	0.002	0.01
Magnesium	0.002	0.001
Lead	0.002	--
Oxygen	0.089	0.14
Nitrogen	0.003	0.01
Hydrogen	0.002	0.003

Method and Experimental Procedure

Zirconium-Oxygen Phase Diagram

Knowledge of the phase diagrams of the Zircaloy 2- and Zircaloy 3-oxygen systems is essential in preparing suitable diffusion specimens to determine diffusion coefficients, but no information is available on either system. However, it is believed that the zirconium-oxygen system^(B-4) is very similar to the Zircaloy-oxygen systems since the basic structure of the alloys are not changed from that of zirconium. That is, alpha and beta Zircaloy alloys have the same structures as alpha and beta zirconium. Therefore, the zirconium-oxygen system was used as a source of oxygen-concentration data needed for diffusion studies of the Zircaloy materials. A partial phase diagram of the zirconium-oxygen system is reproduced in Figure B-1. The portion of the diagram of interest for this study is that from 1000 to 1500 C. In this range the boundary between beta and alpha plus beta represents the maximum solubility of oxygen in beta (solid solution) zirconium. The boundary between alpha plus beta and alpha represents the lowest oxygen concentration required to maintain a single phase of alpha (solid solution) zirconium. The boundary between alpha and alpha plus ZrO_2 represents the maximum solubility of oxygen in alpha zirconium.

Concentration-Gradient Technique

The concentration-gradient technique^(B-5) was used to determine the diffusion coefficients for oxygen in beta-phase Zircaloy 2 and Zircaloy 3. Essentially, the method consists of analyzing the concentration gradient in a cylindrical specimen after the specimen has reacted with oxygen at a given temperature for a predetermined length of time. The diffusion coefficient was determined from the concentration gradient by a graphical method.

Specimens having gradients were prepared as follows. A Zircaloy 2 (or Zircaloy 3) cylinder about 1 cm in diameter and 4 cm long was dry abraded with 240-grit silicon carbide paper. After the dimensions of the cylinder were measured, the specimen was placed in the Vycor furnace tube of a modified Sieverts apparatus^(B-2). The sample was then induction heated in a vacuum for 1 hr at the temperature of the run. Temperatures were measured under black-body conditions with an optical pyrometer. With the sample at the desired temperature, an amount of oxygen (based on the maximum solubility in beta phase at desired temperature) calculated to maintain a thin oxide film on the sample was added to the reaction chamber. The sample was heated for a length of time sufficient to prepare a suitable gradient; that is, enough oxygen was diffused to just begin to affect the core. At the end of this time, the sample was quenched as rapidly as possible to room temperature. The film on the sample contained the phases shown in the phase diagram, Figure B-1. Proceeding from right to left on the

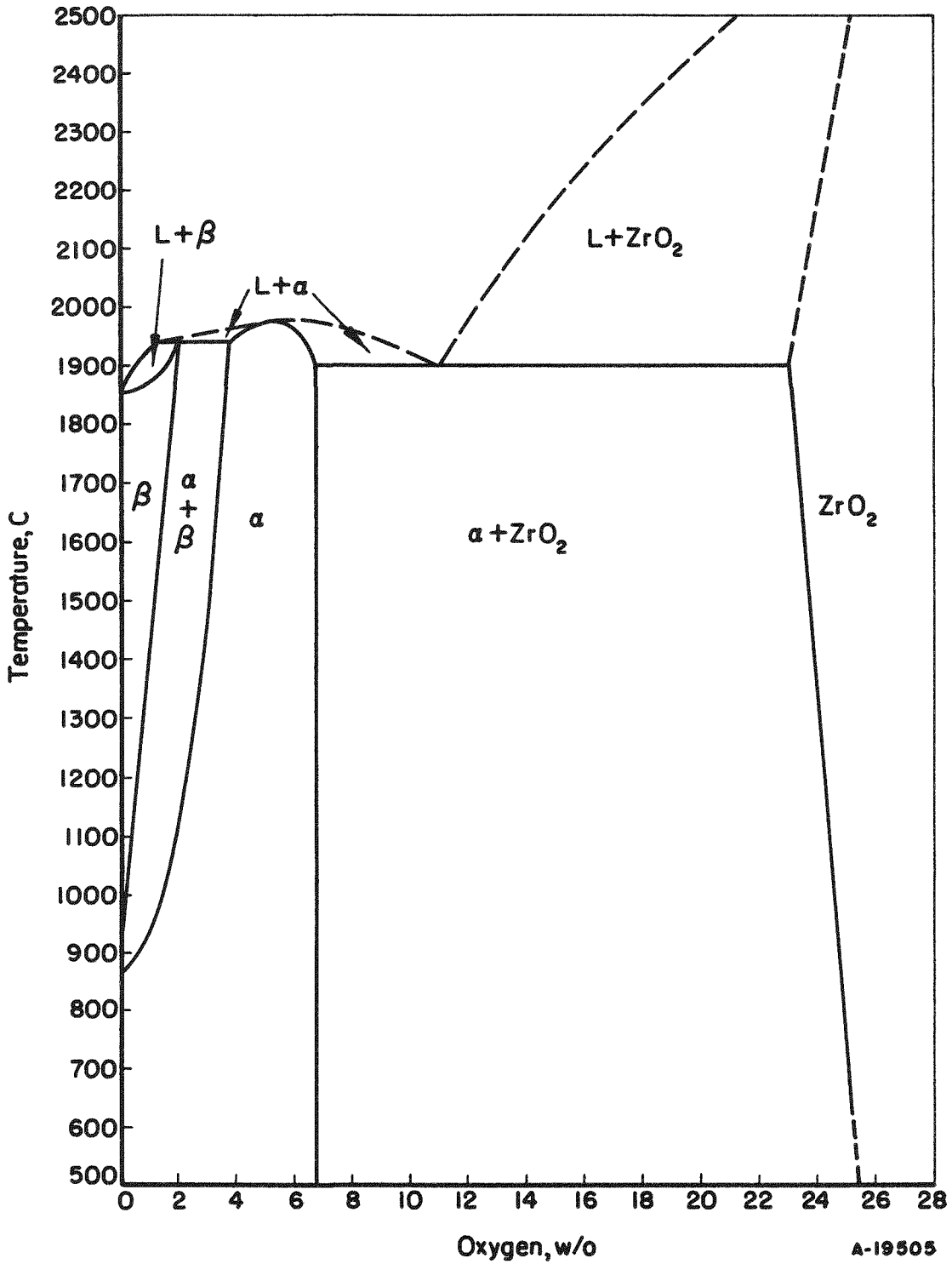


FIGURE B-1. PARTIAL PHASE DIAGRAM OF THE ZIRCONIUM-OXYGEN SYSTEM

diagram at the temperature of the run, the outer layer is ZrO_2 ; beneath this is a very thin layer of alpha solid solution. Beneath this is the beta core which contains the oxygen gradient being measured. It should be noted that two-phase regions are not produced by diffusion in a heterogeneous binary system(B-6).

Since diffusion occurs from the ends of the cylinder as well as the sides, lengths equal to the radius were cut from each end of the specimen and discarded. This insured that the remaining sample would have a concentration gradient as uniform as possible from end to end. Layers of equal weight were machined from the remainder of the sample; each layer was analyzed for oxygen by the vacuum-fusion method. Diffusion coefficients were then determined by the graphical method, using the average oxygen concentrations of the layers, the average radii, and the time. The thin surface layer, which contains alpha and oxide phases, was not used in the calculations.

Moving-Boundary Technique

The diffusion coefficients of oxygen in the alpha phase of Zircaloy 2 (and Zircaloy 3) were determined by the moving-boundary technique described by Jost(B-5)*. This method was developed by Wagner for the case of diffusion into a heterogeneous system of given over-all concentration. The mathematical treatment of this case is based on the fact that a displacement, ξ , of the phase boundary produced by the diffusion of a single species is proportional to the square root of the time of diffusion, i. e.,

$$\xi = 2\gamma\sqrt{Dt}, \quad (B-1)$$

where

ξ = displacement of the phase boundary, cm

γ = a dimensionless parameter characteristic of the system

D = diffusion coefficient, cm^2/sec

t = time, sec.

The parameter, γ , is defined as follows:

$$\frac{C_s - C_{II, I}}{C_{II, I} - C_o} = \sqrt{\pi}\gamma \exp\gamma^2 \operatorname{erf}\gamma, \quad (B-2)$$

*Jost presents the solution of Fick's law for movement of a boundary in a plate. Brief calculations showed that for small displacements of the boundary in a cylinder, the equations for plates could be used in calculating diffusion coefficients without introducing significant errors.

where C_S , $C_{II, I}$, and C_O are concentrations of the diffusing species at various phase boundaries. In the present case, for a given temperature, C_S is the maximum solubility of oxygen in the alpha phase, $C_{II, I}$ is the oxygen concentration at the alpha plus beta-alpha boundary, and C_O is the oxygen concentration at the beta-alpha plus beta boundary. The term $\text{erf } \gamma$ is the "gaussian error function". Values of $\text{erf } \gamma$ may be found in Jost^(B-7) and Carlslaw and Jaeger^(B-8). The value for γ was determined from Equation B-2 by a graphical method.

To determine the value of the diffusion coefficient, it is necessary to have values of ξ , t , and γ at a given temperature. The slope of the plot of ξ versus $t^{1/2}$ is equal to $2\gamma\sqrt{D}$, from which D may be evaluated.

Experimental techniques used to obtain the moving-boundary measurements are as follows. A cylindrical specimen about 1 cm in diameter by 4 cm long was prepared as described above for the gradient method. A calculated quantity of oxygen, C_O , was then added to the sample in order to saturate completely the beta phase at the experimental temperature. This sample was heated at temperature for 6 to 8 hr to distribute the oxygen uniformly throughout the sample. To check the uniformity of the distribution, a cross section was examined metallographically. The sample was then cut into three cylinders.

Each cylinder was heated in an oxygen atmosphere at temperature for various periods of time. A calculated quantity of oxygen was reacted to maintain an oxide film at all times but to keep its thickness at a minimum. At the end of the heating period, the sample was quenched as rapidly as possible to room temperature and cut in half diametrically. The cross section was examined metallographically to determine the movement of the alpha-beta boundary. The diameter of the beta core was measured and subtracted from the original diameter of the cylinder. From this, the displacement of the boundary was determined. Then, the diffusion coefficient was determined from the slope of a plot of the displacement, ξ , against $t^{1/2}$.

Results and Discussion

The diffusion coefficients for oxygen in alpha and beta Zircaloy 2 were determined in the range 1000 to 1500 C at 100 C intervals. Attempts were made to obtain coefficients at 1600 C; however, no suitable gradients or moving boundaries could be prepared. The experimental times (less than 5 minutes) necessary to prepare optimum diffusion samples were so short that errors in the measurement of the time required to quench to room temperature introduced large errors in the estimation of actual diffusion times. The data obtained on a gradient prepared in beta Zircaloy 2 at 1400 C for 5 min is shown in Figure B-2. The thicknesses of the layers machined from the cylinder and the average oxygen concentration of each

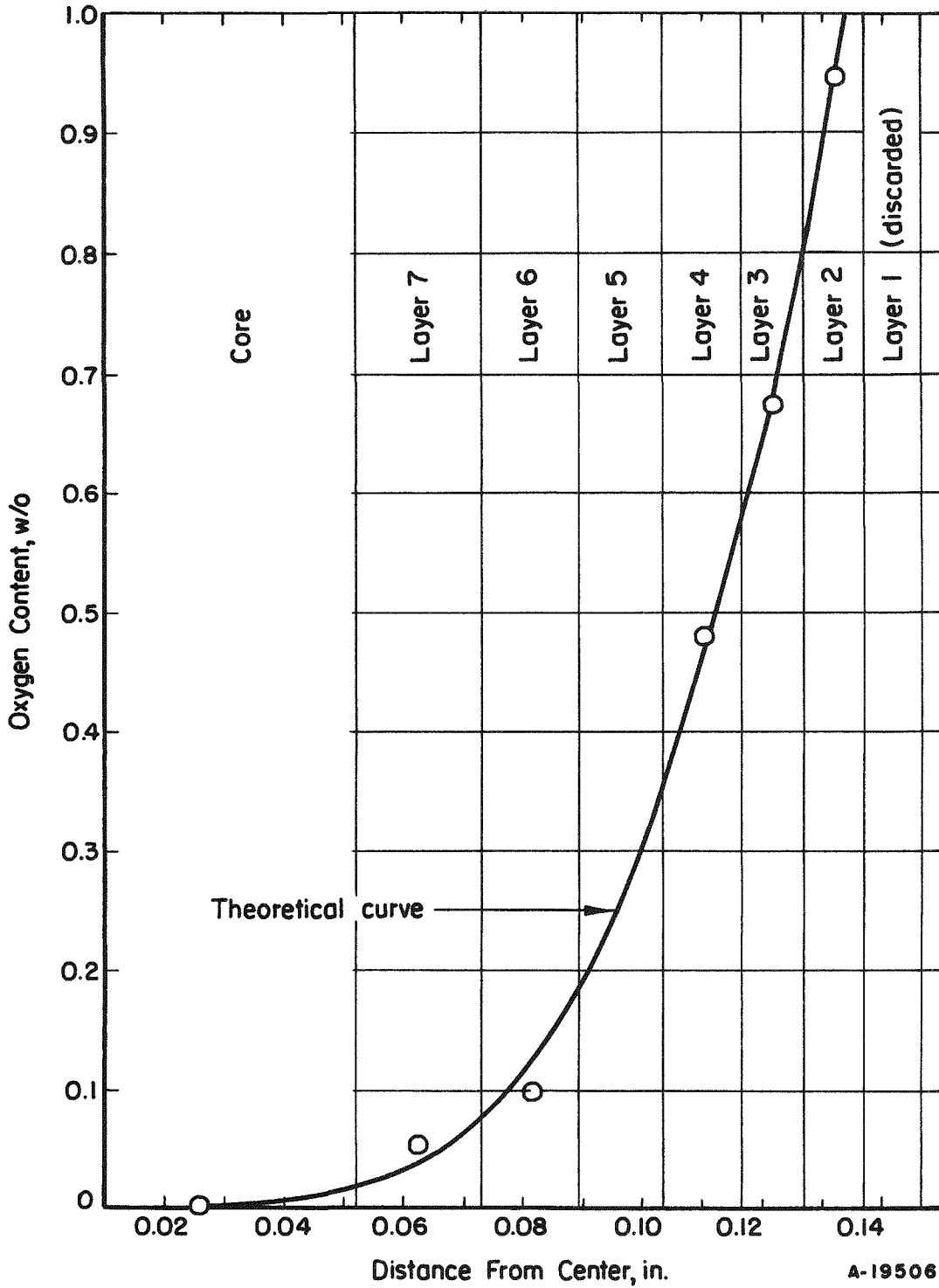


FIGURE B-2. OXYGEN CONCENTRATION GRADIENT PREPARED IN BETA ZIRCALOY 2 AT 1400 C FOR 5 MIN

layer are shown. Layer 5 was lost in analysis and no value was obtained. The solid line is the theoretical curve derived from diffusion theory (B-5) for this gradient. It is seen that there is good agreement between the experimentally determined concentrations and the theoretical curve. In Figure B-3 is shown a typical plot of the alpha-beta boundary displacement, ξ , against $t^{1/2}$ for alpha Zircaloy 2 at 1200 C. The slope of the line is equal to $2\gamma\sqrt{D_\alpha}$. At 1200 C, the value of γ is 0.895. From these values the diffusion coefficient was calculated. All the data are given in Table B-2. The diffusion coefficients for oxygen in alpha Zircaloy 2 range from 1.8×10^{-8} cm² per sec at 1000 C to 1.7×10^{-6} cm² per sec at 1500 C. Those for oxygen in beta Zircaloy 2 range from 8.2×10^{-7} cm² per sec at 1000 C to 2.4×10^{-5} cm² per sec at 1500 C.

In Figures B-4 and B-5 are shown the variations of the diffusion coefficients with temperature for alpha Zircaloy 2 and beta Zircaloy 2, respectively. The logarithms of the diffusion coefficients are plotted against the reciprocal of temperature (Arrhenius-type plot). Equations for the best straight lines through the points were determined by the method of least squares. The equation for the diffusion coefficient, D_α , in cm² per sec, for oxygen in alpha Zircaloy 2 is:

$$D_\alpha = 0.196 \exp [(41,000 \pm 1500)/RT]. \quad (B-3)$$

For oxygen in beta Zircaloy 2,

$$D_\beta = 0.0453 \exp [(28,200 \pm 2400)/RT]. \quad (B-4)$$

The diffusion coefficients for oxygen in alpha and beta Zircaloy 3 were determined at 1100 and 1400 C. The values also are given in Table B-2 and plotted in Figures B-4 and B-5. It is seen that they are in good agreement with those for Zircaloy 2. Apparently, the alloying constituents in the range studied have very little effect on the diffusion of oxygen.

The diffusion coefficients for oxygen in beta Zircaloy 2 and Zircaloy 3 are greater (about 10 times) than those for nitrogen in high-purity beta zirconium (B-2). This difference probably arises from the differences in the size of the diffusing species, oxygen and nitrogen, and not from differences in the alloying constituents. The atomic radius of oxygen is 0.60 Å and that of nitrogen is 0.71 Å. Since oxygen is the smaller atom, it would be expected to diffuse faster.

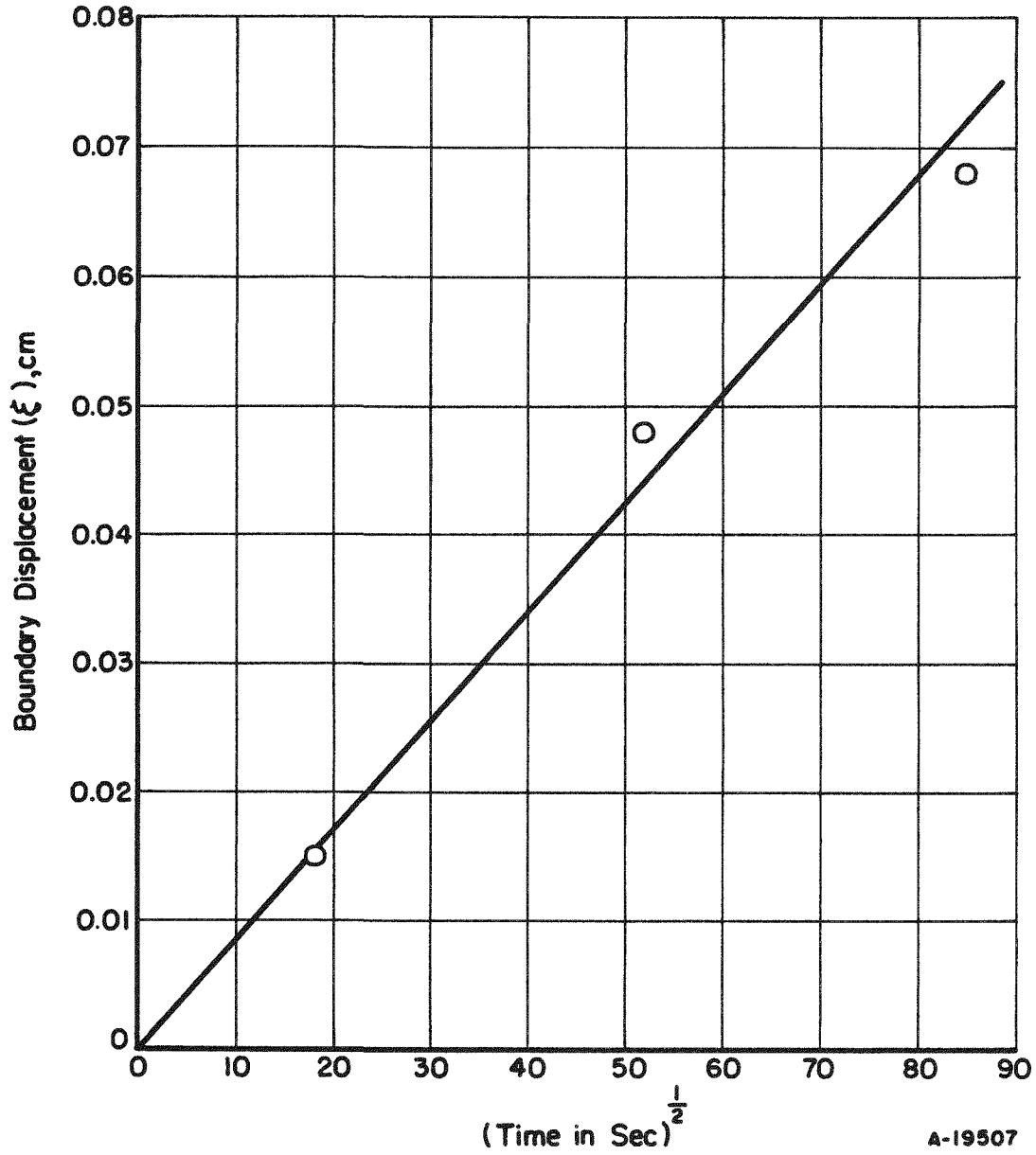


FIGURE B-3. VARIATION OF DISPLACEMENT OF ALPHA-BETA BOUNDARY WITH TIME FOR OXYGEN IN ALPHA ZIRCALOY 2 AT 1200 C

TABLE B-2. DIFFUSION COEFFICIENTS FOR OXYGEN IN
ALPHA AND BETA ZIRCALOY 2 AND ZIRCALOY 3

Material	Diffusion Coefficient, cm ² per sec, at Temperature Indicated					
	1000 C	1100 C	1200 C	1300 C	1400 C	1500 C
Zircaloy 2, alpha	1.8×10^{-8}	4.8×10^{-8}	2.3×10^{-7}	3.6×10^{-7}	7.9×10^{-7}	1.7×10^{-6}
Zircaloy 2, beta	8.2×10^{-7}	1.4×10^{-6}	2.4×10^{-6}	3.8×10^{-6}	8.1×10^{-6}	2.4×10^{-5}
Zircaloy 3, alpha	--	5.8×10^{-8}	--	--	1.4×10^{-6}	--
Zircaloy 3, beta	--	1.4×10^{-6}	--	--	6.5×10^{-6}	--

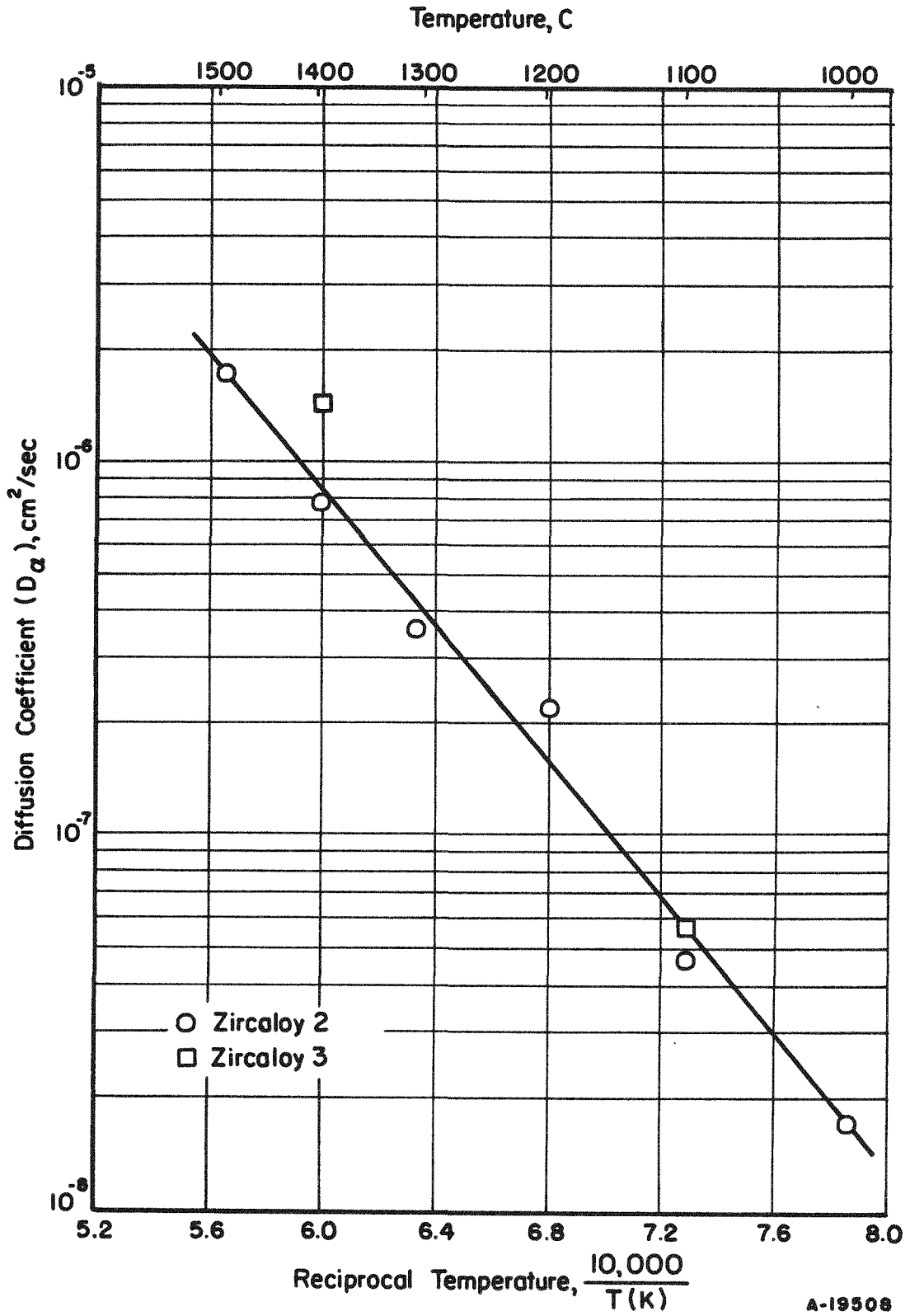
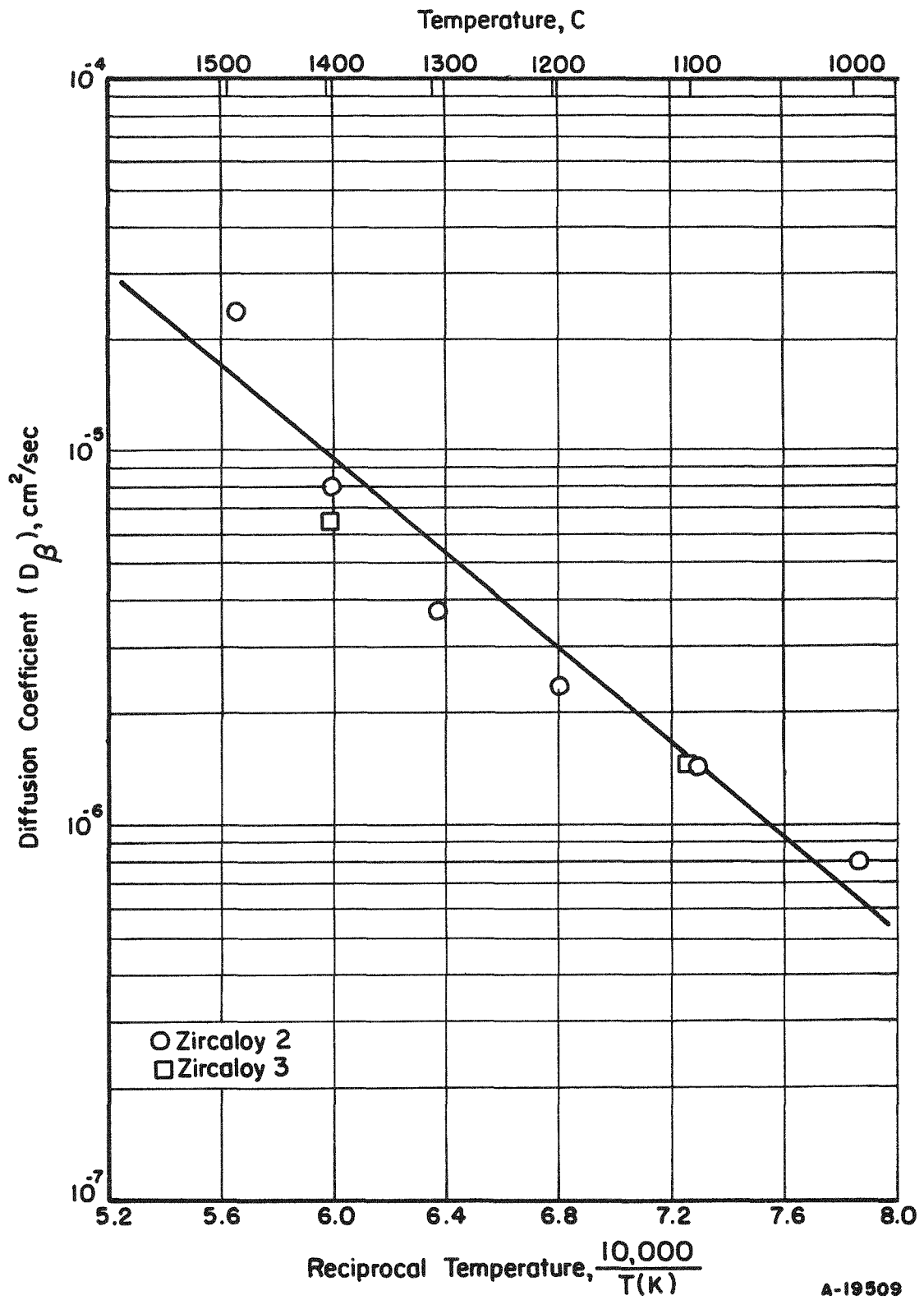


FIGURE B-4. TEMPERATURE VARIATION OF THE DIFFUSION COEFFICIENT FOR OXYGEN IN ALPHA ZIRCALOY 2 AND ZIRCALOY 3



A-19509

FIGURE B-5. TEMPERATURE VARIATION OF THE DIFFUSION COEFFICIENT FOR OXYGEN IN BETA ZIRCALOY 2 AND ZIRCALOY 3

References

- (B-1) Lustman, B., "Zirconium-Water Reactions", WAPD-137, Westinghouse Electric Corporation, Atomic Power Division, Pittsburgh, Pennsylvania (December 1, 1955).
- (B-2) Mallett, M. W., Belle, J., and Cleland, B. B., J. Electrochem. Soc. 101, 1 (1954).
- (B-3) Hoge, H. J., J. Research Natl. Bur. Standards, 44, 321 (1950).
- (B-4) Domagala, R. F., and McPherson, D. J., Trans. Am. Inst. Mining Met. Engrs., 200, 238 (1954).
- (B-5) Mallett, M. W., Baroody, E. M., Nelson, H. R., and Papp, C. A., J. Electrochem. Soc., 100, 103 (1953).
- (B-6) Rhines, F. N., Surface Treatment of Metals, American Society for Metals, Cleveland, Ohio (1941), pp 122 ff.
- (B-7) Jost, W., Diffusion, Academic Press, Inc., New York, New York (1952), pp 71 ff.
- (B-8) Carlslaw, H., and Jaeger, J. C., Conduction of Heat in Solids, Oxford University Press, London (1948).

39

SECTION C

MEASUREMENT OF STEAM-ZIRCALOY 2
REACTION RATES

R. C. Crooks, P. G. Hershall, H. A. Sorgenti,
A. W. Lemmon, Jr., and R. B. Filbert, Jr

SECTION C

MEASUREMENT OF STEAM-ZIRCALOY 2
REACTION RATES

R. C. Crooks, P. G. Hershall, H. A. Sorgenti,
A. W. Lemmon, Jr., and R. B. Filbert, Jr.

The reaction between solid Zircaloy 2 and steam at 50 psia was measured over the temperature range 1000 to 1690 C. Several measurements were made on the reaction between molten Zircaloy 2 and steam with initial molten-metal temperatures of about 1900 C and 2050 C.

The observed order of reaction n for reactions below 1690 C varied from about 1.25 to 2.6, with an average value of 1.75, and appeared to be independent of temperature. Reactions for reaction times between 5 sec and 2 hr were best correlated on the basis of a second-order reaction, as

$$v^2 = 0.1132 \times 10^6 e^{\frac{-34,000 \pm 1440}{RT}} t,$$

with v in units of ml hydrogen per cm^2 and t in units of sec.

Photomicrographs of the sectioned Zircaloy samples after reaction with steam showed a dense outer layer of zirconia overlying a layer of alpha solid solution of oxygen in the metal.

The reaction rate between molten Zircaloy 2 and steam does not correlate with initial temperature. The reasons for this are not known. However, as might be expected, the reaction rates of the molten Zircaloy 2 with steam are higher than those which would be predicted from an extrapolation of the reaction-rate correlation of solid Zircaloy 2.

An effort was made to measure the total extent of reaction between molten Zircaloy 2 droplets and hot water. The results indicate that in only a few of the runs were appreciable fractions of the droplets molten when they reached the water surface. For these, reaction levels of 39 to 45 w/o of the zirconium reacted appear possible. This amount of reaction is considerably higher than the 12 w/o which would be predicted by the Aerojet-General tests (C-4). The explanation appears to be the difference in free fall distance. Of importance is the observation that there was no indication of explosion or extreme reactivity (such as to vaporize the Zircaloy 2 and/or cause a complete reaction of the droplet with water to take place).

PART 1. CONVENTIONAL EXPERIMENTS

Introduction

As a part of the program on the prediction of the amount of reaction that may occur between Zircaloy and water, additional measurements were made on the rate of reaction between Zircaloy 2 and steam at temperatures over 1000 C. Bostrom(C-1)* reported measurements of the reaction of Zircaloy 2 at temperatures of 1300, 1450, 1600, and 1750 C and immersed in water at a pressure near atmospheric by observing the volume of hydrogen formed. Hayes and co-workers(C-2, C-3) measured the weight increases on specimens of pure zirconium exposed to steam for 1 and 24 hr at temperatures between 450 and 1000 C.

In this present investigation, rates of reaction between Zircaloy 2 and steam at 50 psia were measured at temperatures from 1000 C to about 2050 C (approximately 200 C above the melting point of Zircaloy 2). Steam at 50-psia pressure was used in these experiments.

In this work, the reaction between Zircaloy 2 and steam was measured by determination of gas (hydrogen) evolution as indicated in the reaction



In some experiments, the reactions were measured by the weight increases of the specimens or by vacuum-fusion analysis of the specimens.

Photomicrographs of the Zircaloy 2 specimens used in the reaction-rate experiments were taken to show the results of the reaction of steam with Zircaloy 2 at high temperatures.

Experimental Methods

The Zircaloy 2 specimens were heated by electrical induction and reacted with flowing steam at a pressure of 50 psia. Hydrogen formed as a product of the steam-Zircaloy reaction was separated from the steam by passing the mixture through a water-cooled condenser. The resultant hydrogen was measured by displacement of water in a 1-liter burette or by passing through a wet-test gas meter. Temperatures were measured with platinum-type thermocouples for temperatures below 1700 C, and with an optical pyrometer for temperatures above 1700 C.

*References at end of Section C.

The specimens were mounted inside a Vycor tube and protected by argon cover gas during the initial heating period. Steam flow rates were measured by a rotameter and were adjusted to provide a large excess of the steam reactant.

For the reaction between solid Zircaloy 2 and steam, the specimen was 2 in. in length by 0.5 in. in diameter with a hole drilled along the axis in one end for a thermocouple well. The Zircaloy specimen rested upon a vertical thermocouple protection tube.

For the reaction between liquid Zircaloy 2 and steam, the sample was contained in a graphite cup which rested on a graphite rod inserted into the bottom section of the cup. Steam was introduced for timed periods through a 7-mm Vycor tube which directed a jet of steam on the surface of the molten Zircaloy. The extent of reaction was determined by vacuum-fusion analysis of the specimen for oxygen.

Reactions of Zircaloy at temperatures up to 1600 C for periods between 5 sec and 2 min were determined by measurement of the weight gains or the oxygen contents of the reacted specimens.

Materials

Billets of Zircaloy 2 supplied by the Westinghouse Atomic Power Division were used for the preparation of samples. Material from the billets was forged and rolled to form rods about 5/8 in. in diameter. From these rods, samples were machined to the form shown in Figure C-1, and the surface was smoothed to a uniform finish with No. 600 alumina abrasive.

Graphite containers to hold molten Zircaloy were made of AGX graphite (National Carbon Company) as shown in Figure C-2. Samples for the liquid Zircaloy 2 experiments were machined from cold-rolled bars to small rods having a length of 0.5 in. and a diameter of 0.5 in.

Steam for the reaction experiments was taken from the 60-psig service steam lines. Spot checks showed that the air and other noncondensable gas impurities in the steam amounted to less than 0.01 per cent by volume.

Equipment

The arrangement of equipment and method used to measure the reaction between Zircaloy 2 and 50-psia steam are illustrated in Figure C-3. The specimen was supported on a thermocouple protection tube and enclosed inside a Vycor tube; it was inductively heated to the reaction temperature by power applied through the induction coil. During the initial heating period, the Zircaloy sample was protected by a small flow of argon cover

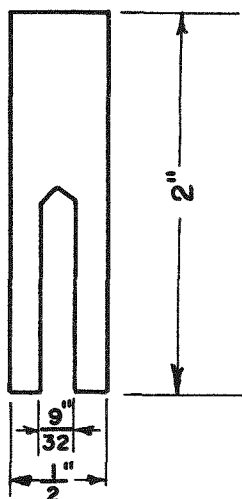


FIGURE C-1. ZIRCALOY 2 SPECIMEN

Transverse Section

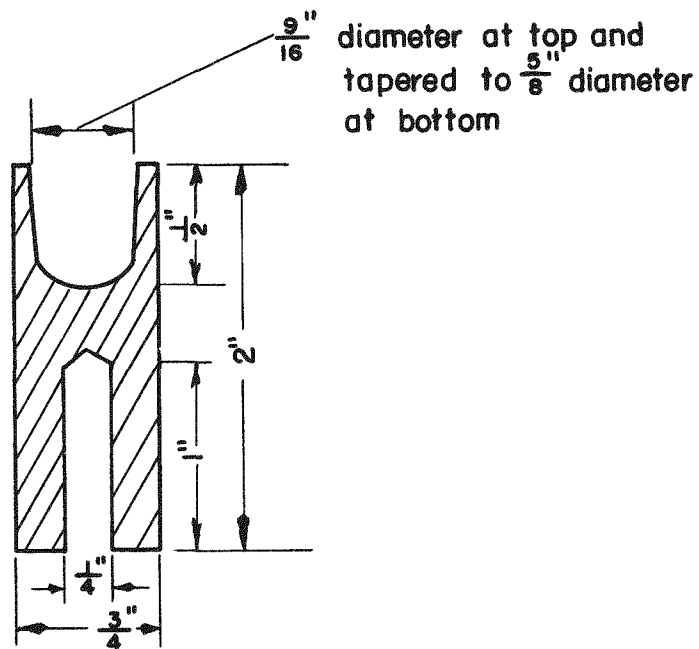


FIGURE C-2. GRAPHITE CRUCIBLE FOR MOLTEN ZIRCALOY 2 SPECIMEN

Transverse Section

44

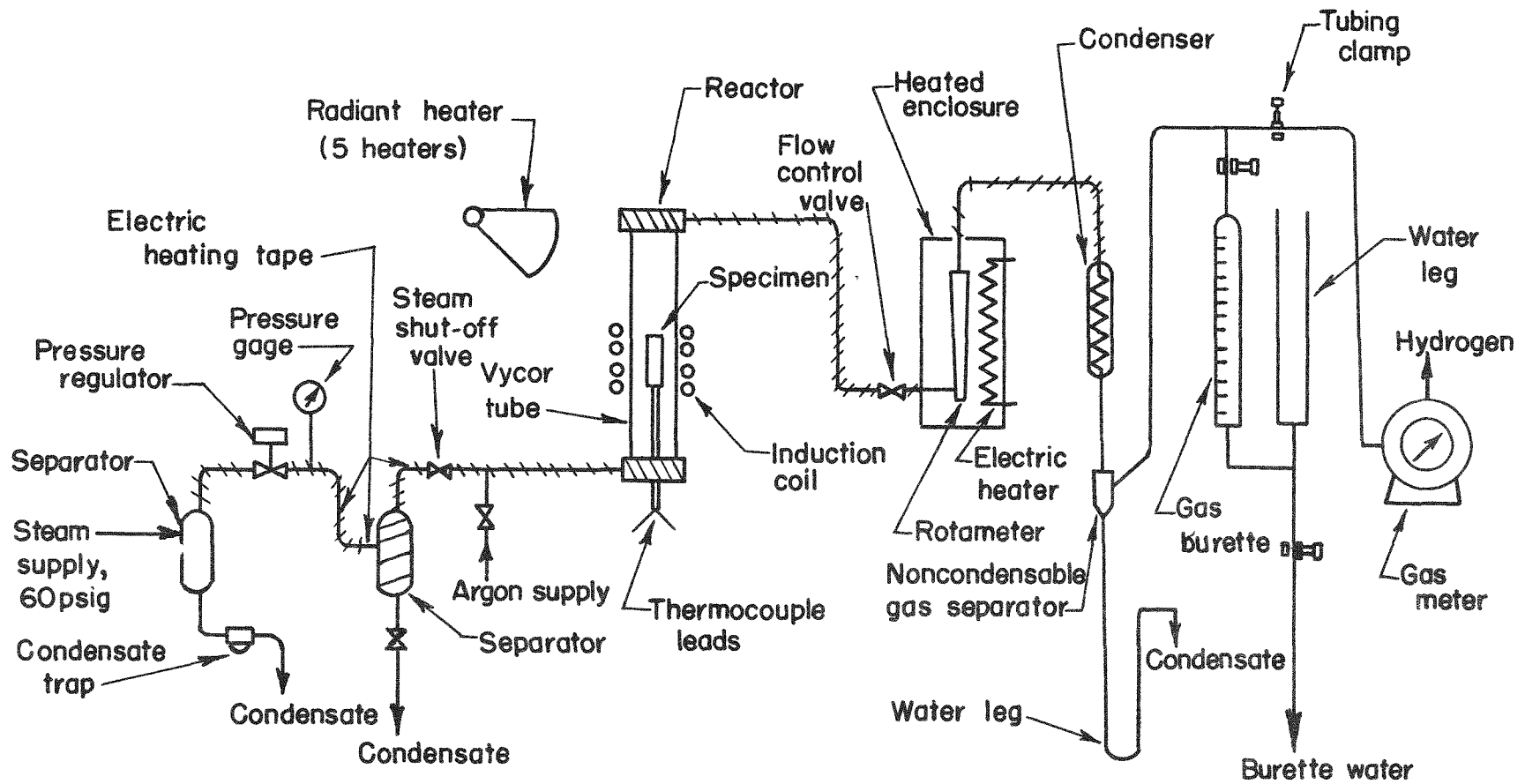


FIGURE C-3. DIAGRAM OF EQUIPMENT USED TO MEASURE RATES OF REACTION BETWEEN ZIRCALOY 2 AND STEAM AT 50 PSIA

gas. Steam for the reaction was passed through condensate separators and electrically heated copper tubing lines to ensure condensate-free steam; the steam pressure was controlled by a Mason-Neilan pressure regulator.

All lines and apparatus between the first steam separator and the water-cooled condenser were electrically heated to maintain the equipment above the condensing temperature of 50-psia steam (139 C). Copper tubing, valves, the end pieces of the reactor unit, and the second steam separator were warmed by electrically heated tapes. Chromel-Alumel thermocouples at several locations were used to measure the equipment temperatures, and temperatures were adjusted to about 150 C by regulation of the power-supply voltage. The rotameter was in an electrically heated enclosure in which the temperature was maintained above the saturation temperature. Heat to prevent condensation was supplied to the reactor unit by five 375-w heater lamps.

The reactor unit consisted of a Vycor tube, 1.5 in. in diameter and 11 in. long, closed with steel endpieces sealed by lead gaskets. Each endpiece was drilled and tapped to receive copper-tubing connectors and to provide passages to the Vycor tube section. A thermocouple protection tube, with closed end, passed through the bottom endpiece and was cemented in a drilled 3/8-in. pipe plug. The reactor assembly was mounted between parallel strips in a supporting frame and tightened by a clamp screw located in the upper part of the frame. The Zircaloy sample was supported on the end of the thermocouple protection tube, which passed into the thermocouple well in the sample. Thermocouples of platinum-platinum 10 w/o rhodium or platinum 6 w/o rhodium-platinum 30 w/o rhodium were inserted in the protection tube for measurement of the sample temperature. The thermocouple head was located near the geometric center of the specimen.

Steam flow rates were adjusted by the flow control valve and measured by a calibrated rotameter. The water-cooled condenser separated the steam from the hydrogen evolved by the Zircaloy-steam reaction, and condensate was removed through a water leg. Hydrogen gas from the reaction was measured by collecting it in the 1-liter burette or, for the faster reactions, by passing it through the gas meter.

For the experiments on the reaction between molten Zircaloy and steam, the graphite crucible (Figure C-2) was supported on a carbon rod which was mounted in the lower endpiece of the reactor assembly. The steam inlet line was connected to the top endpiece of the reactor assembly, and the steam outlet line to the lower endpiece. A Vycor tube, 7 mm in diameter, introduced the steam as a jet which impinged upon the surface of the molten Zircaloy.

Procedure for Measuring Reaction Rates Between Solid Zircaloy 2 and Steam

The Zircaloy 2 samples were cleaned by washing them successively with carbon tetrachloride, benzene, and acetone. With a sample in position in the reactor unit, the system was purged with argon and heated to about 150 C by the electric heater tapes and radiant heaters. The flow control valve was adjusted to allow a predetermined flow of argon gas at 50 psia. Then, the argon gas volume "blank" was obtained by displacing argon gas with steam at 50 psia while the Zircaloy sample was at a low (ca. 200 C) temperature. After the argon "blank" was measured, the steam was purged by argon and the sample heated to the desired reaction temperature, in an argon atmosphere, by induction heat.

With the sample at reaction temperature, steam was passed through the reactor and the hydrogen gas from the reaction was measured at definite time intervals. The argon "blank" described above was used to correct the measured gas volumes for the argon present in the system at the start of the reaction. Slight corrections were applied also for the volume of non-condensable gases present in the steam supply.

The passage of steam through the reactor greatly increased the heat losses from the samples, and a large increase in power to the induction coil was required. Sample temperatures dropped as much as 100 or 200 C below the desired temperature before the power adjustment was effective. This sometimes took as long as 5 min.

With the reaction times of less than about 2 min, it was difficult to measure accurately the volume of hydrogen produced by the Zircaloy-steam reaction. Accordingly, several runs were made in which the extent of reaction was measured by weight increase of the specimen and, in some cases, by vacuum-fusion analysis of the Zircaloy specimen for oxygen. In these runs, steam was introduced into the reactor for measured periods of 5 sec to 2 min, after which the reactor was rapidly purged with a flow of argon.

Procedure for Measuring Reaction Rates Between Molten Zircaloy 2 and Steam

A Zircaloy 2 slug shaped to fit approximately the cup of the graphite crucible (Figure C-2) was placed in the reactor, with the crucible supported by a carbon rod inserted into the bottom of the crucible. Graphite crucibles were baked in a furnace at about 800 C for about 1 hr while packed in carbon to remove traces of oil or other volatile impurities that might have been in the graphite. The Zircaloy specimens were cleaned with carbon tetrachloride, benzene, and acetone, and weighed about 10 g.

At the beginning of each run, after all essential parts of equipment had been heated to about 150 C, the flow control valve was set to allow flow of argon at a pressure of 50 psia. Then, the specimen was heated to the reaction temperature with the induction heater and while argon gas was slowly flowing through the system. The specimen temperatures were measured with the optical pyrometer at the point where the Zircaloy specimen had melted. This reading gave an optical-temperature melting point, and served as a calibration point for the optical temperature-measuring system. The Zircaloy specimen was then further heated to the desired reaction temperature.

With the specimen at the reaction temperature, the system was first brought to 50 psia pressure with argon flow. Then, for the reaction, the argon flow was turned off and at the same time steam at 50 psia allowed to flow into the system. After the steam had flowed into the system for the desired time interval, the steam flow was rapidly shut off, the argon flow simultaneously started in order to displace the steam from the system, and the induction power turned off. Rapid displacement of steam from the reaction tube was accomplished by opening the flow control valve fully and passing argon through the system under atmospheric pressure.

The cooled Zircaloy specimen was subsequently examined for the extent of reaction by vacuum-fusion analysis for oxygen and hydrogen. Prior to sampling for the vacuum-fusion analysis, the specimen was arc melted under a static argon atmosphere to distribute the contained oxygen throughout the sample. Some of the hydrogen may have been lost from the sample during the melting. However, in other work, it had been shown that significant hydrogen loss did not occur in this type of melting with materials containing 50-250 ppm of hydrogen. Since the maximum hydrogen content of these samples is only about 120 ppm, no significant hydrogen loss is expected.

Results and Discussion

Nomenclature and Equations

The units and equations used to describe the results of this work are defined below

A'	constant in the Arrhenius equation
A	reaction area of specimen, cm ²
C	temperature, degrees centigrade
E _A	Arrhenius energy of activation, cal/g-mole
K	absolute temperature, degrees Kelvin
k	reaction rate constant, in units of (STP ml H ₂ /cm ²) ⁿ /min
n	reaction rate order (see equation below)

psia	absolute pressure, lb/sq in.
R	gas constant, 1.987 cal/(g-mole)(K)
T	absolute temperature, degrees Kelvin
t	reaction time, sec
v	extent of reaction by specific hydrogen gas evolution (STP ml H ₂)/(cm ² surface).

The results of this work are organized and compared with the data of other workers upon the basis of the empirical relationship

$$v^n = k t,$$

where the quantity n is hereinafter referred to as the "order of the reaction". The dependence of the reaction rate constant upon temperature is represented by the Arrhenius equation,

$$k = A' e^{\frac{-E_A}{RT}}$$

The reaction area A of the solid Zircaloy 2 specimens (Figure C-1) included the outside area plus one-half the area of the thermocouple well. In the case of the liquid Zircaloy experiments, the reaction area was taken as the projected area of the graphite crucible opening.

Reaction Between Solid Zircaloy 2 and Steam

The results of measurements on the reaction between Zircaloy 2 and steam at temperatures from 1000 C to 1700 C are shown in Figure C-4. Shown also on the same plot are curves taken from Bostrom(C-1). The reaction rates observed in this work agree well with those observed by Bostrom at about 1300 C, but become considerably less than the rates measured by Bostrom at higher temperatures.

The orders of reaction n were taken as the reciprocals of the slopes of the curves in Figure C-4, and are shown plotted against the temperature of reaction in Figure C-5. This figure shows that the calculated values for n indicate no appreciable trend with temperature for the results of this work. Calculated values for n from the data of Bostrom (for Zircaloy 2) and from Hayes and co-workers(C-2) (for zirconium metal) are shown for comparison on the same plot. The average order of reaction for this work is n = 1.75. The over-all average for all values of n shown on the chart is 1.94.

The results of this experimental work are shown also in Figures C-6 and C-7, which present the data as the extent of reaction v plotted as a function of time on the basis of a reaction order of 1.75. As noted in

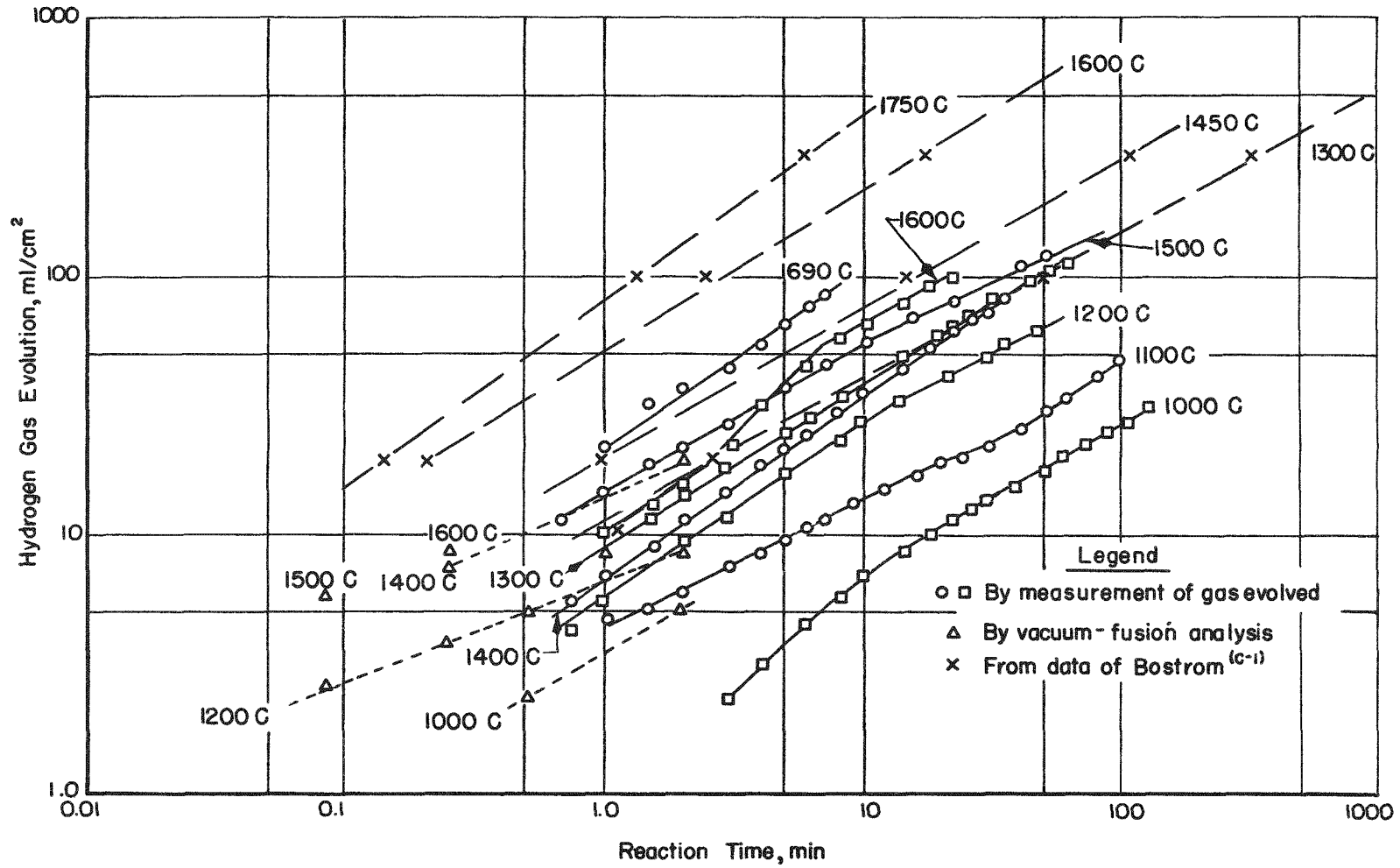


FIGURE C-4. REACTION BETWEEN ZIRCALOY 2 AND STEAM

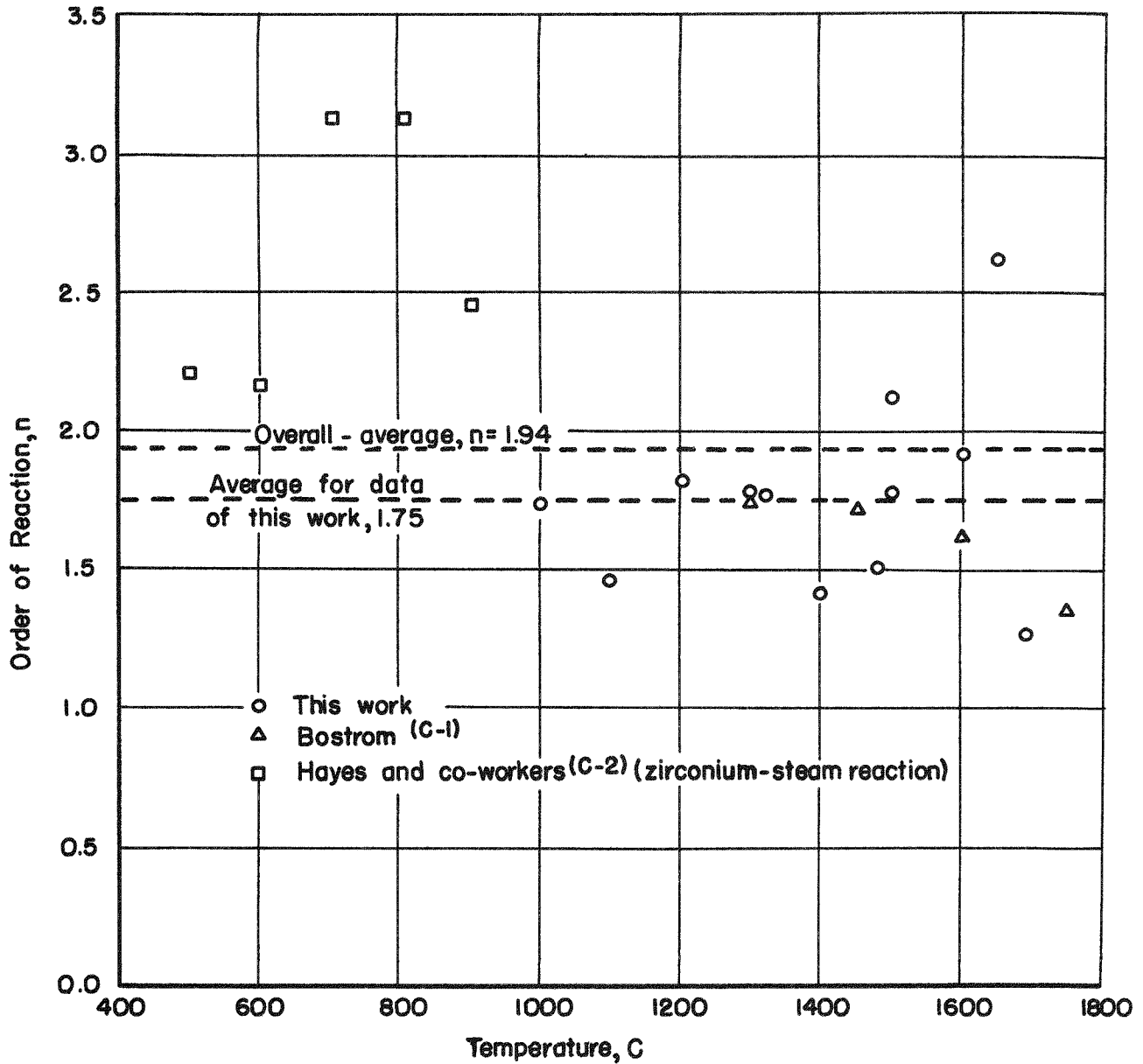


FIGURE C-5. ORDER OF REACTION OF STEAM WITH ZIRCALOY 2 AND ZIRCONIUM METAL

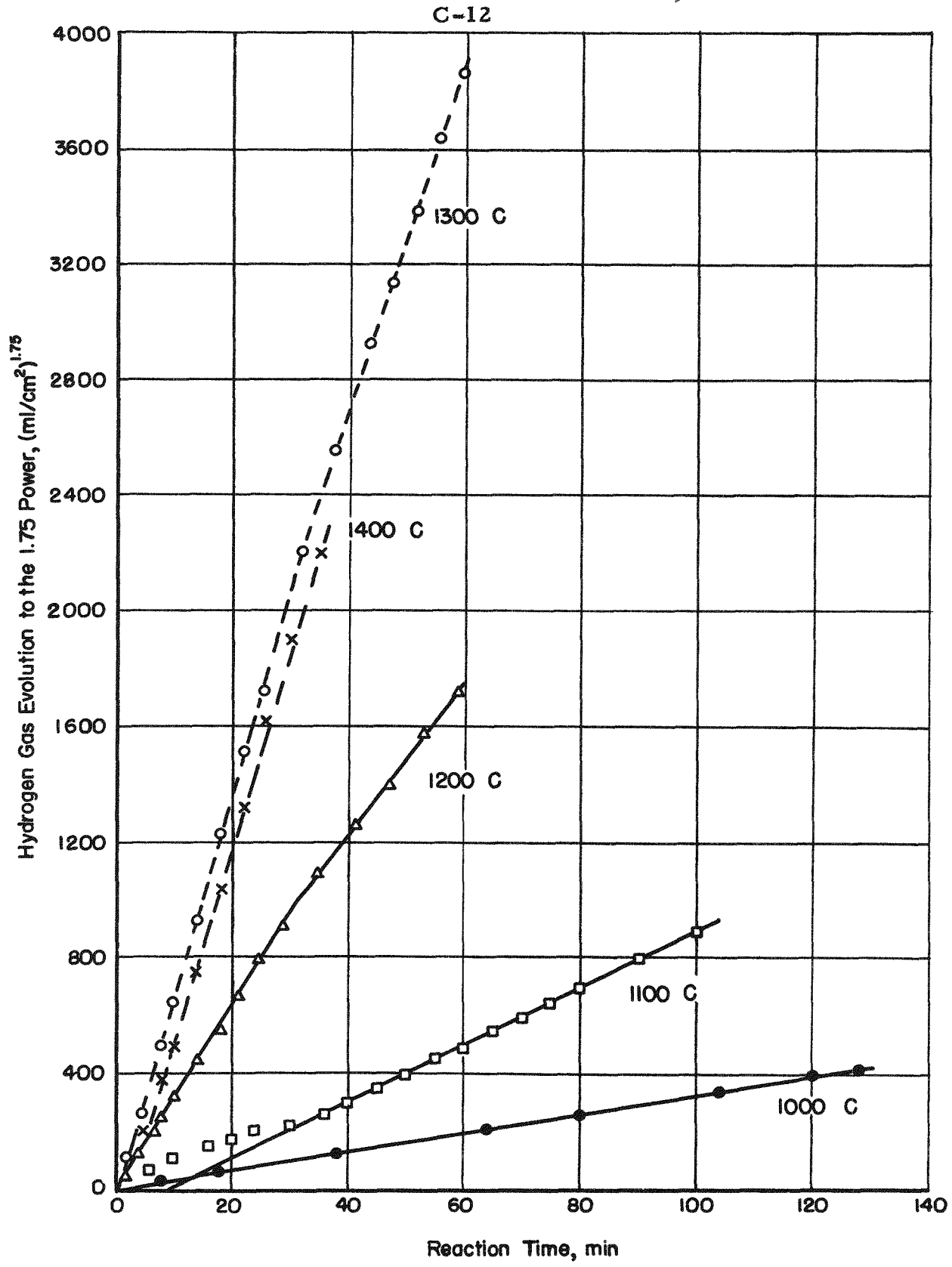


FIGURE C-6. REACTION BETWEEN ZIRCALOY 2 AND STEAM PLOTTED AS A 1.75-ORDER REACTION

1000 to 1400 C

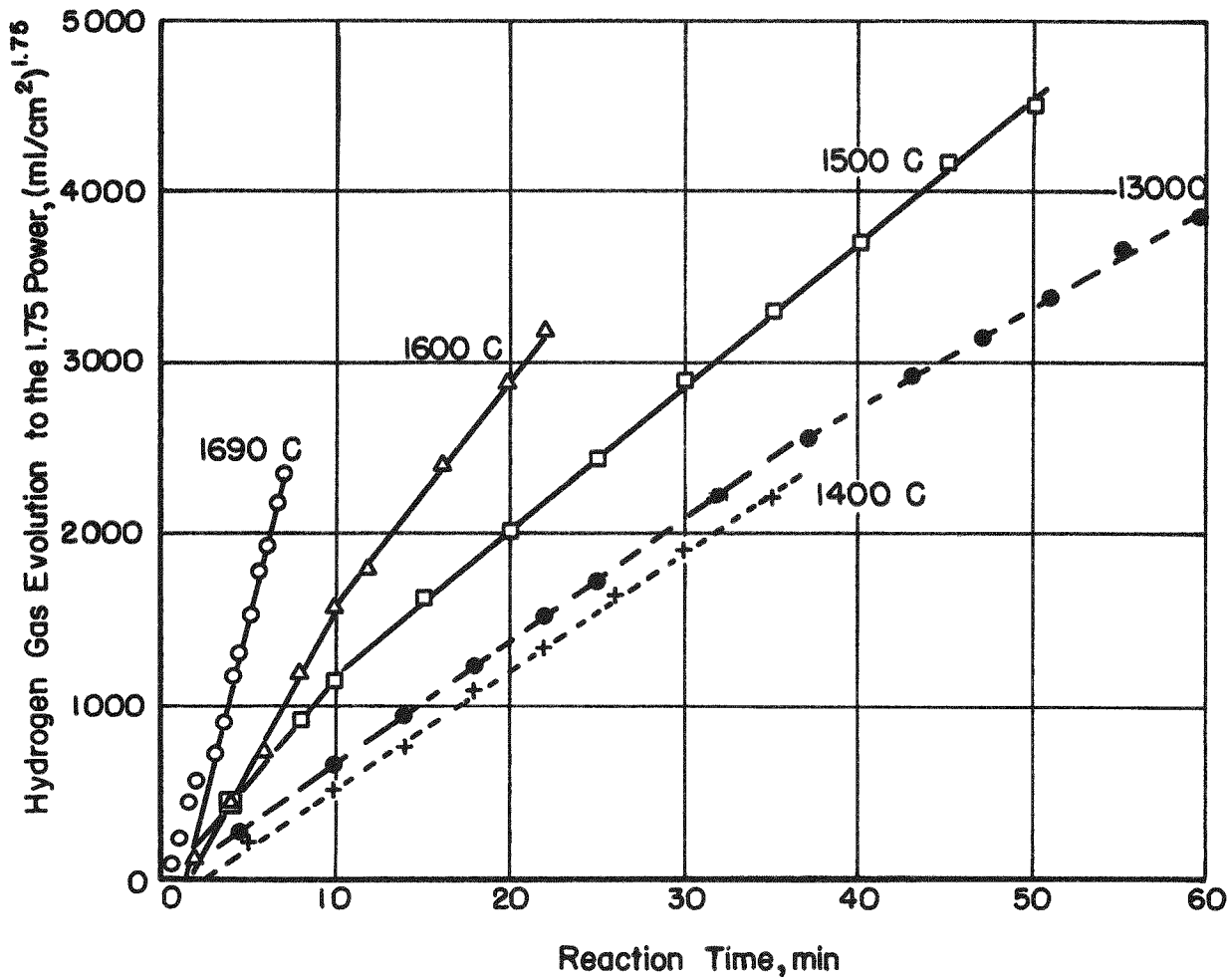


FIGURE C-7. REACTION BETWEEN ZIRCALOY 2 AND STEAM
PLOTTED AS A 1.75-ORDER REACTION

1300 to 1690 C

Figure C-5, an average value of 1.75 was obtained in this work for the order of reaction between Zircaloy 2 and steam. Figure C-8 illustrates how a representative run appears when the data are plotted at various assumed orders of reaction; in this instance, the data appear to be represented best by the reaction order of 2.0.

The experimental data may be represented by the equation

$$v^n = k t ,$$

where n is the order of reaction and k is the reaction velocity constant. The dependence of the reaction velocity constant on the absolute temperature can be represented by the Arrhenius equation,

$$k = A' e^{\frac{-E_A}{RT}} .$$

Plots of the reaction velocity constant k as a function of the reciprocal absolute temperature are shown in Figures C-9, C-10, and C-11 for assumed reaction orders of $n = 1.4$, 1.75 , and 2.0 , respectively. Values of k were obtained from slopes of the reaction curves in which v^n was plotted as a function of t . The k curves at the different reaction orders represent the empirical temperature correlations possible over a range of reaction orders which includes most of the experimental data.

The reaction rate constants for reaction periods between 5 sec and 120 min show best agreement with the 2.0-order correlation. The 1.75-order correlation, based on the average value of n for this experimental work, fairly well represents runs at reaction times longer than 5 min but generally gives low values for k for reaction periods less than 2 min. The 1.4-order correlation still represents well the longer runs but shows a progressive deviation away from the points which represent reaction times less than 2 min.

Empirical correlations for the Zircaloy 2 and steam reaction as a function of temperature are represented by the correlation lines on Figures C-9 and C-11 and expressed analytically as follows:

For 2.0-order reaction (Figure C-11):

$$v^2 = 0.1132 \times 10^6 e^{\frac{-34,000}{RT}} t .$$

For 1.75-order reaction (Figure C-10):

$$v^{1.75} = 0.1482 \times 10^5 e^{\frac{-31,420}{RT}} t .$$

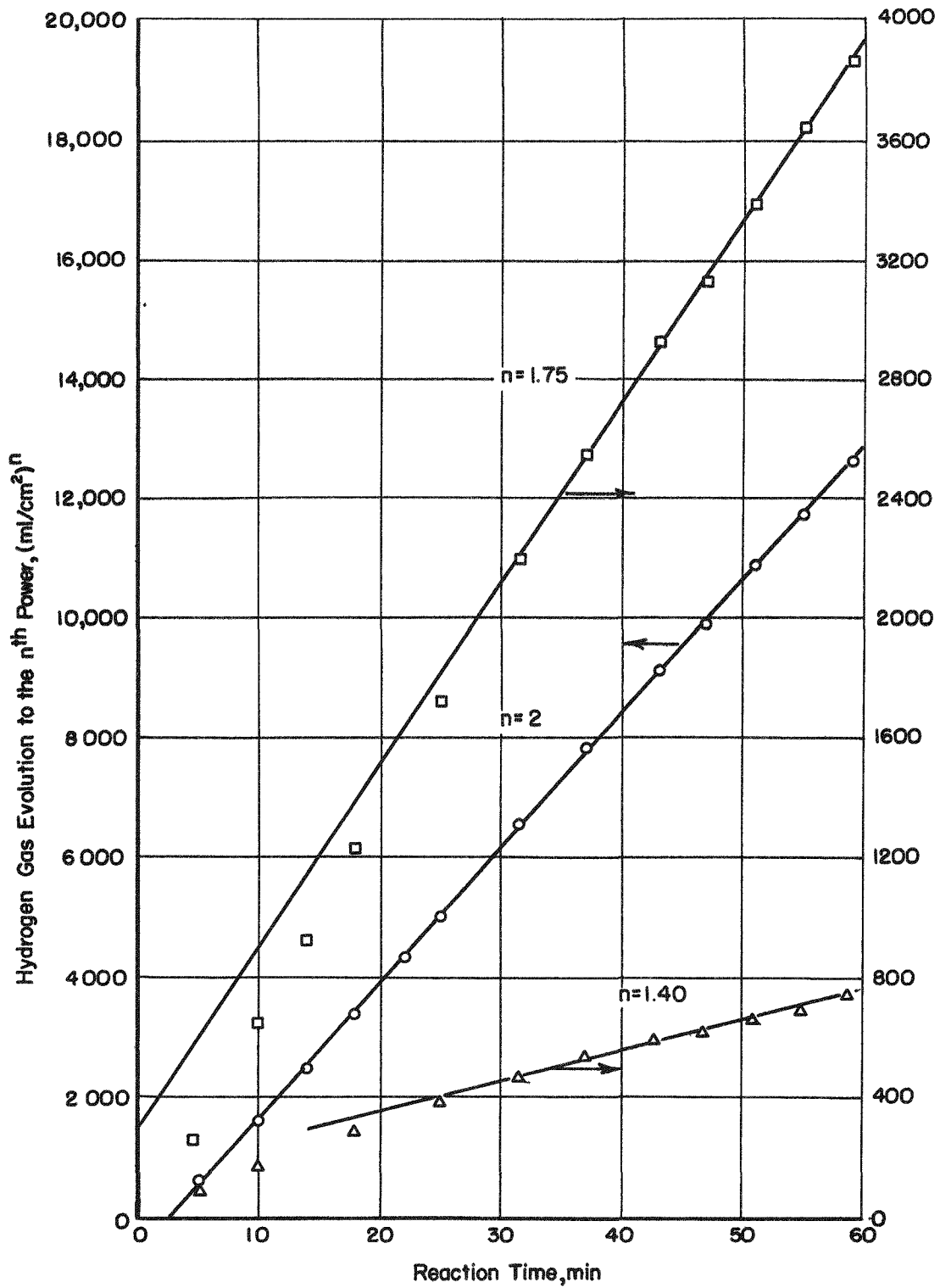


FIGURE C-8. EFFECT OF PLOTTING REACTION DATA AT VARIOUS ASSUMED ORDERS OF REACTION

Run 10, 1300 C.

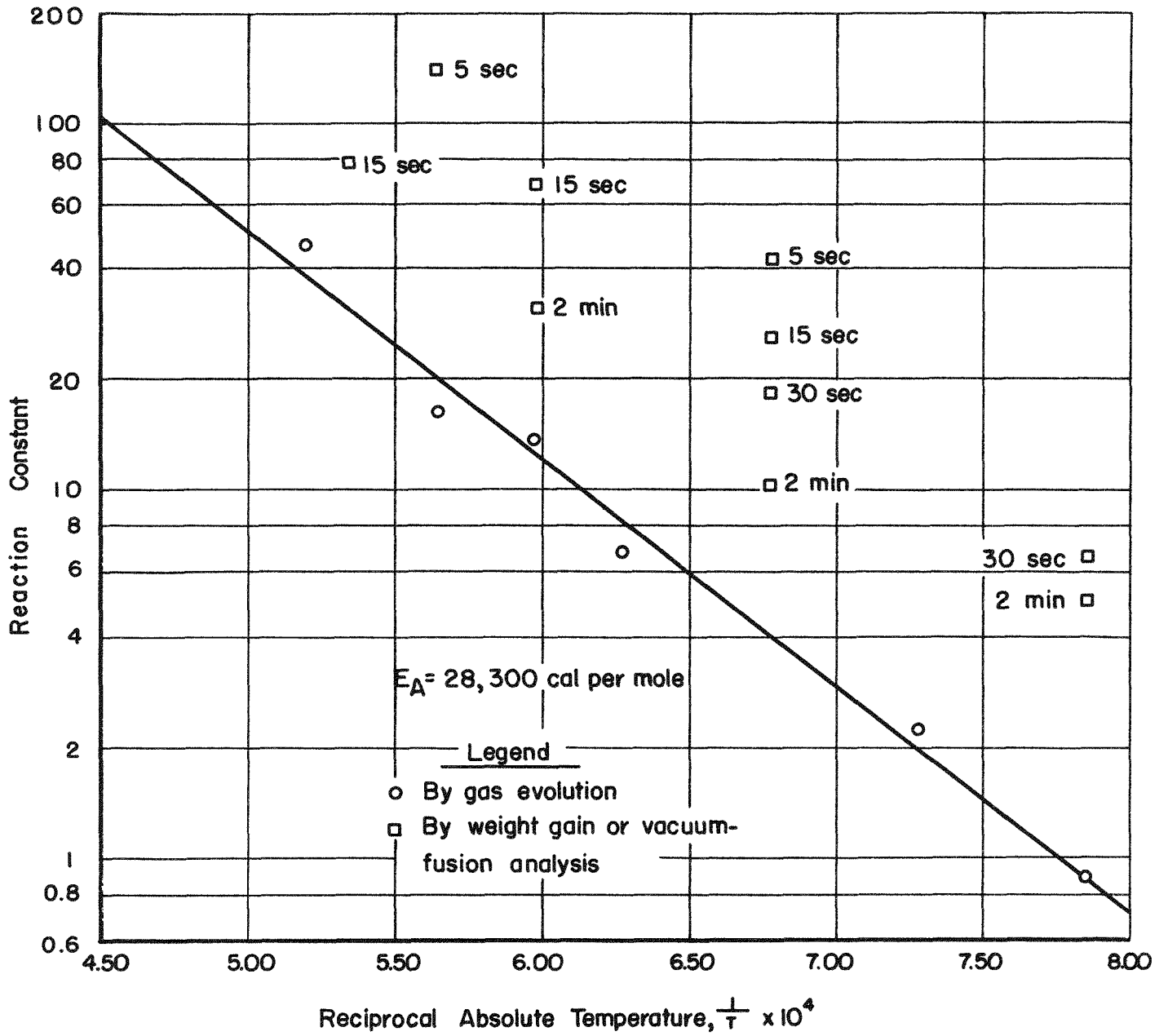


FIGURE C-9. EFFECT OF TEMPERATURE ON THE 1.4-ORDER REACTION RATE CONSTANT

56

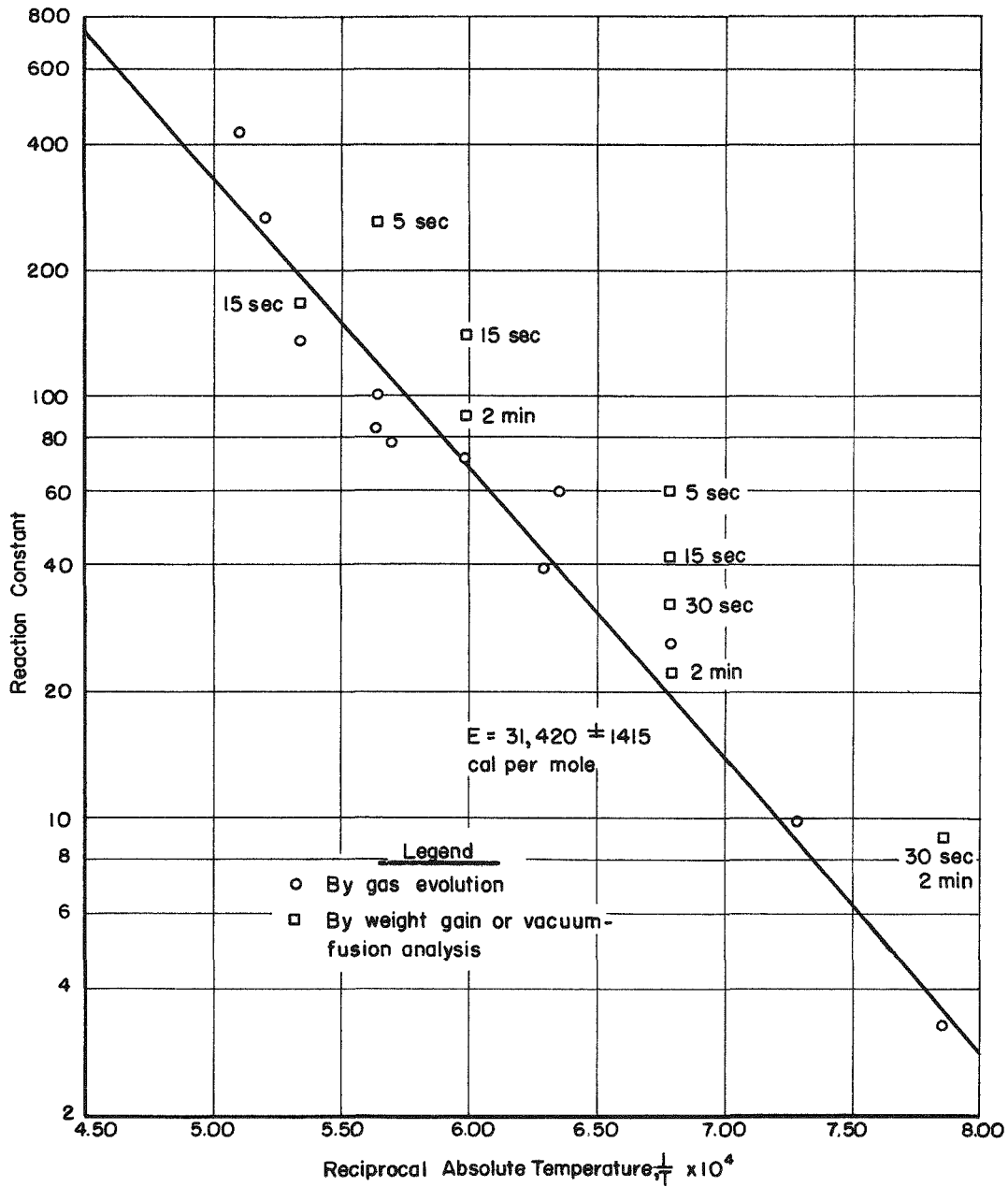


FIGURE C-10. EFFECT OF TEMPERATURE ON THE 1.75-ORDER REACTION RATE CONSTANT

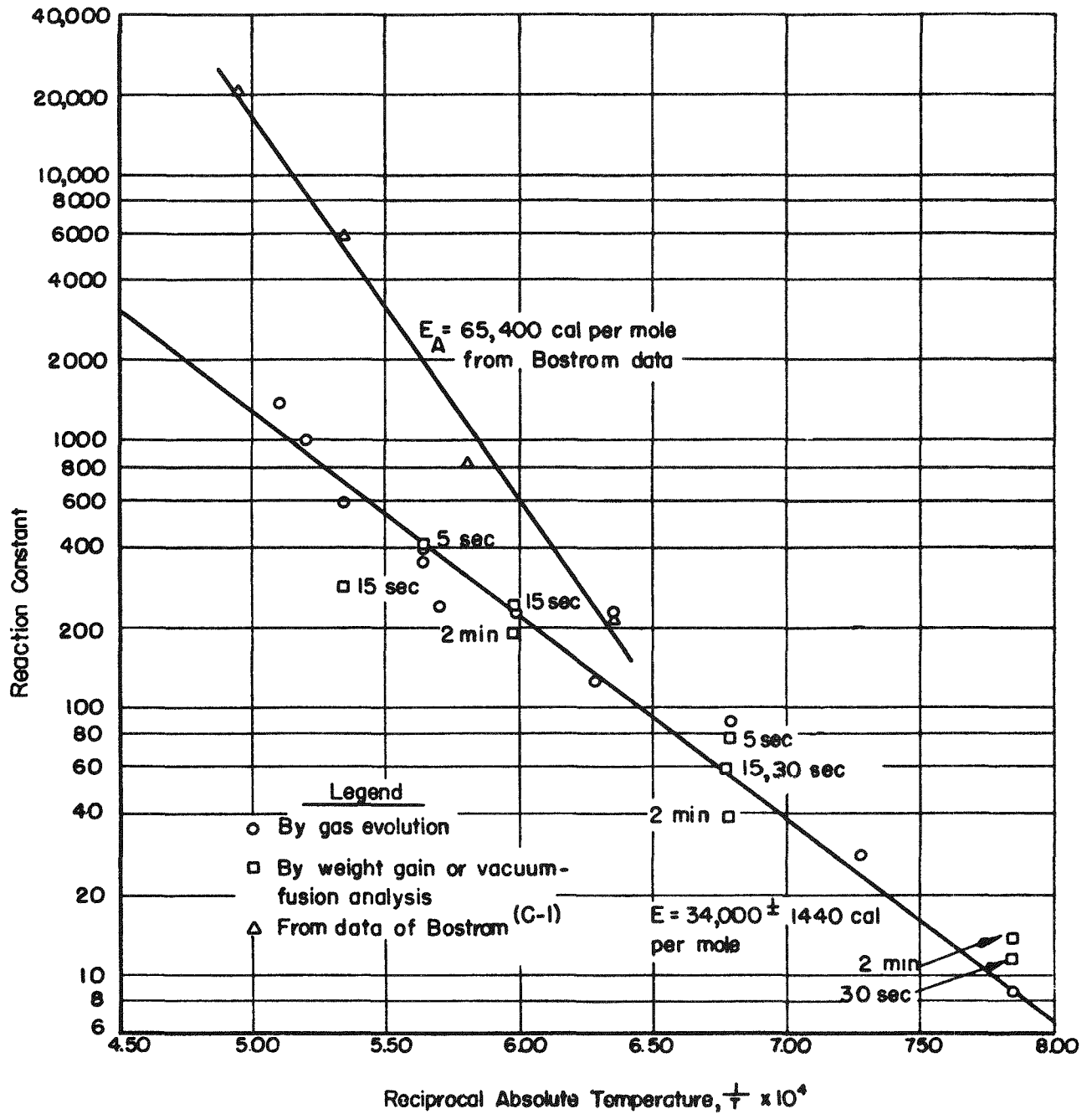


FIGURE C-11. EFFECT OF TEMPERATURE ON THE 2.0-ORDER REACTION RATE CONSTANT

For 1. 4-order reaction (Figure C-9):

$$v^{1.4} = 0.1050 \times 10^4 e^{\frac{-28,300}{RT}} t$$

Reaction rate constants were calculated from the reaction data of Hayes and co-workers^(C-2) and shown on extended k plots (Figures C-12 and C-13) together with the experimental data obtained in this work. Hayes' data are for the reaction between zirconium and steam rather than between Zircaloy 2 and steam, but cover a temperature range between 500 C and 1000 C. The extrapolated k-correlation lines from the Zircaloy 2 data come quite close to the k values for zirconium-steam at about 500 C. At temperatures between 600 and 1000 C, the k values for the zirconium reaction become about one-tenth as large as the k values for Zircaloy 2. Nevertheless, there is agreement to within one order of magnitude for values of k which extend over a range between about 0.001 and 1000.

Pressure appeared to have little, if any, effect on the rate of reaction at steam pressures above atmospheric. The effect of pressure of steam reacting with Zircaloy 2 at 1500 C is shown in Figure C-14. The reaction rate when using 20-psia steam did not differ significantly from the reaction rate resulting from the use of 50-psia steam. The differences between the reactions are probably well within the variations in the experimental data.

Between 4 and 13 per cent of the hydrogen formed in the reaction of steam with Zircaloy 2 is absorbed in the sample. Table C-1 shows the contents of oxygen and hydrogen in Zircaloy 2 after reaction with steam.

TABLE C-1. OXYGEN AND HYDROGEN FOUND IN ZIRCALOY 2
AFTER REACTION WITH 50-PSIA STEAM

Run	Reaction Temp, C	Reaction Time, min	Oxygen Content ^(a) , STP ml O ₂ per cm ² surface	Hydrogen Content ^(a) , STP ml H ₂ per cm ² surface	Theoretical Hydrogen Formed ^(b) , STP ml H ₂ per cm ² surface	Relative Quantity of Hydrogen Found in Sample, per cent
19	1000	2	3.4	0.4	6.8	5.9
8	1000	120	6.0	12.0	--	--
21	1200	2	5.3	0.5	10.6	4.7
9	1200	60	29.	5.3	58.	9.2
22	1400	2	6.9	0.9	13.8	6.5
7	1400	35	30.	6.3	60.	10.5
25	1600	0.08	4.8	1.2	9.6	12.5
16	1600	22	48.	12.	96.	12.5

(a) By vacuum-fusion analysis.

(b) Theoretical hydrogen formed taken as twice the volume of oxygen found.

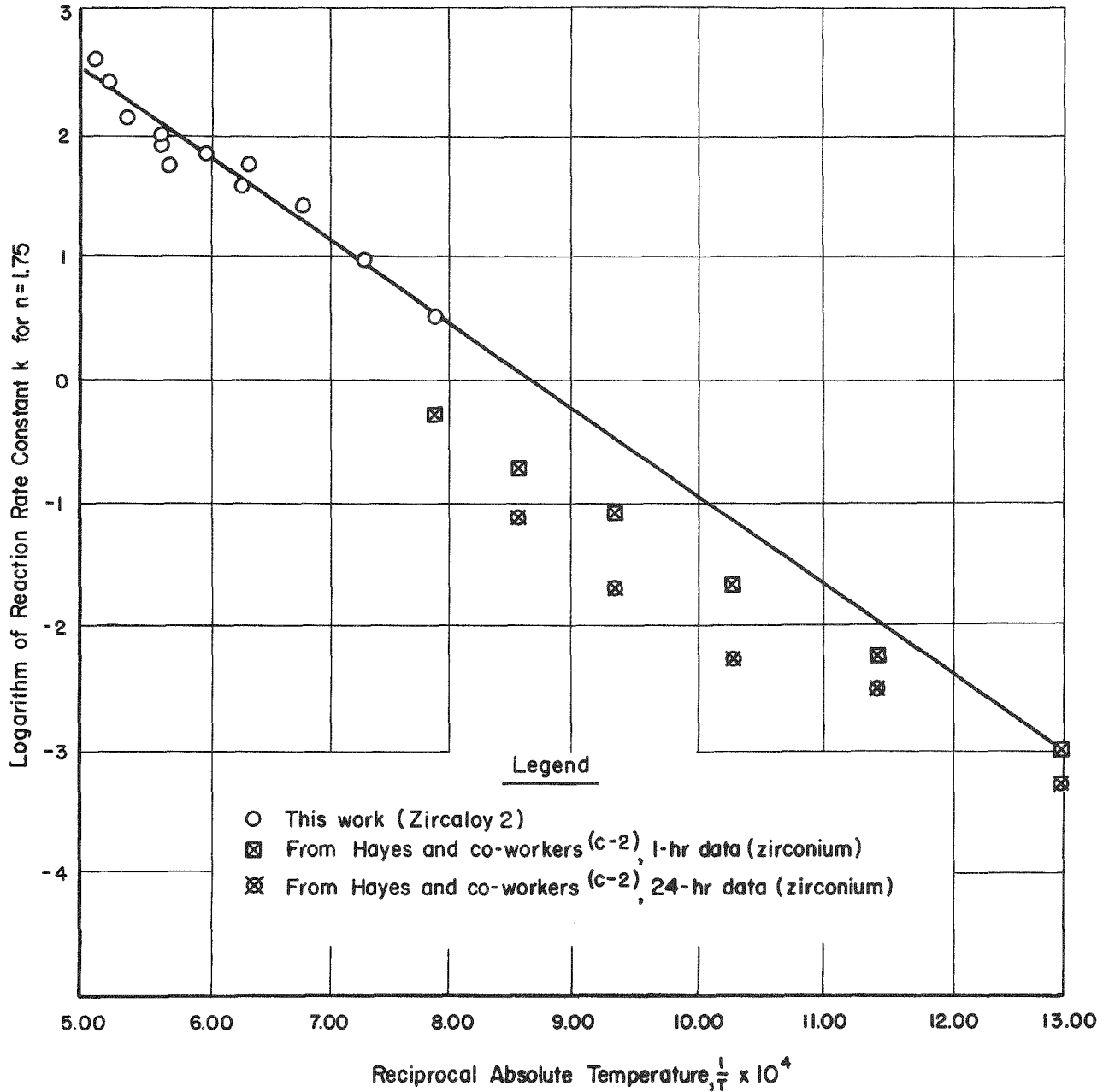


FIGURE C-12. EXTENDED-TEMPERATURE PLOT OF THE 1.75-ORDER REACTION RATE CONSTANT

Reaction of Zircaloy 2 and Zirconium With Steam.

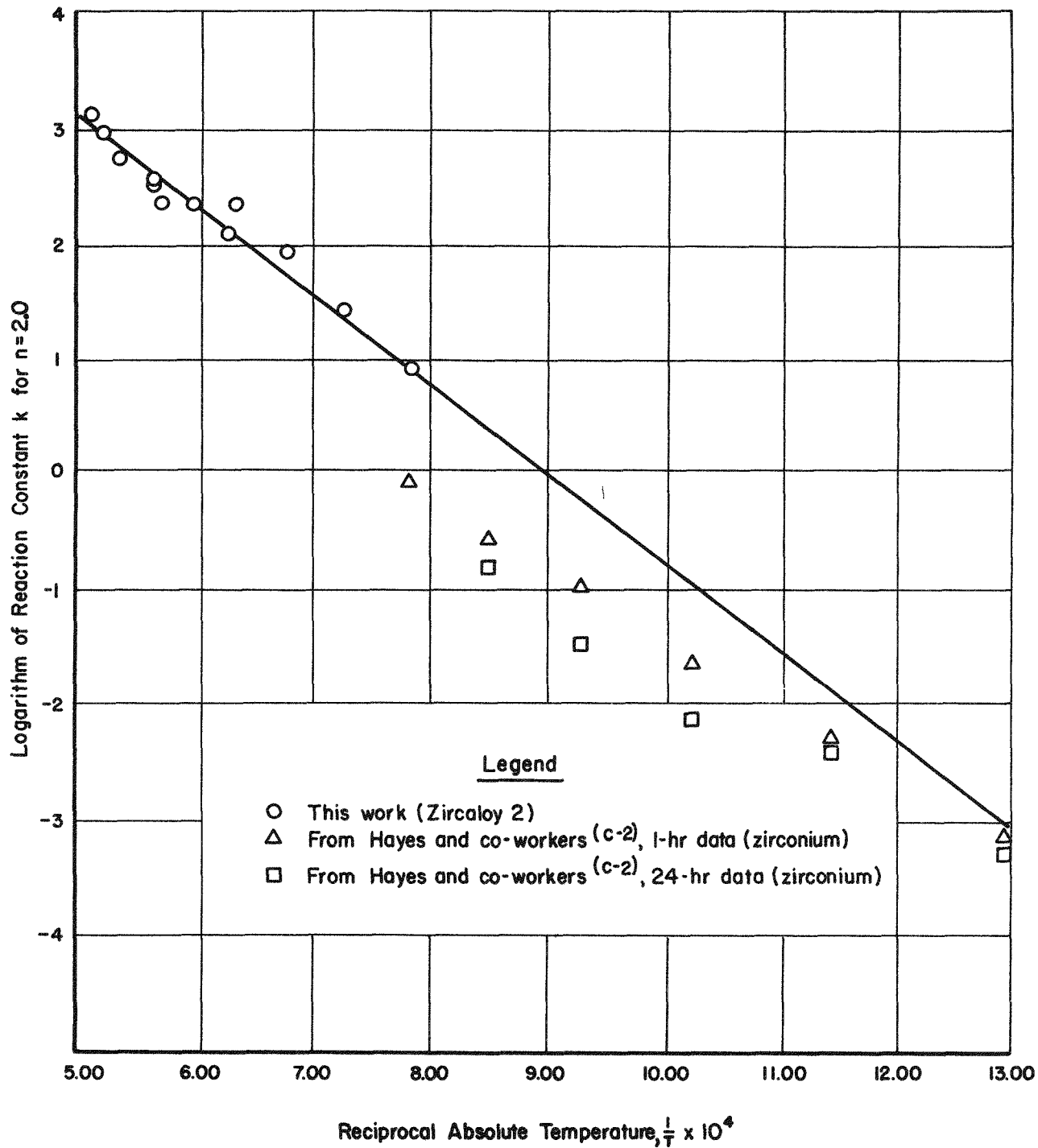


FIGURE C-13. EXTENDED-TEMPERATURE PLOT OF THE 2.0-ORDER REACTION RATE CONSTANT

Reaction of Zircaloy 2 and Zirconium With Steam.

61

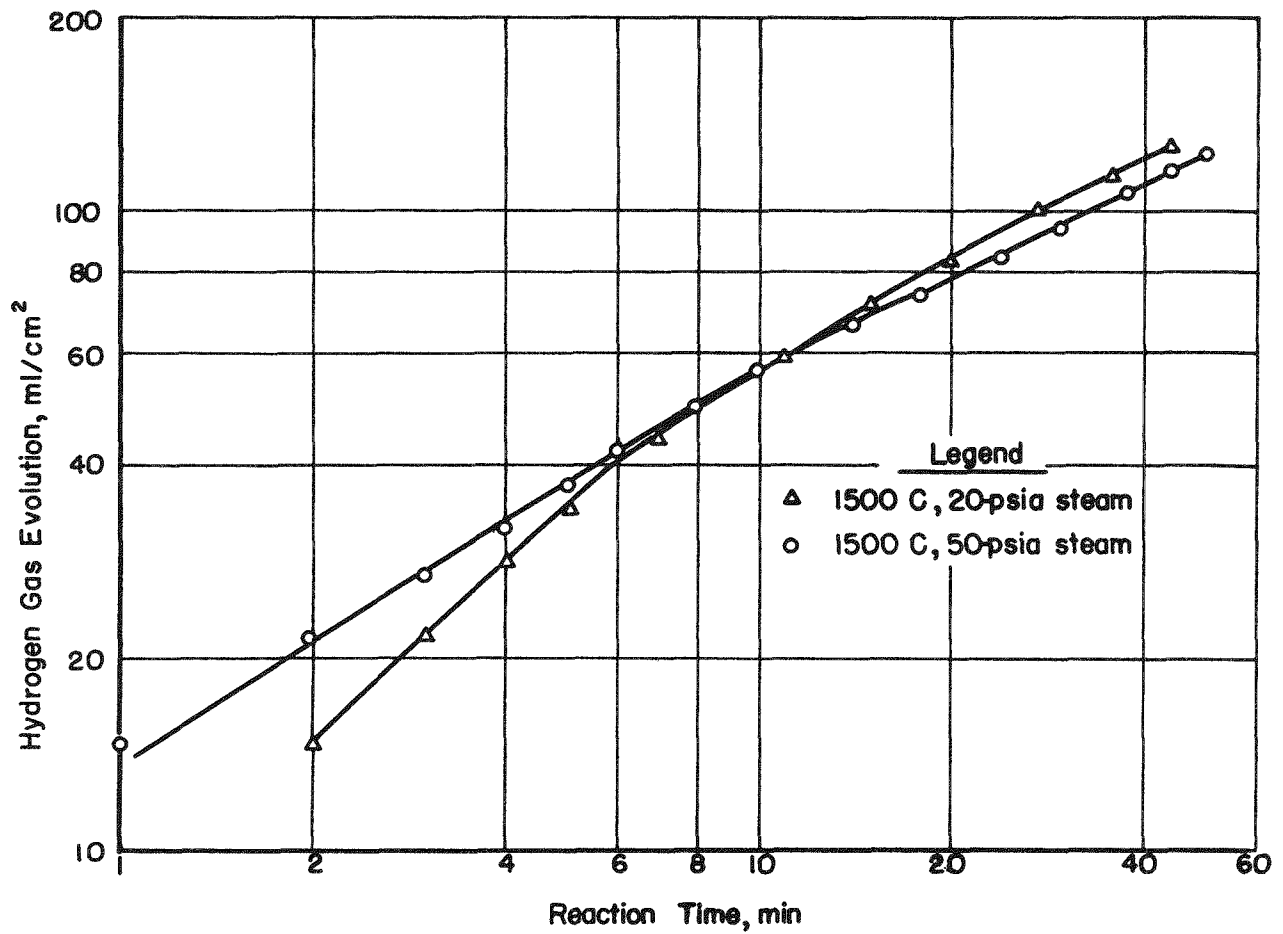


FIGURE C-14. EFFECT OF PRESSURE ON REACTION BETWEEN ZIRCALOY 2 AND STEAM

Photographs of cross sections of Zircaloy 2 after reaction with steam are shown in Figures C-15 to C-22. The sections show a characteristic outer layer of zirconium oxide which overlies a layer of alpha-phase solid solution of oxygen in zirconium. Underneath the alpha-phase layer appears the transformed beta phase.

From photographs of several specimens, the thicknesses of the zirconium dioxide and alpha-phase layers were obtained and are given in Table C-2. As the reaction temperature was increased, the ratio between the thicknesses of the zirconia layer and the alpha-phase layer considerably decreased in value.

TABLE C-2. THICKNESS OF ZIRCONIA AND ALPHA-SOLID-SOLUTION LAYERS NEAR SURFACE OF ZIRCALOY 2 AFTER REACTION WITH 50-PSIA STEAM

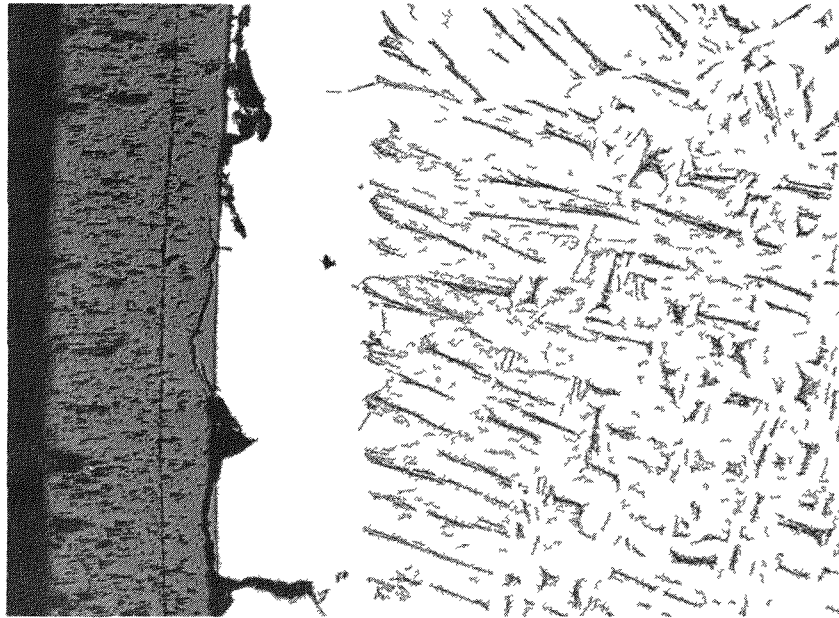
Run	Temp, C	Reaction Time, min	Extent of Reaction (v), ml H ₂ per cm ²	Thickness of Layers, mm		Ratio of Thicknesses, mm ZrO ₂ mm Alpha
				Zirconia	Alpha Phase	
19	1000	2	5.2	0.024	0.008	3.0
8	1000	120	31.	0.23	0.20	1.2
21	1200	2	8.8	0.030	0.028	1.1
9	1200	60	74.	0.22	0.045	4.9
22	1400	2	20.	0.060	0.084	0.72
7	1400	35	82.	0.28	0.38	0.74
25	1600	0.08	8.4	0.028	0.044	0.64

Reaction Between Molten Zircaloy 2 and Steam

The results of experiments on the reaction between molten Zircaloy 2 and steam are illustrated in Figure C-23 and shown in more detail in Table C-3. The extent of reaction is expressed as STP ml hydrogen evolved per sq cm projected area of the graphite crucible opening.

Considerable scatter of the data is evident from the plot shown as Figure C-23. No reasonable correlation with the initial temperature of the Zircaloy can be suggested. The lack of correlation with temperature may be due to any one of several factors. Among these factors is the uncertainty of temperature, since the temperature of the molten Zircaloy

63



100X

1 Per Cent HF Etchant

N31579

FIGURE C-15. ZIRCALOY 2 AFTER REACTION AT 1000 C WITH 50-PSIA STEAM FOR 120 MIN

Transverse section at edge in which appears an outer layer of zirconia phase overlaying first a layer of alpha-solid-solution phase and next the transformed beta phase.

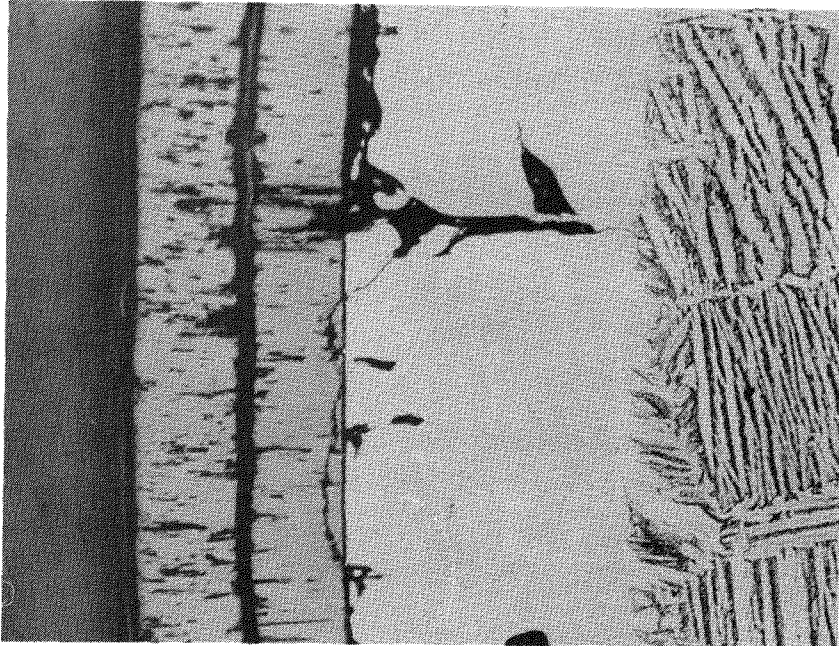


100X

1 Per Cent HF Etchant

N31577

FIGURE C-16. ZIRCALOY 2 AFTER REACTION AT 1200 C WITH 50-PSIA STEAM FOR 60 MIN

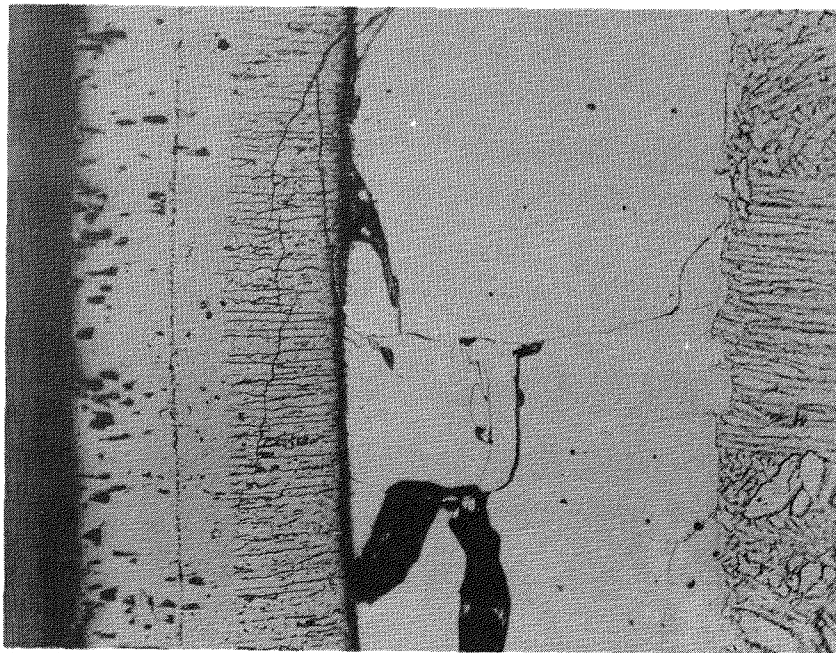


100X

1 Per Cent HF Etchant

N31575

FIGURE C-17. ZIRCALOY 2 AFTER REACTION AT 1400 C WITH 50-PSIA STEAM FOR 35 MIN

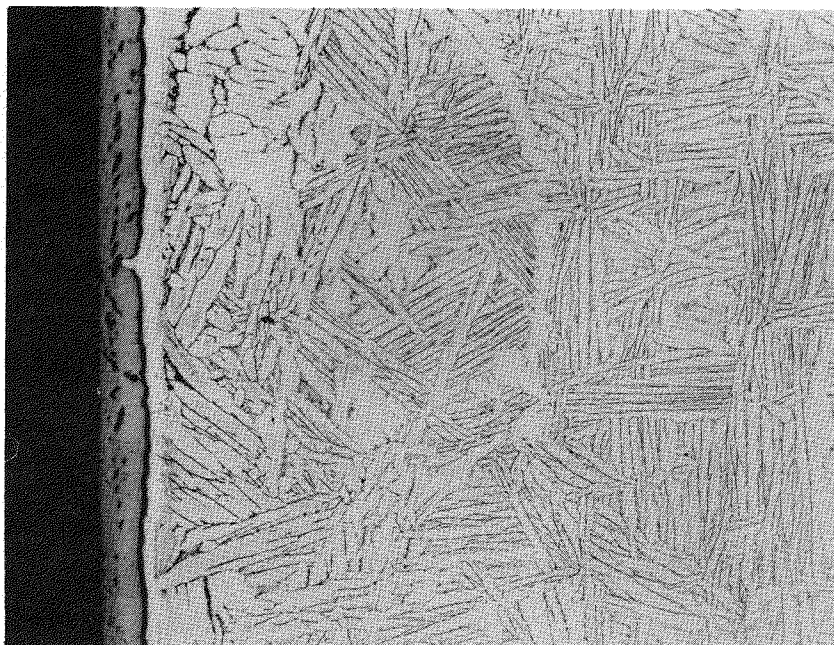


100X

1 Per Cent HF Etchant

N31581

FIGURE C-18. ZIRCALOY 2 AFTER REACTION AT 1600 C WITH 50-PSIA STEAM FOR 22 MIN



250X

1 Per Cent HF Etchant

N31583

FIGURE C-19. ZIRCALOY 2 AFTER REACTION AT 1000 C WITH 50-PSIA STEAM FOR 2 MIN

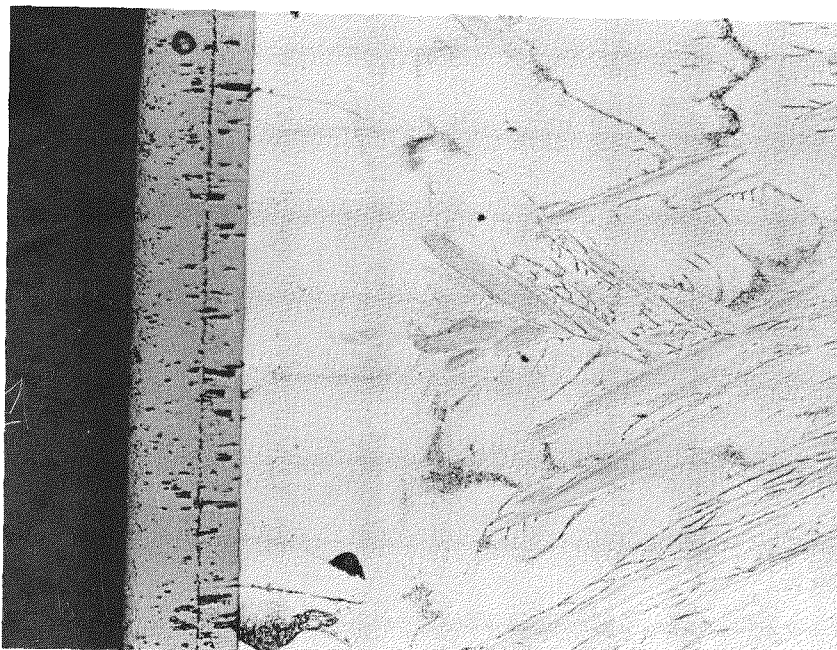


250X

1 Per Cent HF Etchant

N31587

FIGURE C-20. ZIRCALOY 2 AFTER REACTION AT 1200 C WITH 50-PSIA STEAM FOR 2 MIN

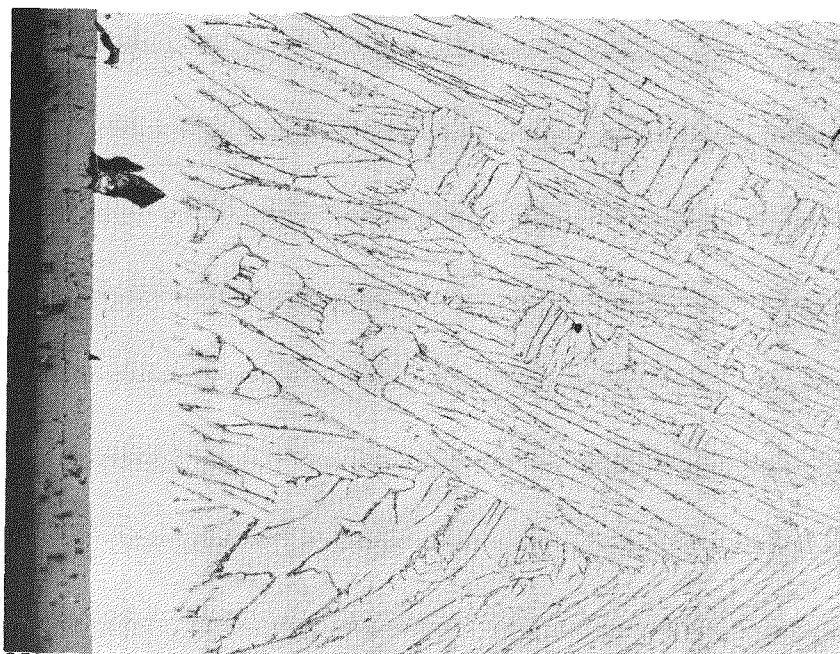


250X

1 Per Cent HF Etchant

N31589

FIGURE C-21. ZIRCALOY 2 AFTER REACTION AT 1400 C WITH 50-PSIA STEAM FOR 2 MIN



250X

1 Per Cent HF Etchant

N31591

FIGURE C-22. ZIRCALOY 2 AFTER REACTION AT 1600 C WITH 50-PSIA STEAM FOR 5 SEC

67

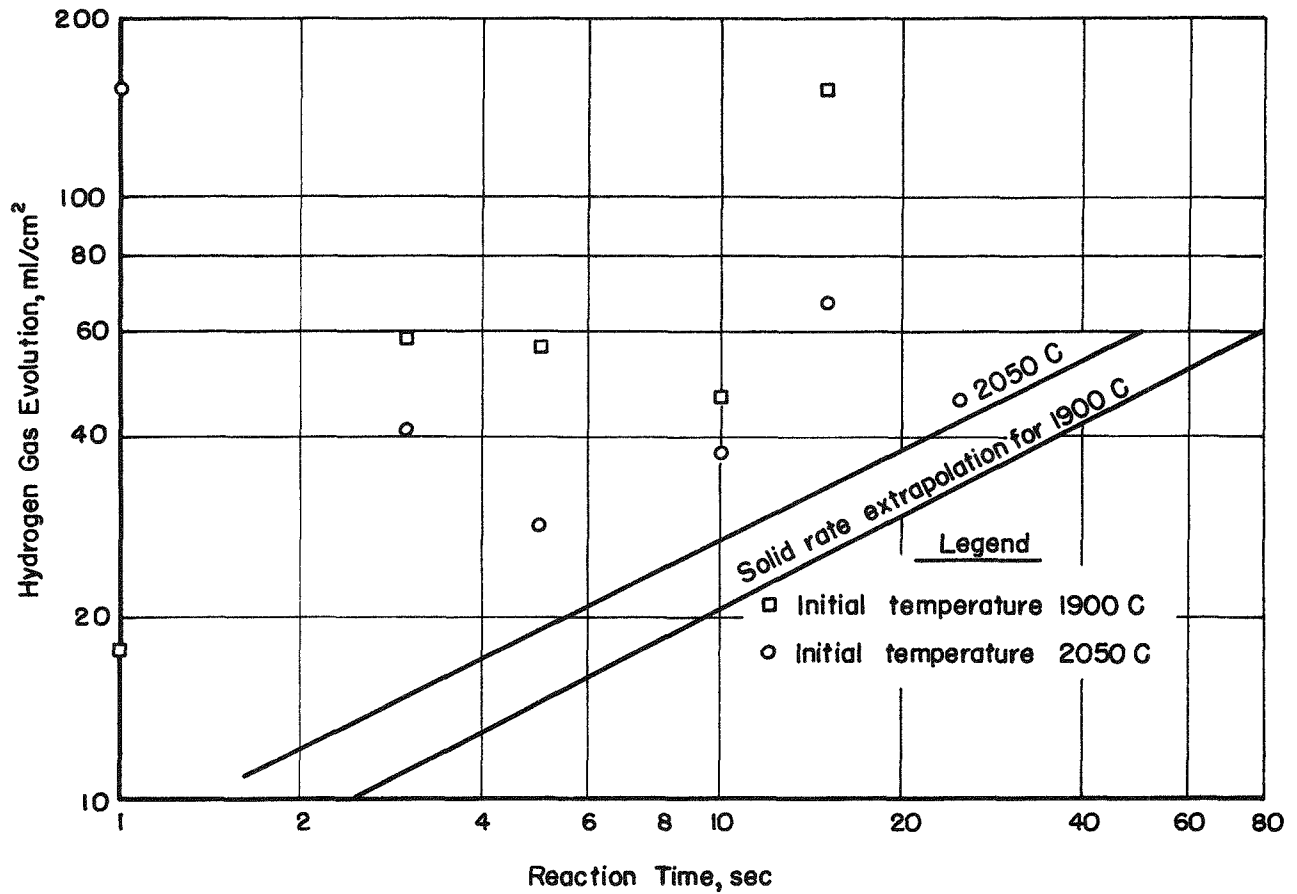


FIGURE C-23. REACTION BETWEEN LIQUID ZIRCALOY 2 AND STEAM AT 50 PSIA

increased what appeared to be several hundred degrees upon contact with steam. Also, the variations in the disturbing effects of the steam on the surface of the molten Zircaloy cannot be evaluated.

TABLE C-3. REACTION BETWEEN MOLTEN ZIRCALOY 2 AND STEAM

Steam jet directed on surface of molten Zircaloy in graphite crucible.

Run	Initial Temp ^(a) , C	Reaction Time, sec	Oxygen Content, w/o		Hydrogen Content, w/o		Extent of Reaction ^(b) , STP ml H ₂ per cm ²	Average Rate of Reaction, STP ml H ₂ per (cm ²)(min)
			Found	Corrected for Blank	Found	Corrected for Blank		
48	1900	0 ^(c)	0.12	--	0.0014	--	--	--
47	1900	1	0.34	0.22	0.0052	0.0038	17.7	1062.
46	1900	3	0.75	0.63	0.0032	0.0018	58.3	1166.
45	1900	5	0.73	0.61	0.0027	0.0013	56.7	680.
44	1900	10	0.65	0.53	<0.001	--	46.9	281.
40	1900	15	1.81	1.69	0.012	0.0106	151.	604.
35	2050	1	1.81	1.69	0.0097	0.0083	151.	9060.
38	2050	3	0.60	--	<0.0010	--	41.2	824.
34	2050	5	0.43	0.31	<0.0010	--	28.4	341.
36	2050	10	0.53	0.41	0.0038	0.0024	37.5	225.
32	2050	15	0.88	0.76	0.0026	0.0012	67.0	278.
39	2050	25	0.63	0.51	0.0016	0.0002	46.3	111.

(a) Temperature of molten Zircaloy surface was greatly increased by the heat of reaction with steam.

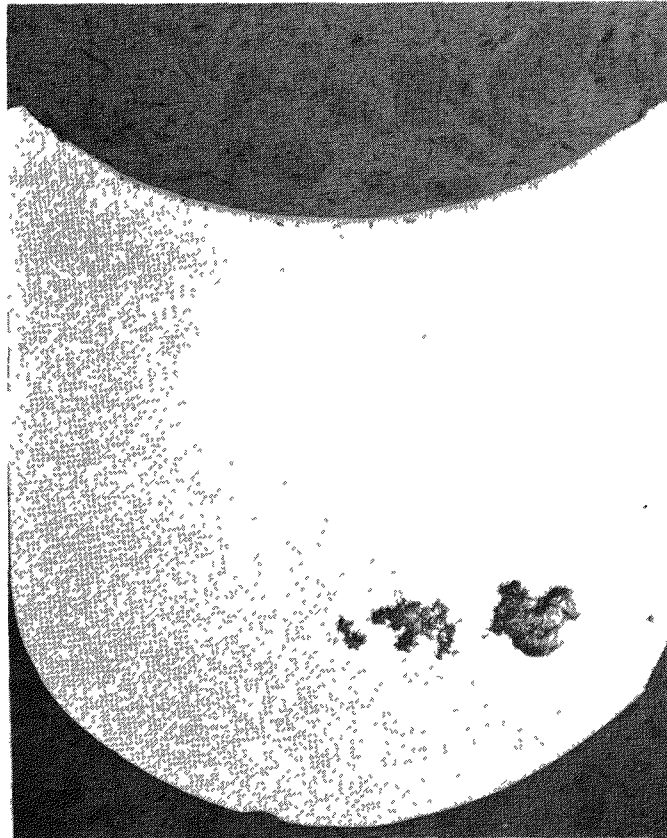
(b) Specific reaction expressed on basis of hydrogen liberated as gaseous product as calculated from analysis of sample.

(c) Sample heated in argon stream only to determine oxygen and hydrogen pickup in absence of added steam.

The rates of reaction of molten Zircaloy 2 with steam are compared in Figure C-23 with the extrapolated rates from the correlation for the reaction rates of solid Zircaloy 2 with steam. All observed rates are higher than would be predicted from extrapolating the reaction rates of solid Zircaloy 2. Because of the large scatter in the data on molten Zircaloy 2, no correlation is possible. It is possible that variations from run to run of the type discussed above contributed to the scatter. Future effort is needed on further studies of molten-metal reaction rates.

Figures C-24 and C-25 show the results of reaction of molten Zircaloy 2 with steam at 50 psia after a reaction interval of about 1 sec. Layers of zirconia and alpha solid solution of oxygen are directly under the top

60



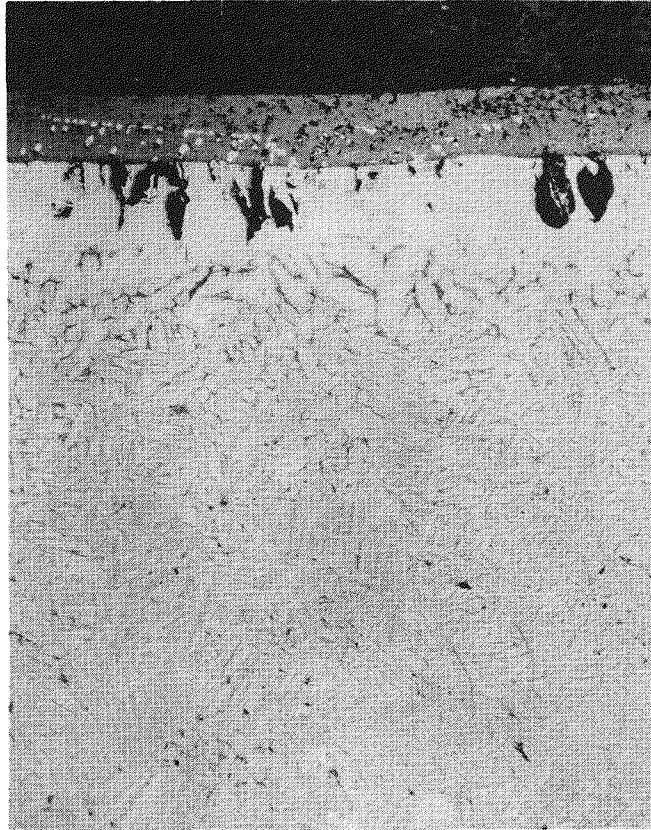
7X

1 Per Cent HF Etchant

N31667

FIGURE C-24. VERTICAL SECTION OF ZIRCALOY 2 SPECIMEN AFTER REACTION AS MOLTEN METAL AT 1900 C WITH STEAM AT 50 PSIA FOR 1 SEC

Zirconia and alpha layers appear at top surface.



100X

1 Per Cent HF Etchant

N31594

FIGURE C-25. ZIRCALOY 2 AFTER REACTION AS
MOLTEN METAL AT 1900 C WITH
STEAM AT 50 PSIA FOR 1 SEC

Vertical transverse section at surface.

surface of the sample. Figures C-26 and C-27 show another Zircaloy sample after exposure to steam for a period of 5 sec. The nodular-shaped areas visible in Figure C-27 are believed to be crystallites of zirconium carbide produced by reaction with the containing crucible.

Because of the large uncertainties in the reaction-rate data on molten Zircaloy 2, it is recommended that an extrapolation of the rate expression for solid Zircaloy 2 be used for the molten metal until better data are available.

PART 2. DROP-TEST EXPERIMENTS

Introduction

In the related investigation, described in Part 1, the rate of reaction between Zircaloy 2 in the solid and molten states and steam at 50 psia has been determined at various temperatures. In this program, the reaction of molten Zircaloy 2 with water at temperatures in the range 90 to 200 F was investigated. Measurements of the total extent of reaction between molten Zircaloy 2 droplets and hot water were desired to provide data for checking the computations in Section D.

Apparatus

A 2-w Lepel high-frequency induction coil was used to melt the 1/12-in. -diameter Zircaloy 2 rod. The water-cooled, 1/8-in. OD copper-tubing induction coil used was 1 in. long, had 8 turns, an outside diameter of 0.59 in. and an inside diameter of 0.39 in. It was coated with G-E 1201 Red Enamel (Glyptal) to prevent water vapor from condensing on the coil turns and causing shorts.

Figure C-28 illustrates the arrangement of the coil and rod. The purpose of the baffles was to aid in the elimination of water vapor from the coil region because the coil was found to arc occasionally even with the Glyptal coating. The smaller opening through which the argon was forced to flow prevented the water vapor from rising above the top baffle. The water vapor, then, condensed on the baffles instead of the coil.

The coil was situated about 4 in. from the surface of the water, which was contained in a glass column of 4-in. inside diameter and over-all height of 22.5 ft. The bottom of the column had valves to allow flow of water in and out of the column, as well as provision for recovery of samples which had been dropped to the bottom.

72

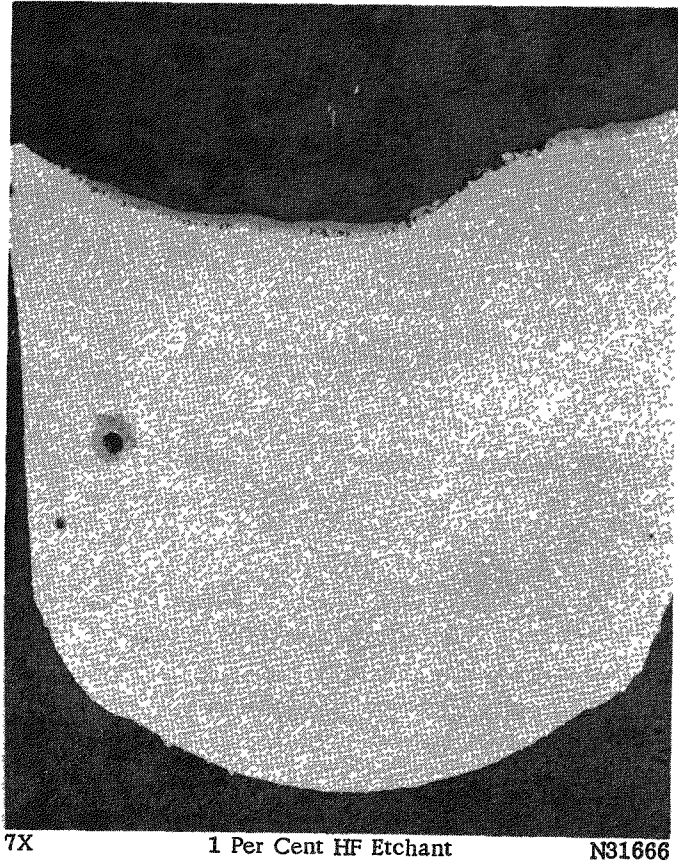
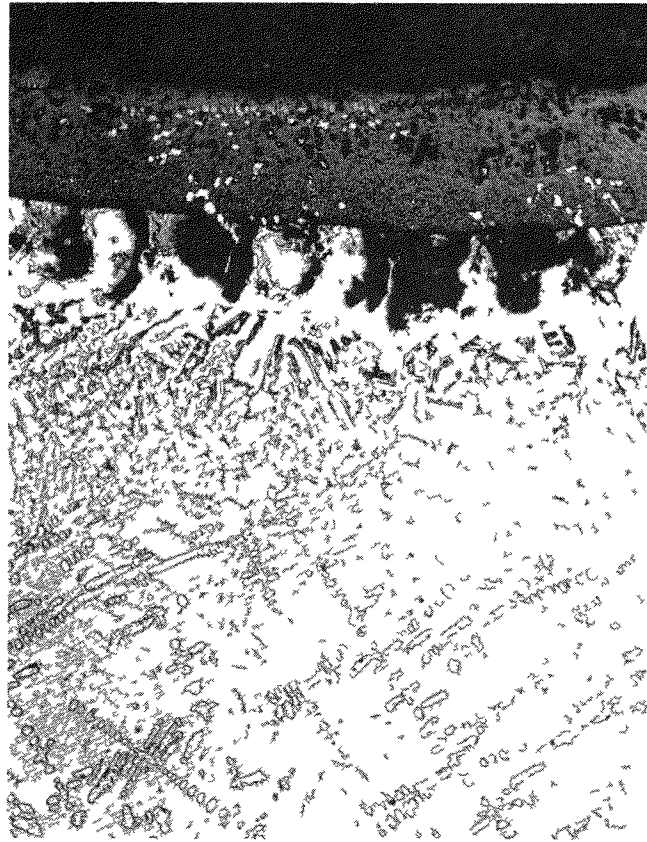


FIGURE C-26. VERTICAL SECTION OF ZIRCALLOY 2 SPECIMEN AFTER REACTION AS MOLTEN METAL AT 1900 C WITH STEAM AT 50 PSIA FOR 5 SEC

73



100X

1 Per Cent HF Etchant

N31596

FIGURE C-27. ZIRCALOY 2 AFTER REACTION AS
MOLTEN METAL AT 1900 C WITH
STEAM AT 50 PSIA FOR 5 SEC

Vertical transverse section at surface.

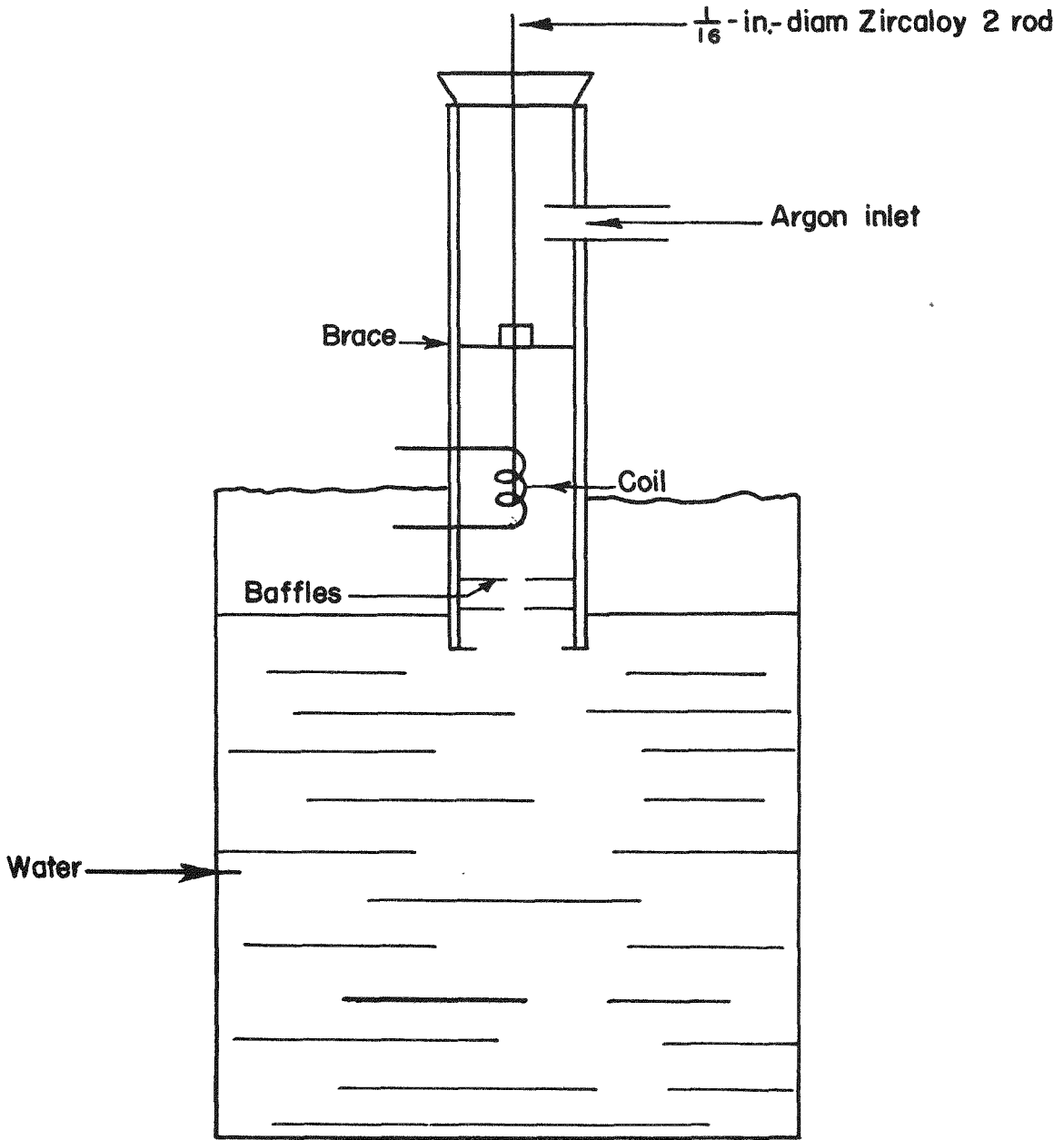


FIGURE C-28. SCHEMATIC SKETCH OF COIL AND ROD ARRANGEMENT FOR DROP-TEST APPARATUS

Procedure

The first step in making a run was to fill the glass column with water. The water was heated to different temperatures by directly combining various proportions of steam and cold water in a mixing tee. After the temperature of the water was determined, a weighed Zircaloy 2 rod was carefully inserted through the top opening (see Figure C-28) and fed into the axis of the coil. Reaction time, determined with a stop watch, was measured as the interval between the instant the molten droplet entered the water until it ceased glowing. When the droplet ceased glowing, the observer also noted the corresponding distance of fall.

For each run at a given water temperature, about 8 to 10 molten drops were allowed to fall. At the conclusion of a run, the water was removed, and the balls were recovered, dried, and weighed. The remaining unmelted rod also was weighed.

Results

Qualitative observation of the liquid Zircaloy 2 drops during the runs did not establish whether or not the drops were molten until the time they hit the water. However, calculation showed that the latent heat of melting of a ball of Zircaloy 2 of the size used in the experiment was about 27 cal. Assuming free-fall conditions, the time of fall was roughly 0.15 sec for the 4-in. distance above the water surface. The heat loss due to radiation at 2070 K during this time would be only 1 cal. A value of about 10^{-3} cal was obtained for the forced convection heat loss, again assuming free-fall conditions. Thus, it appears that the ball could not have lost sufficient heat before striking the water surface to cause significant solidification.

The luminescence of the drops appeared to increase at the water surface, reaching a peak at a depth of 3 to 4 ft. After this, the luminescence diminished until the ball ceased to glow. The increased luminescence may have been caused partly by increasing temperature owing to reaction, but almost certainly was caused in large part by the higher emissivity of the oxide coating formed by the reaction.

All the reacted pellets had essentially the same appearance and size. They were slightly flattened spheres with a characteristic hole in one of the flat ends extending about half way through the pellet. A hard, black, shell-like coating could be readily removed by scraping, revealing a gray-black much thinner and more closely adhering film. This film could be readily scratched through. This procedure revealed the silver-white unreacted alloy.

The chief results of the experiment are presented in Tables C-4, C-5, and C-6.

Table C-4 gives values of water temperature at the start of each run, the period of luminescence of the pellets, the depth of the water at which the pellets ceased glowing, and the measured thickness of the oxide layer determined from photomicrographs. Also shown is the difference in degrees Fahrenheit between the water temperature and its boiling point, $T_b - T$.

Table C-5 shows the amount of reaction which occurred in the Zircaloy 2 pellets as determined by several techniques. First, the weight gain was interpreted as being due entirely to chemical reaction and equivalent to the hydrogen and oxygen contained by the reacted pellets. The values listed in Column 3 were determined by dividing the weight increase of the pellets collected from one run by the weight of the metal melted from the rod, equal to the initial weight of the pellets, of course. In Run 4, the Zircaloy rod was apparently fed too rapidly into the coil causing a piece of the rod to be cut from the main rod and to fall unmelted into the water column. A correction was made for the weight of this piece and the adjusted result reported. No values are reported for Runs 5 and 6 due to loss of several balls and/or loss of their oxide coatings. In Run 7, one ball was lost, but an interpretation of the values for the other pellets gave the result reported. Some question also exists regarding Run 3. There is a possibility that an extra pellet from another run may have led to the extremely high value reported.

Values of the gas contents in the pellets, as computed from available photomicrographs, are given in Column 4 in Table C-5. Volumes of oxide coatings on the pellets and volumes of oxygen diffusion layers were estimated and used to obtain these results.

In Table C-5 are included vacuum-fusion results for four of the runs. The sample for analysis was one-half the pellet. The sample was degreased with cp acetone and then analyzed by dropping it with a tin flux on a bed of graphite chips at 1200 C (2192 F) and rapidly raising the temperature to 2150 C (3902 F). All evolved gases were collected and analyzed by the low-pressure, fractional-freezing method.

Also included in Table C-5 are values for the average weight of the reacted pellets in different runs. These are seen to be quite uniform.

Table C-6 gives some correlational data for the drop-test runs and the solid Zircaloy 2-steam and liquid Zircaloy 2-steam runs reported in Part 1. The correlating parameter used in the table was the w/o hydrogen in the sample.

TABLE C-4. DATA FOR FALL OF ZIRCALOY 2 DROPLETS THROUGH WATER

Run	Water Temp., F	$T_b - T^{(a)}$	Period of Luminescence, sec	Distance of Fall to End of Luminescence, ft	Oxide Layer Thickness, in.
1	92	119	2.8	--	0.0040
6	110	101	3.6	8.0	0.0024
7	124	87	3.5	8.9	0.0028
2	138	73	4.3	9.25	0.0018
8	148	63	6.2	14.8	0.0047
5	164	47	6.8	16.1	--
4	166	45	7.8	18.4	0.0026
3	174	37	9.4	20.2	0.0032
9	200	11	9.25	21.6	0.0068

(a) Boiling temperature, $T_b = 211$ F.

TABLE C-5. PELLET WEIGHTS AND GAS CONTENTS AFTER REACTION

Run	Initial Water Temp., F	Weight Gain of Pellets ^(a) , w/o	Calculated From Photo-micrographs	Gas Content, w/o			Average Weight of Reacted Pellets, g	
				Vacuum-Fusion Analysis				
				O ₂	H ₂	Total		
1	92	3.78	1.85	--	--	--	0.57	
6	110	--	2.21	3.21	0.051	3.26	--	
7	124	(6.45)	--	3.10	0.046	3.15	0.53	
2	138	4.85	2.86	--	--	--	0.62	
8	148	9.6	6.48	1.79	0.0212	1.81	0.59	
5	164	--	--	--	--	--	0.54	
4	166	(4.63)	2.45	--	--	--	--	
3	174	(14.1)	3.68	--	--	--	0.58	
9	200	11.5	7.40	3.14	0.0553	3.20	0.62	
							Average	0.58

(a) Values in parentheses are questionable.

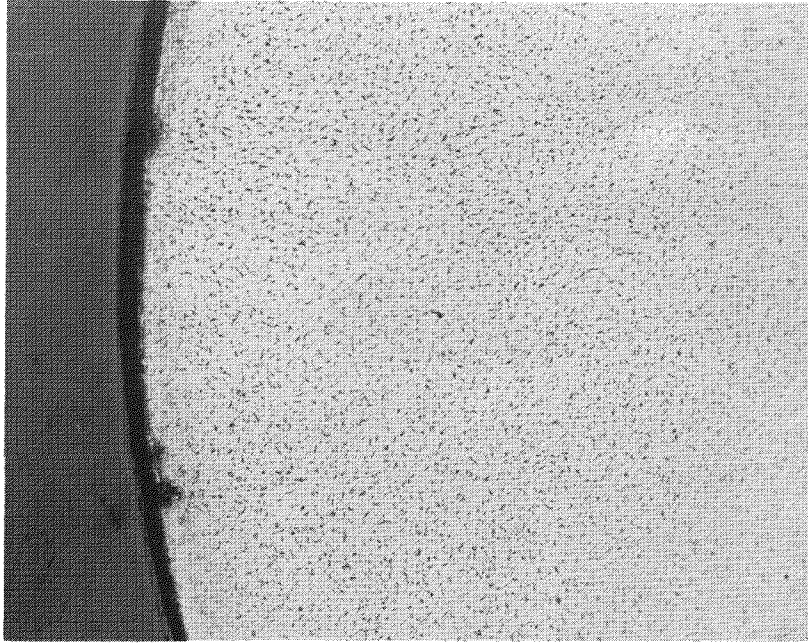
TABLE C-6. HYDROGEN GAS RETAINED IN VARIOUS EXPERIMENTS

Total Time of Run, sec	Per Cent Hydrogen Retained at Temperature, C						
	1000	1200	1400	1600	1900	2050	Drop Test
1	--	--	--	--	0.765	0.059	--
3	--	--	--	--	0.213	0.085	--
3.5	--	--	--	--	--	--	12.6 (Run 7)
3.6	--	--	--	--	--	--	11.8 (Run 6)
5	--	--	--	12.5	0.185	0.104	--
6.2	--	--	--	--	--	--	9.4 (Run 8)
9.25	--	--	--	--	--	--	14.0 (Run 9)
10	--	--	--	--	0.077	0.358	--
15	--	--	--	--	0.331	0.192	--
25	--	--	--	--	--	0.415	--
120	5.9	9.4	6.5	--	--	--	--

Figure C-29 shows a cross section of the Zircaloy 2 rod after the rod has been heated by the induction coil in the argon atmosphere. The single phase region in the interior and the absence of an oxide skin shows that no appreciable oxidation took place in the specimen. Figures C-30 and C-31 show typical examples of the pellets from Runs 3 and 6. Figures C-32 and C-33 show a typical pellet from Run 9. Figure C-34 shows graphically the relation between time and distance-of-fall values from Table C-4. The relatively small scatter of the data from the average line shows that the time-distance measurements are quite reliable. Figure C-35 shows graphically how the period of luminescence varies with water temperature. The plot appears to be essentially linear. A plot of oxide-layer thickness versus period of luminescence, Figure C-36, shows, for comparison with the drop-test data, three molten metal points reported in Part 1 for which photomicrographs were available.

Figure C-37 shows the amount of reaction, obtained by the various methods, for each of the runs made. Although this information is shown as a function of the water temperature, a single value for reaction with water at its boiling point is desired.

It should be added that an important negative result was attained from these experiments, viz., the fact that no explosion ensued when the liquid pellets struck the water. Furthermore, the reaction was not so vigorous as to vaporize the metal or bring about complete reaction of the metal with water.

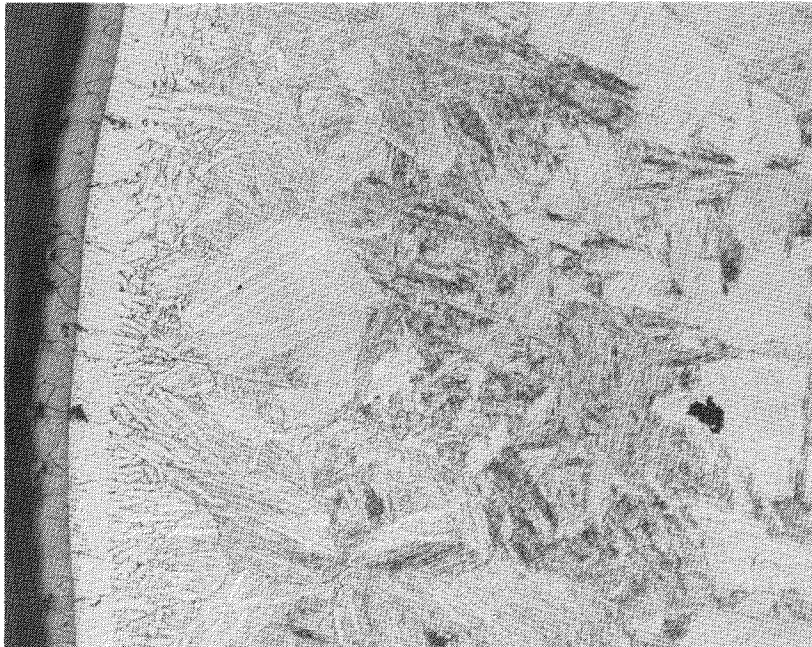


250X

30 Lactic, 30 HNO₃, 1 HF

N29062

FIGURE C-29. PHOTOMICROGRAPH OF UNREACTED ROD

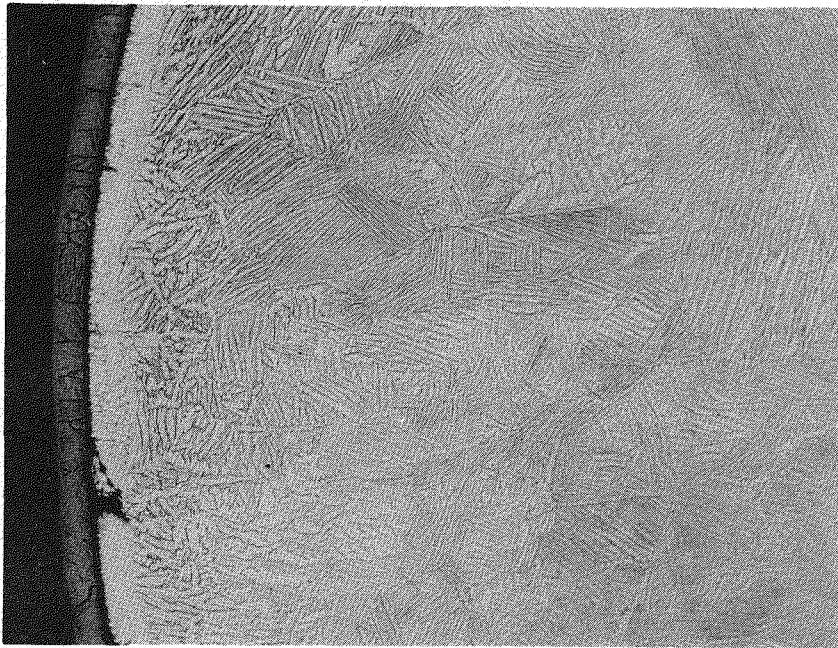


100X

1 Per Cent HF on Wheel

N28948

FIGURE C-30. REACTED ZIRCALOY 2 FROM RUN 3



100X

1 Per Cent HF on Wheel

N31325

FIGURE C-31. REACTED ZIRCALOY 2 PELLET FROM RUN 6

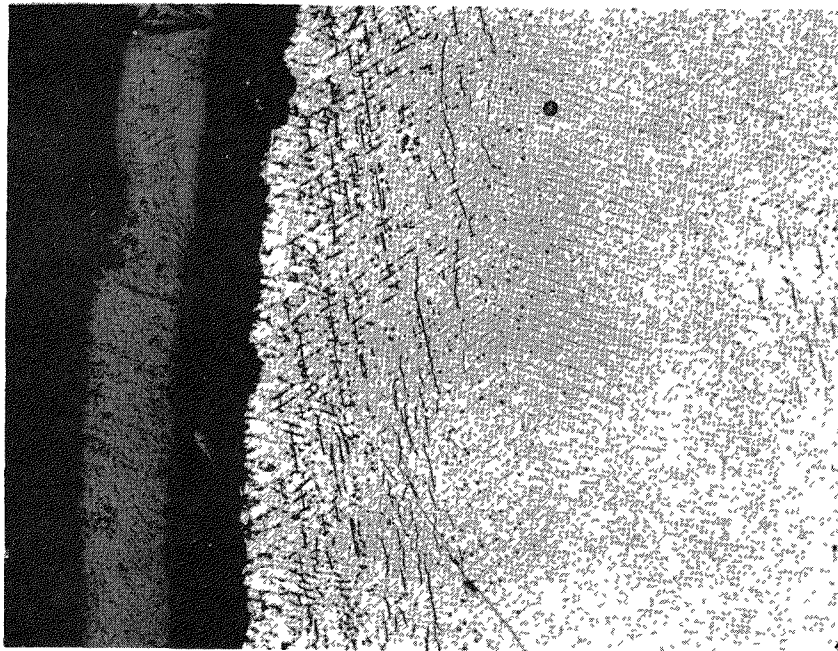


15X

1 Per Cent HF on Wheel

N31340

FIGURE C-32. PHOTOMACROGRAPH OF REACTED ZIRCALOY 2 PELLET FROM RUN 9



100X

1 Per Cent HF on Wheel

N31335

FIGURE C-33. PHOTOMICROGRAPH OF REACTED ZIRCALOY 2 PELLET FROM RUN 9

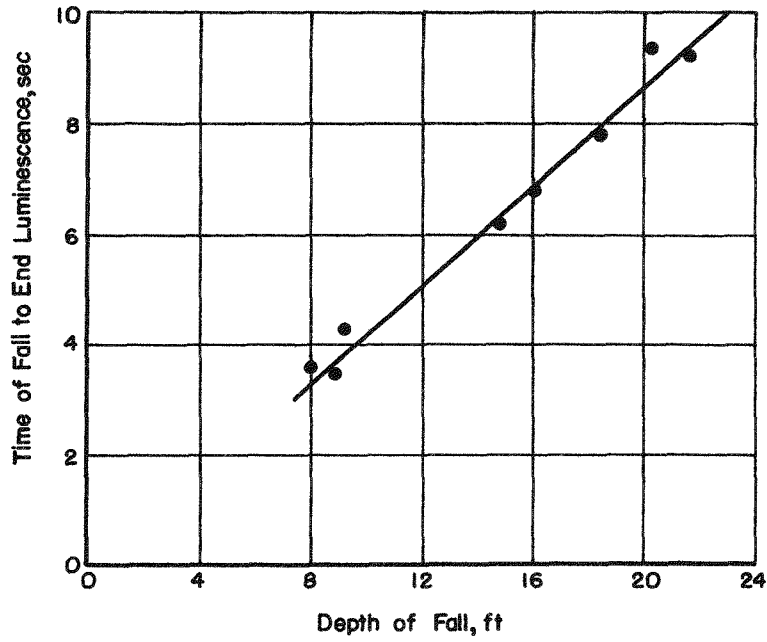


FIGURE C-34. TIME AND DEPTH OF FALL TO END OF LUMINESCENCE

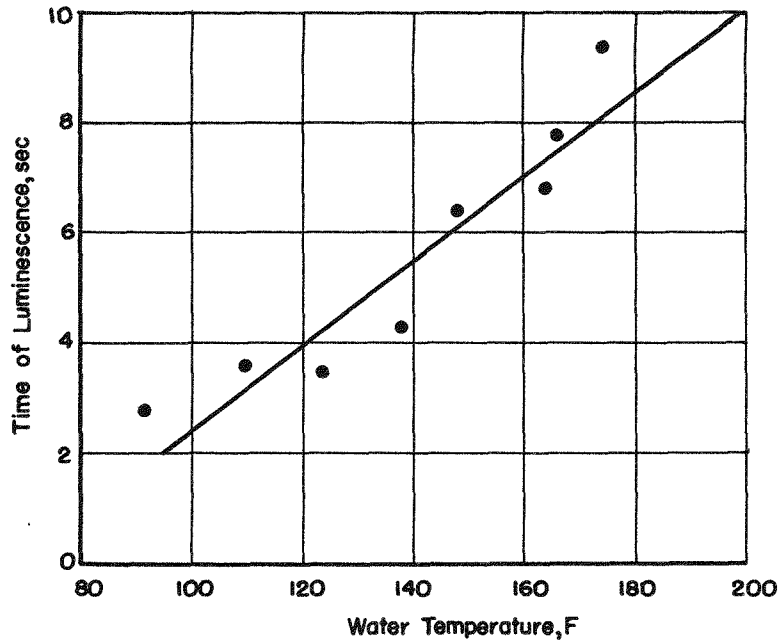


FIGURE C-35. EFFECT OF WATER TEMPERATURE ON TIME OF LUMINESCENCE

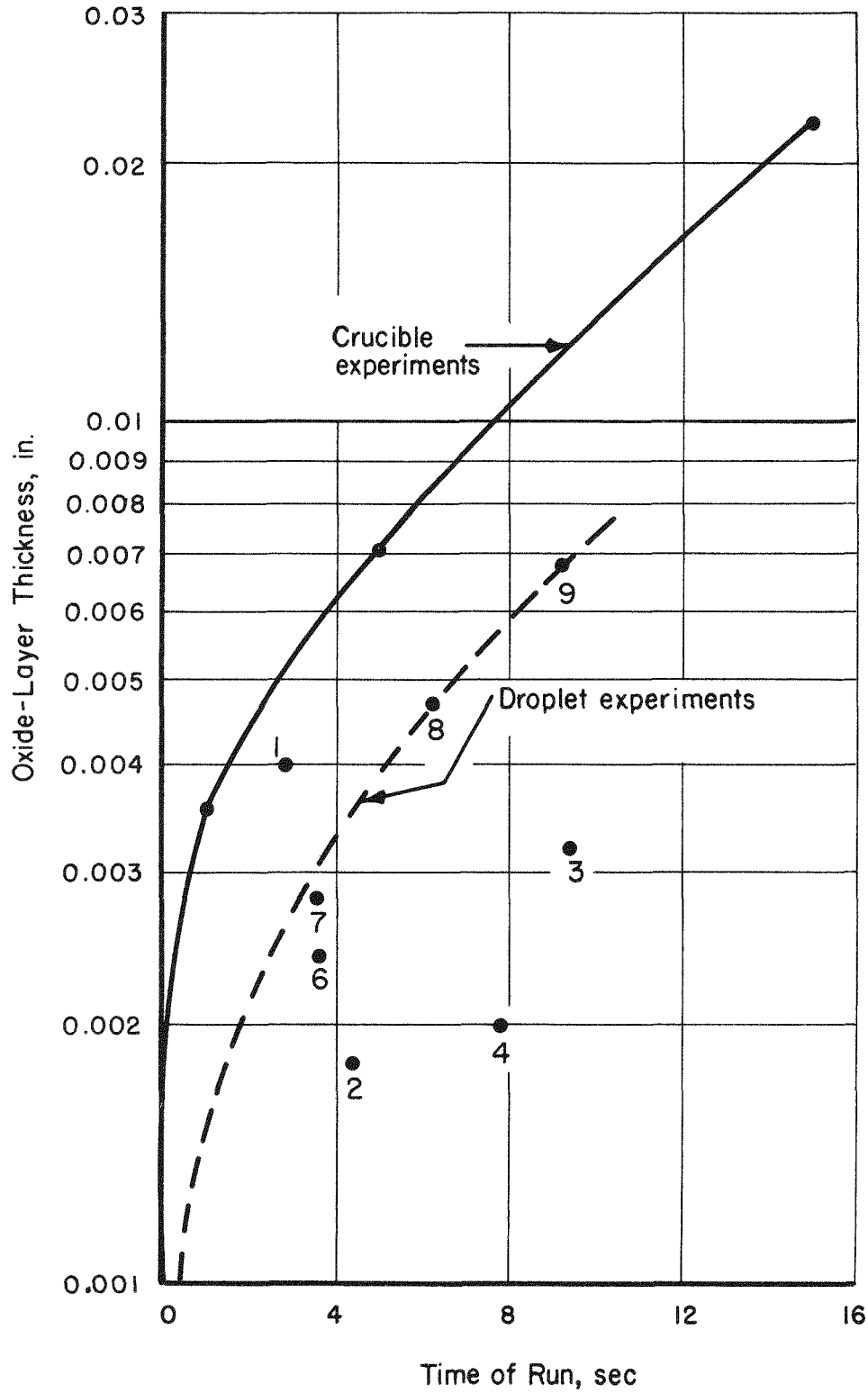


FIGURE C-36. EFFECT OF REACTION TIME ON OXIDE-LAYER THICKNESS

84

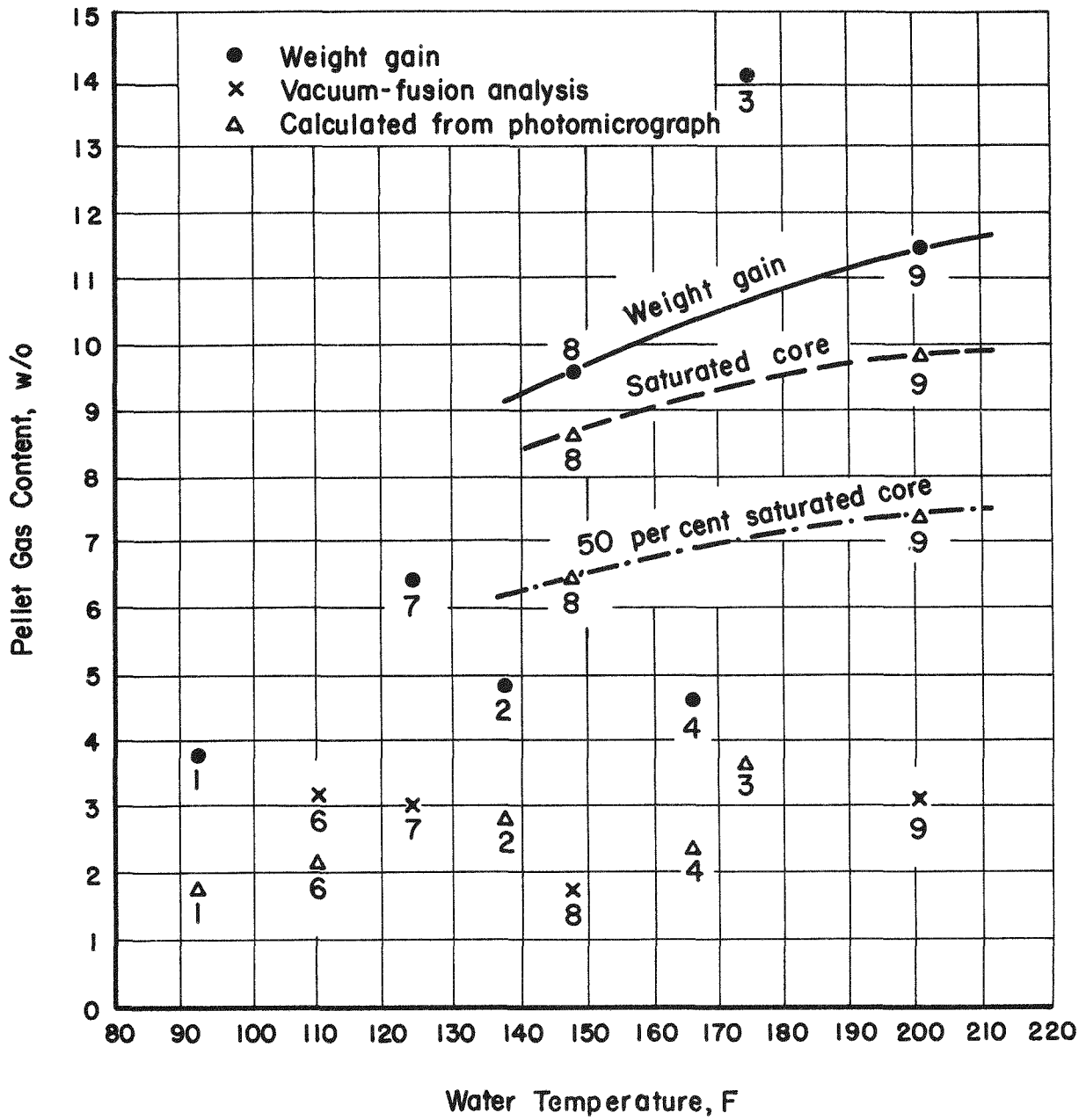
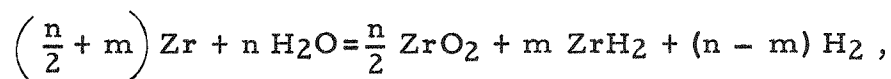


FIGURE C-37. PELLETT GAS CONTENTS

Discussion

It is apparent from Figure C-35 and qualitative observations that the drop-test pellets were not effectively molten for a large fraction of the luminescent period. On the other hand, the heat loss during free fall is not enough to freeze the ball; therefore, it appears that cooling may be rapid enough to freeze molten droplets early in their fall through water.

The oxide layers observed in the drop tests were thinner than those formed in the liquid runs which were initiated at 1900 C and made for the same length of time. Photomicrographs also show this difference qualitatively. Some drop-test prints show an oxide layer structure similar to that of samples of the solid Zircaloy 2 samples which were reacted with steam at temperatures in the range 1000 to 1700 C as reported in Part 1. Furthermore, the amount of hydrogen retained, as determined by vacuum-fusion analyses for the three types of runs (i. e., solid Zircaloy 2-steam, liquid Zircaloy 2-steam, and liquid Zircaloy 2 droplets-water), indicate a break in the values for the solid runs and drop-test runs on the one hand, and the true liquid runs on the other hand. As was expected (see Table C-6), the liquid runs showed a smaller hydrogen retention than did the solid runs. The oxide ZrO_2 apparently had not begun to decompose appreciably even at 1900 C. If the reaction is indicated by the over-all equation



where m is the number of moles of hydrogen retained as hydride and $n - m$ the net number of moles of hydrogen evolved, it follows that for the liquid runs the ratio m/n was roughly 0.0005 to 0.0080 whereas for the drop tests and solid runs m/n was 0.05 to 0.14. The hydrogen analyses, therefore, suggest that sufficient heat had been lost to the water to solidify the metal after a portion of the reaction had occurred, but that the bulk of the reaction, in which hydrogen entered the metal, occurred after solidification.

As calculations of heat loss of the ball during transit from the rod to the water surface indicate losses equivalent to less than a 4 per cent conversion of liquid to solid phase, it is safe to say that the ball is in essentially the same condition when striking the water, despite the fact that the calculations were made assuming free-fall conditions. The radiative loss, which is proportional to the time of transit, could hardly be doubled in value if friction and profile drag are considered. The sudden increase in emissivity (see Section A) and the possible increase in temperature due to the high reaction rate at a thin oxide layer immediately after the drop hits the water probably brings about a peak in the luminescence shortly after the drop contacts the water. The rapid increase in oxide-layer thickness thereafter rapidly reduces the reaction rate so that the rate of cooling overtakes the rate of heating and the luminescence declines. Apparently, the

emissivity stays essentially constant after an initial layer of oxide has been formed.

Careful consideration of the data shown in Figure C-37, in light of the previous discussion, seems to lead to the conclusion that, in reality, both molten and solid pellets of Zircaloy 2 were dropped into the water. Certainly the data for Runs 2, 4, and 6 cannot represent the same type of phenomena as those for Runs 7, 8, and 9. It seems logical that the pellets from Runs 2, 4, and 6 were mainly solid while those from Runs 7, 8, and 9 were mainly molten. Also, even the pellets collected in any one run may have had quite a range of percentage of the pellet as liquid. Favoring this interpretation also is the fact that the later runs, when the experimental techniques were more refined, are the more acceptable ones. Thus, it appears that present consideration should be limited to the data from Runs 7, 8, and 9. The data from Run 3 can be discarded on the basis that an extra pellet from some other run was included in those weighed as well as because it was an early run.

Even for Runs 7, 8, and 9, however, the scatter between the data collected by the various measurements is considerable. Some explanation may be possible by examining critically the measuring techniques used. The vacuum-fusion values are much lower than the other two observations for these runs. Although the vacuum-fusion technique is known to be satisfactory for both zirconium containing dissolved oxygen and its oxide, there is a definite possibility that the analyses are in error for the oxide-coated pellets. As a check on the possibility that only the dissolved oxygen was recovered and that in the oxide shell was not, the result was computed on this basis from the photomicrographs. For Run 8, the computed value, assuming the core to be half saturated with oxygen, is 2.72 w/o oxygen versus the vacuum-fusion analysis result of 1.79 w/o oxygen. For Run 9 on the same basis, the results would be 2.52 w/o versus 3.14 w/o oxygen. It seems probable that this is a valid explanation for this discrepancy, and it is believed that a much closer check could be obtained if the actual oxygen level in the core were known and could be used for computing the oxygen content from the photomicrographs.

In Figure C-37, much of the difference between the oxygen contents based on weight gain and the computations from the photomicrographs can be resolved by considering the uncertainties introduced by two factors. First, the actual oxygen content is unknown and, second, the photomicrograph calculations are based on one pellet from each run, which cannot be considered a representative sample.

Considering that the weight-gain determinations are an average for all pellets in these runs, a value of about 11.7 w/o oxygen would be predicted for molten pellets of this size (0.2 in. or 5080 μ diameter) dropping into water at its boiling point. This would correspond to having 45 w/o of the zirconium reacted. For comparison, Aerojet-General Report AGC-AE-22(C-4) shows that for a pellet of this size, a maximum of 12 w/o

of the zirconium would be reacted. This large variation must arise from the difference in test conditions, mainly the distance available for free fall.

Obviously, these experiments are in no way conclusive, but it is difficult to explain away these high amounts of reaction in which weight gain measurements are partially verified by photomicrographs. Much additional work should be done to obtain reliable results and a better understanding of these phenomena.

Conclusions

The reaction rates between liquid droplets of Zircaloy 2 and water at various temperatures are in rough qualitative agreement with the reaction rates of solid and liquid Zircaloy 2 with steam given in Part 1. The major uncertainty lies in not knowing for what length of time the balls are in the liquid state during their fall through water. Future refinements in techniques might lead to more quantitative data of considerable value. If further work could be done, it is recommended that the length of fall of the Zircaloy 2 drops through the argon atmosphere be minimized to prevent partial solidification of the drops before striking the water and that some technique be devised for assuring that the droplet is actually molten before being dropped.

Although considerable uncertainty exists in the results obtained, partial confirmation exists that a reaction level amounting to 10 to 12 w/o oxygen (or 39 to 45 w/o of the zirconium reacted) is possible in molten pellets having a 0.2-in. diameter. Variations between these results and those reported by Aerojet-General(C-4) are undoubtedly due to the difference in free-fall distance.

A further conclusion is the corroboration of these drop tests with the liquid Zircaloy 2-steam runs that there was no indication of explosion or extreme reactivity (such as to vaporize the Zircaloy 2 and/or cause a complete reaction of the ball with water).

REFERENCES

- (C-1) Bostrom, W. A., "The High Temperature Oxidation of Zircaloy in Water", WAPD-104, Westinghouse Electric Corporation, Atomic Power Division, Pittsburgh, Pennsylvania (March 19, 1954), CONFIDENTIAL.
- (C-2) Hayes, E. T., et al., U. S. Bureau of Mines Technical Progress Report 9, Contract No. (33-038) 50-1214 E (December 21, 1951).

- (C-3) The Metallurgy of Zirconium, Lustman, B. , and Kerze, F. , Jr. (Editors), First Edition, McGraw-Hill Book Company, Inc. , New York (1955).
- (C-4) Higgins, H. M. , et al. , "The Reaction of Molten Metal with Water", Informal Progress Report AGC-AE-22, Aerojet-General Corporation, Azusa, California (September 14, 1956).

89

SECTION D

COOLING MECHANISM OF ZIRCALOY 2
DROPLETS IN WATER

W. S. Hogan, R. F. Redmond, J. W. Chastain,
and S. L. Fawcett

SECTION D

COOLING MECHANISM OF ZIRCALOY 2
DROPLETS IN WATER

W. S. Hogan, R. F. Redmond, J. W. Chastain,
and S. L. Fawcett

A mathematical analysis was performed in an attempt to determine the amount of chemical reaction and heat transfer which would occur for a molten Zircaloy droplet falling through a steam and water environment. The mathematical model included consideration of the temperature asymmetry in the molten droplet caused by the variation in convective heat transfer from front to rear. The results showed that, using the reaction-rate expression which gave the lower values at short times and including heat of fusion effects, 3 to 7 w/o of the Zircaloy would react for emissivities of 0.8 and 0.25, respectively, for a 0.5-cm droplet size. For some cases where the reaction-rate expression giving higher values was used, the temperature of the pellet increased without limit for the lower emissivity values. Comparison of these results with other work, analytical and experimental, does not establish a reasonable pattern, so definitive conclusions are not possible.

Introduction

The object of this analysis was to determine analytically the degree of cooling and the extent of oxidation that occurs as a molten Zircaloy 2 droplet falls through steam and water.

In this analysis it was necessary to make certain assumptions regarding the model chosen and values of important parameters that were the subjects of concurrent phases of the zirconium-water reaction program.

Formulation of the Problem

The problem of predicting the extent of oxidation of molten Zircaloy droplets with water was first considered by Lustman^(D-1). Lustman considered a simplified model in which the droplet was assumed to be spherical with uniform temperature. Cooling by radiation only was assumed and the latent heat of fusion during solidification of the droplet was neglected. Lustman used the data of Bostrom^(D-2) for the oxidation of Zircaloy in water as a basis for estimating the reaction kinetics of the problem. Lustman's results indicated that the extent of oxidation was a function of

the emissivity and the droplet diameter in that the extent of oxidation increased with decreasing emissivity and decreasing droplet diameter.

The work reported here represents an attempt to improve upon the model considered by Lustman.

Formulation of the Problem

Consider the following chain of events: A droplet of molten Zircaloy forms and starts its fall through steam. After a travel of perhaps several feet, the droplet enters a pool of water at saturation temperature and finally comes to rest at the bottom of the vessel after falling through several feet of water.

During its fall, the droplet gains energy from an exothermic oxidation reaction and loses energy by means of several heat-transfer mechanisms. A detailed energy balance on the droplet is required to determine the temperature distribution and history of the droplet. This is necessary because the reaction kinetics governing the oxidation reaction are temperature dependent.

An examination of the problem during the time when the droplet falls through steam was made first. It was concluded that the extent of oxidation and the amount of heat transfer during this time would be of minor importance to the final result. Hence, this part of the droplet history was postulated to occur with a small change of the initial state of the droplet, which could be estimated.

A preliminary examination of the problem during the time when the droplet falls through water led to the following conclusions:

- (1) Information on the reaction kinetics of the oxidation reaction would be required over short time intervals and at temperatures near the melting point for both solid and liquid phases of the Zircaloy.
- (2) Heat transfer from the droplet by conduction and convection would be comparable to that by radiation for temperatures and droplet sizes of interest.
- (3) Heat transfer by conduction and convection would vary markedly over the droplet surface.
- (4) The calculated extent of oxidation of the droplet would be sensitive to parameters such as reaction rate constants and emissivity under conditions where the heat gained is nearly balanced by the heat losses from the droplet.

- (5) The effect of the liquid-to-solid phase change would be significant in the energy balance.

Reaction-Rate Kinetics

The only data available at the time and pertinent to the problem were the data of Bostrom already mentioned. The difficulty in using the data of Bostrom is that the data do not cover the temperature and time ranges of interest and are for solid Zircaloy. Thus, extrapolations of the experimental data in temperature and time are necessary. Of course, these extrapolations may lead to large uncertainties in the final results, but this can be avoided only by extending the range of the experimental data.

In using Bostrom's data, Lustman based his extrapolations upon a correlating expression of the form

$$y = A e^{-Q/RT} t^{n(T)}, \quad (D-1)$$

where

y = metal oxidized at time t , g per cm^2

t = time after start of oxidation, sec

T = absolute temperature of metal, K

R = gas constant

A , Q , $n(T)$ = are parameters determined from experimental data.

In formulating the present problem, it was desirable to have an expression for the reaction rate which involved both the temperature of the metal and the previous amount of oxidation explicitly. The rate of chemical reaction was assumed to depend on a surface reaction rate and on a diffusion rate through the oxide layer. (D-3) This assumption leads to an equation of the desired form,

$$\frac{dy}{dt} = y' = \frac{\frac{N}{2M}}{1 + \frac{y}{M}}, \quad (D-2)$$

where

y' = reaction rate at time t , $g/(cm^2)(sec)$

M and N are functions of temperature of the form $A e^{-B/T}$, where the A 's and B 's are determined from experimental data.

The following equation was found to correlate Bostrom's data with a maximum deviation of 16 per cent:

$$y' = \frac{4.2 \times 10^2 e^{-\frac{21,700}{T}}}{1 + 3.02 y e^{-\frac{4,400}{T}}} \quad (D-3)$$

The relationship between the correlating expression and the data of Bostrom is shown in Figure D-1. The time and temperature ranges of interest to the present problem are from 0 to 2 sec and near the melting point of Zircaloy (about 2200 K). It will be evident from Figure D-1 that a considerable extrapolation in temperature and in time is involved. Lustman's correlation would appear as straight lines with varying slope on Figure D-1.

In addition to the expression given in Equation (D-3), an expression of the form of Equation (D-2) was obtained which fitted Lustman's correlation over the temperature and time intervals of interest to the present problem. Over this limited range, the best fit was given by

$$y' = \frac{0.0143}{1 + 1.90 \times 10^{-9} y e^{-\frac{51,300}{T}}} \quad (D-4)$$

Figures D-2, D-3, and D-4 compare the various correlations. Both expressions, Equations (D-3) and (D-4), were used in the calculations to be described later.

Heat-Transfer Mechanisms

As the molten droplet of Zircaloy falls through the water, an envelope of steam forms around it, and the droplet carries with it a layer of vapor which is in dynamic equilibrium. Vapor leaves from the trailing side of the droplet and vapor forms around the vapor-liquid interface surrounding the droplet. The heat lost from the droplet can be separated into a radiative term and into a convective term. The convective heat transfer has been studied in detail by Bromley, et al. (D-4). Bromley measured and correlated, on the basis of a physical model, film boiling heat-transfer

94

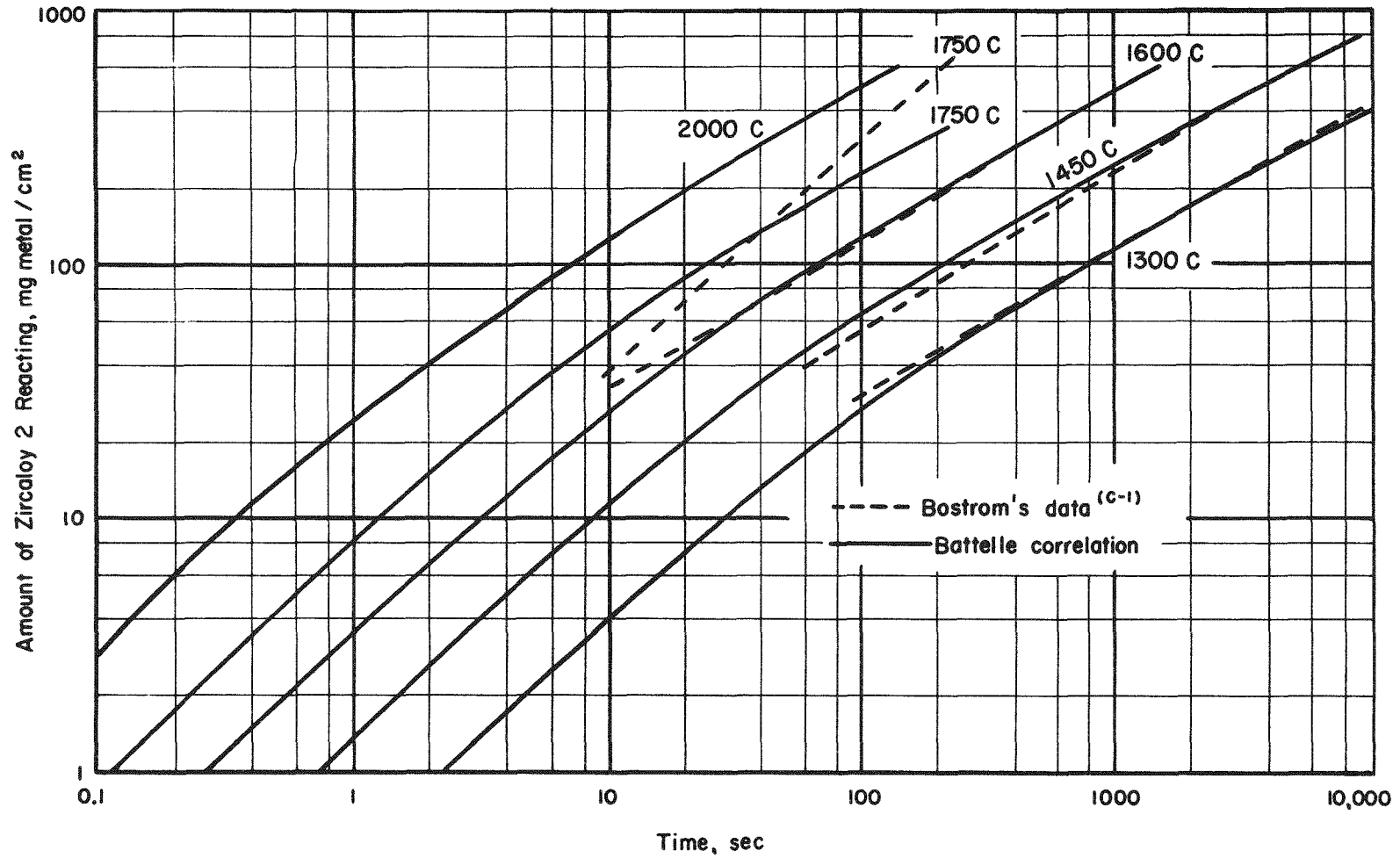


FIGURE D-1. ZIRCALOY 2-WATER REACTION RATES AS A FUNCTION OF TIME

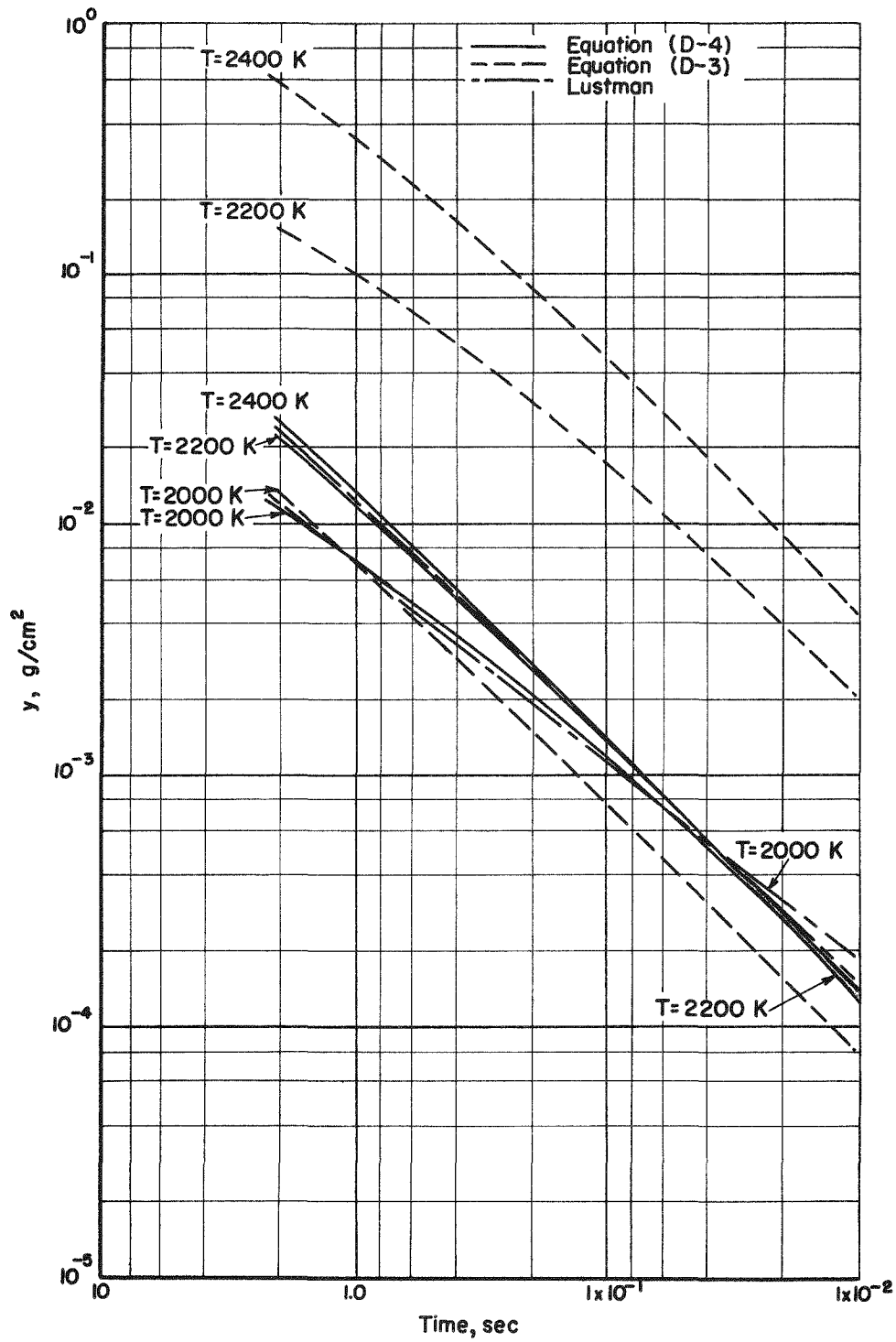


FIGURE D-2 REACTION-RATE CORRELATIONS

Total Reaction as a Function of Time.

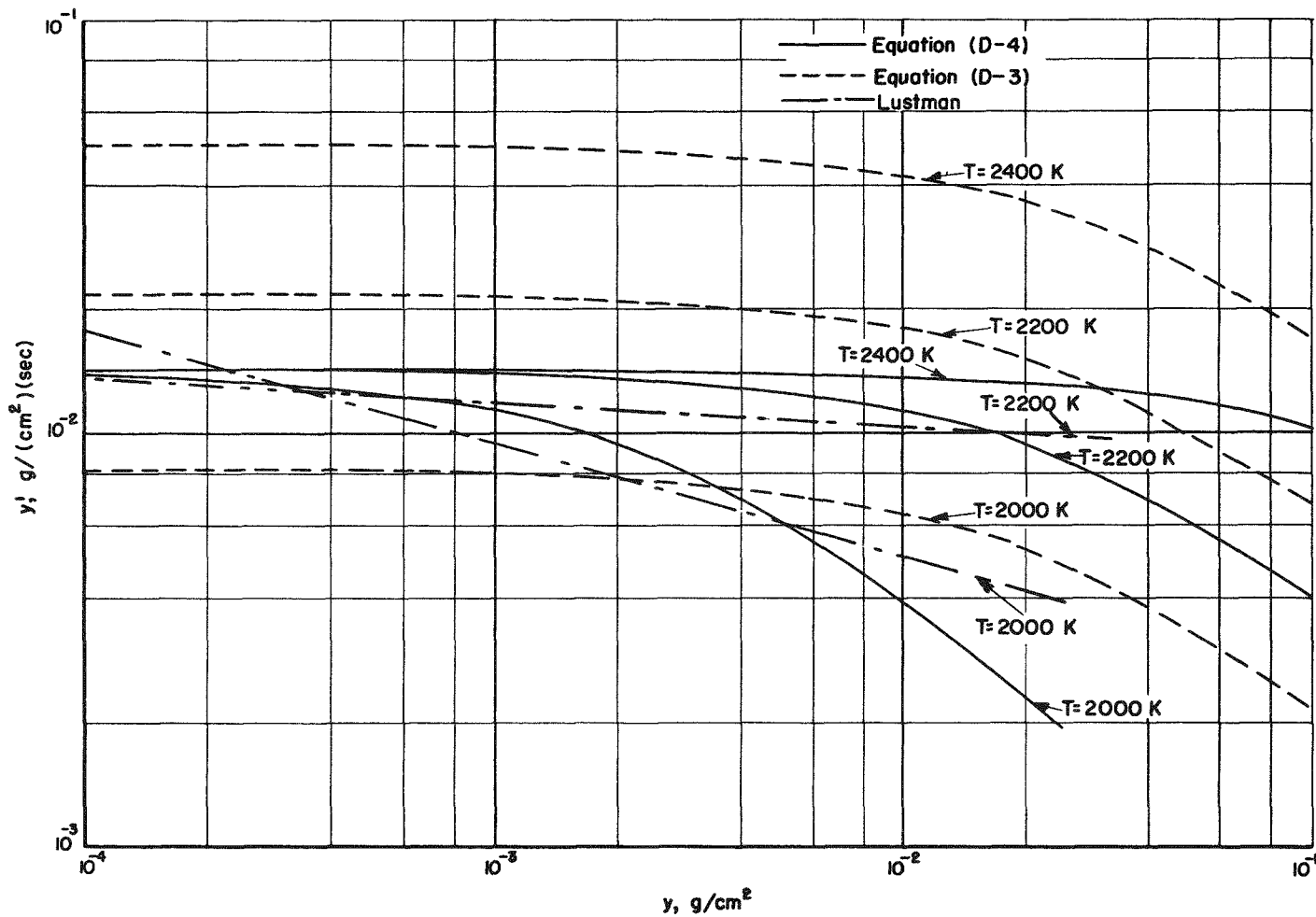


FIGURE D-3. REACTION-RATE CORRELATIONS

Reaction Rate as a Function of Total Reaction

97

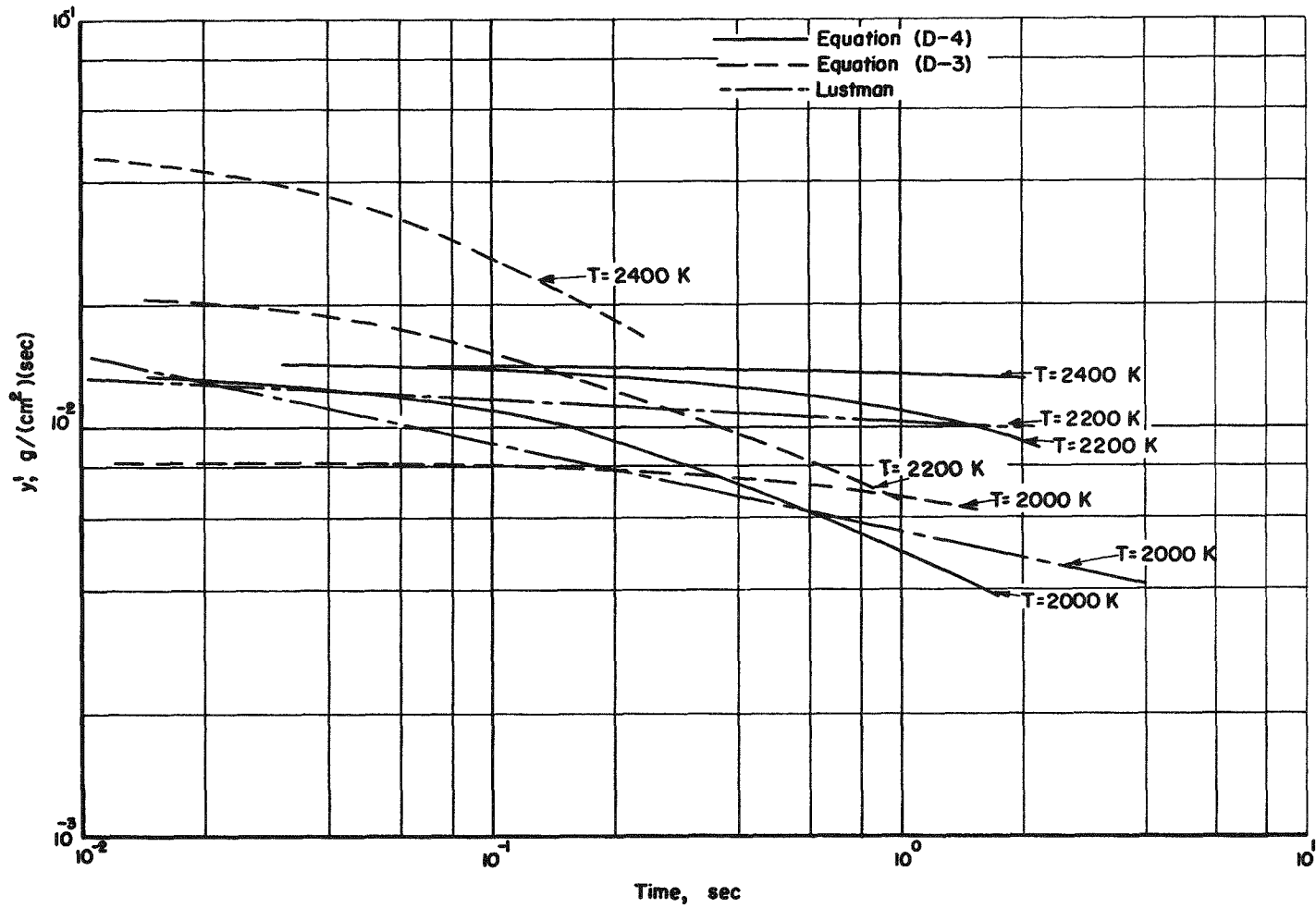


FIGURE D-4. REACTION-RATE CORRELATIONS

Reaction Rate as a Function of Time.

coefficients for cylinders in organic fluids. The correlation obtained by Bromley for $\sqrt{2ag} > 1.5$ is

$$h_c \left[\frac{2a \Delta T N_{pr}}{k^2 \rho (\rho_\ell - \rho) g \lambda' C_p} \right]^{1/4} = 0.63 \left[\frac{v}{\sqrt{2ag}} \right]^{1/2}, \quad (D-5)$$

where

h_c = convective heat transfer coefficient, cal/(cm²)(sec)(C)

a = cylinder radius, cm

N_{pr} = Prandtl number

k = thermal conductivity of vapor, cal/(cm)(sec)(C)

ρ = density of vapor, g per cm³

ρ_ℓ = density of liquid, g per cm³

g = gravitational constant, 980 cm per sec²

λ' = effective heat of vaporization given approximately

$$\text{by } \lambda \left[1 + \frac{0.4 C_p \Delta T}{\lambda} \right]^2, \text{ cal per g}$$

λ = actual heat of vaporization, cal per g

C_p = heat capacity of vapor, cal/(g)(C)

ΔT = temperature difference between surface and liquid, C

v = relative velocity of cylinder to liquid, cm/sec.

An analysis was made of the heat-transfer problem for the case of a sphere (D-5) and this gave a basis for using the correlation of Bromley for spherical geometry. The result was that

$$h_c (\text{sphere}) = (0.6 \text{ to } 0.7) h_c (\text{cylinder})$$

when the sphere radius is substituted for the cylinder radius in Equation (D-5).

An important conclusion drawn from Bromley's work was that the major part of the convective heat transfer occurs on the leading part of the cylinder surface for conditions of interest here. This conclusion has important consequences in formulating the problem of the falling droplet since it introduces asymmetry into the temperature distribution in the droplet.

This, in turn, may have important consequences because the reaction kinetics are temperature dependent.

The convective-heat-transfer coefficient given by Equation (D-5) was calculated for the Zircaloy droplet problem. The physical properties of steam (D-6, D-7) were evaluated at the arithmetic mean temperature of the steam layer around the droplet. It was found that in the temperature range of interest, the heat-transfer coefficient was nearly independent of steam properties. After correcting for spherical geometry, the convective-heat-transfer coefficient could be expressed by

$$h_c = 8.95 \times 10^{-4} \left(\frac{v}{2a} \right)^{1/2} . \quad (D-6)$$

The radiative term of the heat transfer was obtained by assuming the droplet radiated to black-body surroundings. A radiative-heat-transfer coefficient was defined by

$$h_r = \frac{\sigma \epsilon T^4}{\Delta T} \quad (D-7)$$

where

σ = Stefan-Boltzmann constant,
 1.36×10^{-12} cal/(cm²)(sec)(K)⁴

ϵ = emissivity

T = temperature of surface, K

ΔT = T - liquid temperature, K .

Figure D-5 shows a comparison of the radiative and convective heat transfer when spherical droplets have attained terminal velocity in saturated water. It will be noted that the two modes of heat transfer are of similar importance.

Mathematical Formulation

The previous discussion was devoted to the physical laws which are pertinent to the falling-droplet problem, and certain conclusions were drawn regarding the factors which would be significant to the problem. There remains the problem of formulating the equations governing the temperature and oxidation distribution and history of the droplet.

It was apparent at the outset that numerical results would be obtainable only by making simplifying assumptions. In fact it was convenient to

100

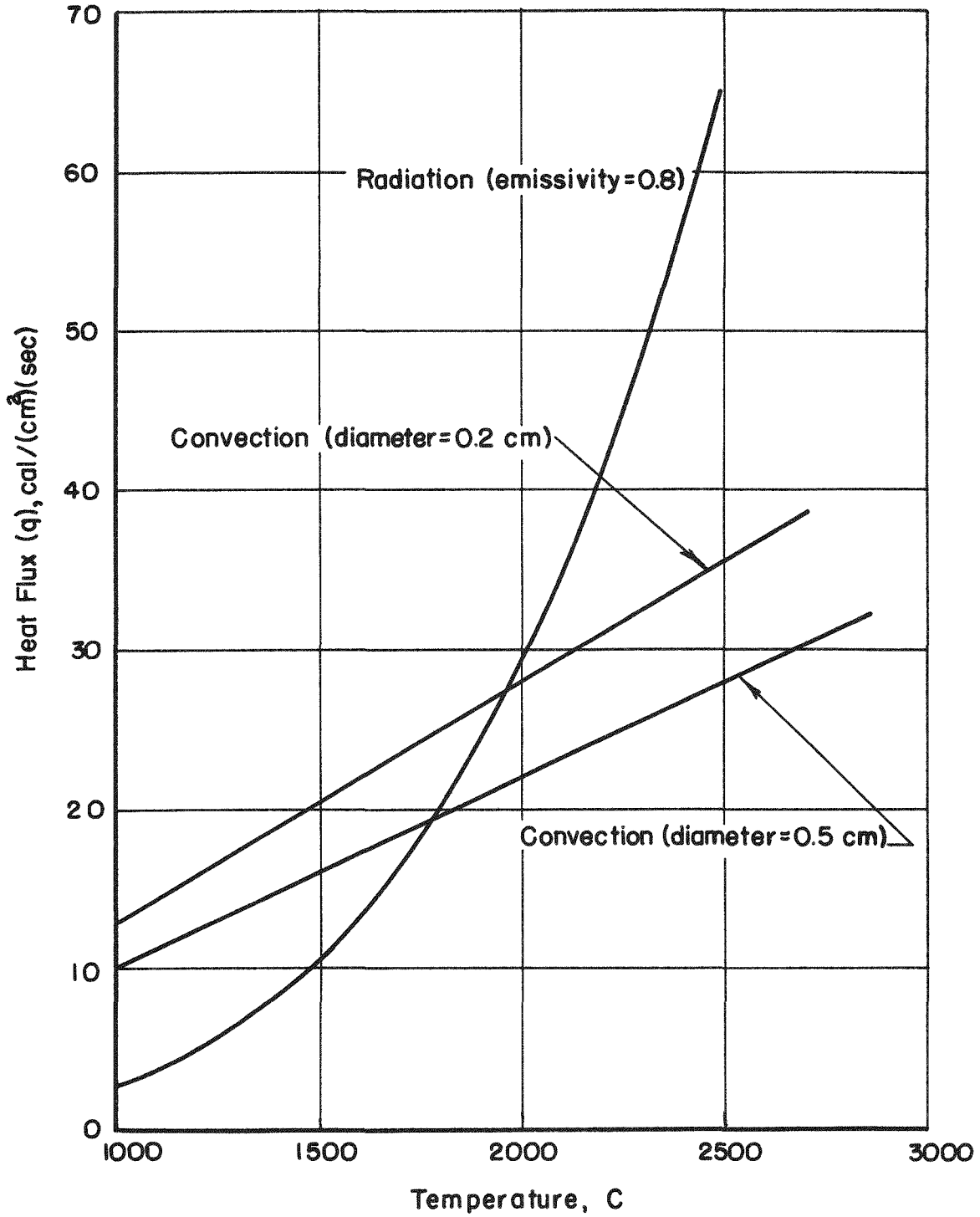


FIGURE D-5. COMPARISON OF HEAT FLUXES DUE TO RADIATIVE AND CONVECTIVE HEAT TRANSFER IN WATER AT TERMINAL VELOCITY

formulate several different problems which together would include all the significant factors but individually would not give a complete description.

The first problem formulated neglected the effect of the phase change of the Zircaloy upon cooling but included the asymmetry of the heat transfer around the droplet surface. In this formulation the reaction kinetics were governed by Equation (D-3), and a value of 1560 cal per g of Zircaloy oxidized was used for the heat of reaction. Calculations were made with droplet diameter, initial state of droplet, and emissivity as parameters.

The second problem formulated was the same as the first problem except that the reaction kinetics were governed by Equation (D-4) and a value of 1100 cal per g was used for the heat of reaction. Again, calculations were made with droplet diameter, initial state of droplet, and emissivity as parameters.

The third problem formulated considered the effect of the phase change but neglected the asymmetry of the heat transfer. The one-dimensional problem was formulated for a thin plate suitably related to the spherical geometry of interest. Calculations were made for a single set of parameters; the reaction kinetics were governed by Equation (D-4), and a value of 1100 cal per g was used for the heat of reaction.

In all of the formulations it was assumed that the heat of reaction was released at the surface of the metal. It was also assumed that the reaction kinetics at a point on the metal surface depended only upon the temperature and previous amount of reaction at that point.

The formulation of the first two problems is similar. It was assumed that the shape of the droplet would be approximately spherical. The temperature distribution and history are given by the solution of a boundary-value problem that may be stated as follows:

$$\alpha \nabla^2 T(r, \theta, t) + \frac{H}{C_p \rho} = \frac{\partial T}{\partial t}(r, \theta, t) \quad (D-8)$$

$$T(r, \theta, 0) = T_0$$

$$\frac{\partial T}{\partial r}(a, \theta, t) = -\frac{q(\theta, t)}{k}$$

where

r = radius variable, cm

θ = azimuthal angle variable, radians

t = time variable, sec

$T(r, \theta, t)$ = temperature at (r, θ, t) , K

$q(\theta, t)$ = surface heat flux at (θ, t) , cal/(cm²)(sec)

H = volume heating term due to radiative decay heating, cal/cm³(sec)

C_p = heat capacity, cal/(g)(K)

ρ = density, g per cm³

k = thermal conductivity, cal/(cm)(sec)(K)

a = radius of sphere, cm

$\alpha = \frac{k}{C_p}$ = thermal diffusivity, cm² per sec

∇^2 = Laplacian operator in spherical coordinates .

The angle θ is the angle defined by the intersection of the radius vector and the velocity vector of the droplet. The volume heating term, H , as it turns out, is not a significant factor, but was included for the sake of completeness.

To facilitate the solution of this problem, it was assumed that the dependence of the heat flux could be adequately represented by the first two terms in a Fourier series expansion in Legendre polynomials:

$$q(\theta, t) = q_0(t) + q_1(t) \cos \theta .$$

This approximation is reasonable because $q(\theta, t)$ will be a maximum at $\theta = 0$ and a minimum at $\theta = \pi$.

With this simplification, the "solution" of the problem was found to be

$$\begin{aligned} T(r, \theta, t) = & T_0 + \frac{H\alpha t}{k} - \frac{3\alpha}{ak} \int_0^t q_0(t') dt' \quad (D-9) \\ & + \int_0^t \alpha q_0(t-t') \sum_{m=1}^{\infty} \frac{2 \sin \lambda_n \frac{r}{a}}{k r \sin \lambda_n} e^{-\frac{\lambda_n^2 \alpha t'}{a^2}} dt' \\ & + \int_0^t \alpha q_1(t-t') \cos \theta \sum_{m=1}^{\infty} \frac{2 \left[\frac{\sin \nu_n \frac{r}{a}}{\left(\frac{r}{a}\right)^2} - \frac{\nu_n \cos \nu_n \frac{r}{a}}{\left(\frac{r}{a}\right)} \right]}{a k \nu_n \cos \nu_n} e^{-\frac{\nu_n^2 \alpha t'}{a^2}} dt' , \end{aligned}$$

where λ_n and ν_n are solutions of the equations

$$\tan \lambda_n = \lambda_n, \quad \tan \nu_n = \frac{2\nu_n}{2 - \nu_n^2}, \quad n = 1, 2, \dots$$

Equation (D-9) is a solution if $q_0(t)$ and $q_1(t)$ are known explicitly as functions of time. However, in this problem these functions depend upon the surface temperature; hence, Equation (D-9) with $r = a$ is actually an integral equation for the surface temperature.

To complete the formulation of the problem, it is necessary to obtain expressions for $q_0(t)$ and $q_1(t)$. The heat flux, $q(\theta, t)$, may be written as

$$q(\theta, t) = h(\theta, t) \Delta T(\theta, t) - Qy'(\theta, t), \quad (\text{D-10})$$

where

$h(\theta, t) = h_c(\theta, t) + h_r(\theta, t) =$ total (convective and radiative)-
heat-transfer coefficient, $\text{cal}/(\text{cm}^2)(\text{sec})(\text{K})$

$\Delta T(\theta, t) =$ surface temperature at (θ, t) above saturation
temperature, K

$Q =$ heat of reaction, cal per g

$y'(\theta, t)$ is given by Equations (D-3) or (D-4) with the
substitution of $T(a, \theta, t)$ for T . $h_c(\theta, t)$ is given by
Equation (D-6) for $0 < \theta < \frac{\pi}{2}$ and is equal to zero for
 $\frac{\pi}{2} < \theta < \pi$.

$h_r(\theta, t)$ is given by Equation (D-7) with the substitutions
of $T(a, \theta, t)$ for T and $\Delta T(\theta, t)$ for ΔT .

Expressions for $q_0(t)$ and $q_1(t)$ are obtained as follows:

$$q_0 = 1/2 \int_0^\pi q(\theta, t) P_0(\cos \theta) \sin \theta d\theta \quad (\text{D-11})$$

$$q_1 = 3/2 \int_0^\pi q(\theta, t) P_1(\cos \theta) \sin \theta d\theta, \quad (\text{D-12})$$

where

$$P_0(\cos \theta) = 1,$$

$$P_1(\cos \theta) = \cos \theta.$$

Equations (D-8), (D-9), (D-10), (D-11), and (D-12) were used as a basis for an iterative numerical solution for the temperature history and the amount of oxidation. It will be noted that the velocity of the droplet appears in Equation (D-6); however, the velocity can be obtained explicitly as a function of time from the equation

$$\frac{dv}{dt} = g \left(1 - \frac{\rho_w}{\rho_s} \right) - \frac{3\rho_w C_D v^2}{8\rho_s a} \quad (\text{D-13})$$

where

v = droplet velocity, cm per sec

ρ_w = water density, g per cm^3

ρ_s = droplet density, g per cm^3

a = droplet radius, cm

C_D = drag coefficient

g = gravitational constant, 980 cm per sec^2 .

Actually, for the size droplets considered, there is no significant error if terminal velocity is used in Equation (D-6) over the entire droplet history.

The results of the numerical solutions for the problems formulated will be discussed later.

Attention is now given to the formulation of the third problem considered. In this problem, a flat-plate geometry is considered. Chemical reaction and heat transfer occur at the Zircaloy plate surfaces in contact with water at saturation temperature. Initially, the Zircaloy is in the liquid state but with cooling a region of solid Zircaloy forms at the surface and increases in thickness until the entire plate is solidified. This problem is defined by the following equations:

$$\frac{\partial^2 T}{\partial x^2} (x, t) = \frac{1}{\alpha} \frac{\partial T}{\partial t} (x, t) \quad (\text{D-14})$$

$$\frac{\partial T}{\partial x} (0, t) = 0 \quad (\text{D-15})$$

$$\frac{\partial T}{\partial x} (b, t) = \frac{-q(t)}{k} \quad (\text{D-16})$$

$$T(x, 0) = T_0 \quad (\text{D-17})$$

$$\left(\frac{\partial T}{\partial x} \right)_{x=x_0^+}(t) = \frac{\partial x_0(t)}{\partial t} \left(\frac{\Delta H_f \rho}{k} \right), \quad 0 < x_0(t) \leq b \quad (\text{D-18})$$

$$x_0(0) = b \quad (\text{D-19})$$

$$T(x, t) = T_0, \quad 0 < x < x_0(t), \quad (\text{D-20})$$

where

x = distance from plate center, cm

t = time, sec

$T(x, t)$ = temperature at (x, t) , K

T_0 = melting temperature of Zircaloy, K

α = thermal diffusivity of Zircaloy, cm^2 per sec

k = thermal conductivity of Zircaloy, $\text{cal}/(\text{cm})(\text{sec})(\text{K})$

b = plate half thickness, cm

ρ = density of Zircaloy, g per cm^3

ΔH_f = heat of fusion of Zircaloy, cal per g

$q(t)$ = effective heat flux at plate surface at time t ,
 $\text{cal}/(\text{cm}^2)(\text{sec})$.

The expression assumed for $q(t)$ is

$$q(t) = h(t) [T(b, t) - T_c] - Qy'(t), \quad (\text{D-21})$$

where

$$h(t) = \frac{h_c(t)}{2} + h_r(t)$$

$h_c(t)$ is given by Equation (D-6) with v and a suitably defined

$h_r(t)$ is given by Equation (D-7) with $T(b, t)$ substituted for T and

$[T(b, t) - T_c]$ substituted for ΔT .

T_c = saturation temperature of water, K

Q = heat of reaction, cal per g

$y'(t)$ is given by Equation (D-4) with $T(b, t)$ substituted for T .

In this formulation physical properties are assumed to be the same for liquid and solid Zircaloy. Also the volume heat source from gamma heating is neglected. In order to relate the flat plate geometry to the spherical geometry, it is assumed that a good correlation will result if the surface area to volume ratio is the same for the two geometries.

A numerical solution of Equations (D-14) through (D-21) was performed, and for purposes of comparison a numerical solution of the corresponding single-phase (solid Zircaloy) problem was performed. These solutions were performed for one set of parameters ($\epsilon = 0.5$, $a = 0.1$ cm). The results are discussed in the next section.

Results of the Calculations

Typical results of the calculations for the first problem formulated are shown in Figures D-6 through D-11. The values of y_{max} and y_{min} are plotted versus time in Figures D-6 through D-8, which show the relationship between the oxidation on top of the sphere, y_{max} , to that on the bottom, y_{min} . The temperature histories at the top and bottom of the sphere are shown in Figures D-9 through D-11. In all cases a pronounced asymmetry is evident.

Several cases were attempted for which the numerical calculations did not converge. To determine whether or not this was an effect of the numerical method used, the time interval was halved and the calculations were repeated. There was little change in the result. Hence, on the basis of the formulation of the first problem, certain choices for parameter values would lead to large amounts of reaction. Another conclusion is that small changes of parameter values for critical values will cause large changes in amounts of reaction.

Table D-1 lists the information for all of the calculations made for the first problem formulated.

Typical results of the calculations for the second problem formulated are shown in Figures D-12 through D-15. The asymmetry is again evident. In all cases considered the numerical calculations led to convergence. Table D-2 lists the information for all of the calculations made for the second problem formulated.

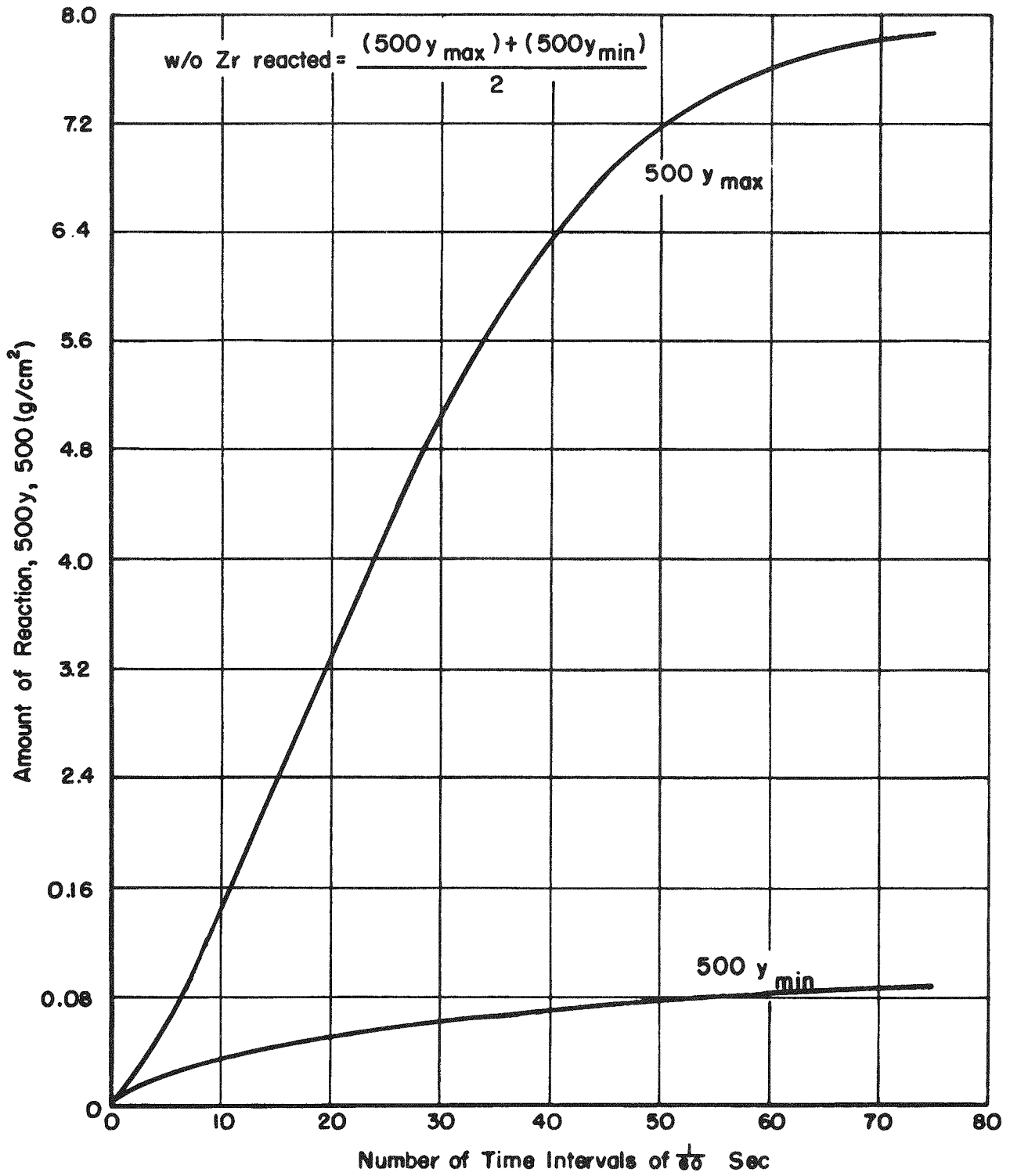


FIGURE D-6. REACTION-TIME CURVES FOR $r = 0.1$ CM,
 $T_0 = 2173$ K, $v_0 = 200$ CM PER SEC, $\epsilon = 0.8$,
 AND $y_0 = 0$

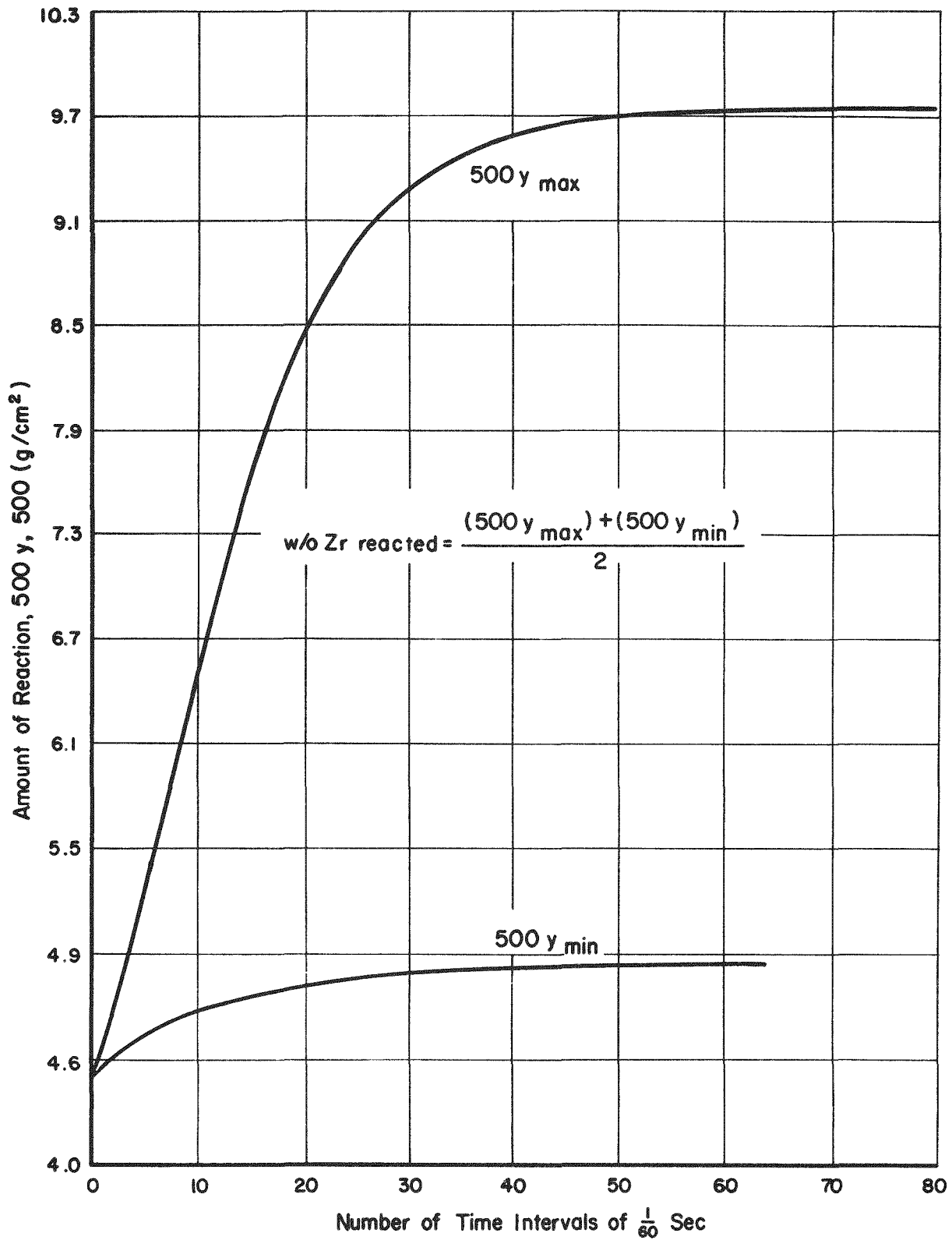


FIGURE D-7. REACTION-TIME CURVES FOR $r = 0.1$ CM,
 $T_0 = 2173$ K, $v_0 = 200$ CM PER SEC, $\epsilon = 0.8$,
 AND $y_0 = 0.009$ G PER CM²

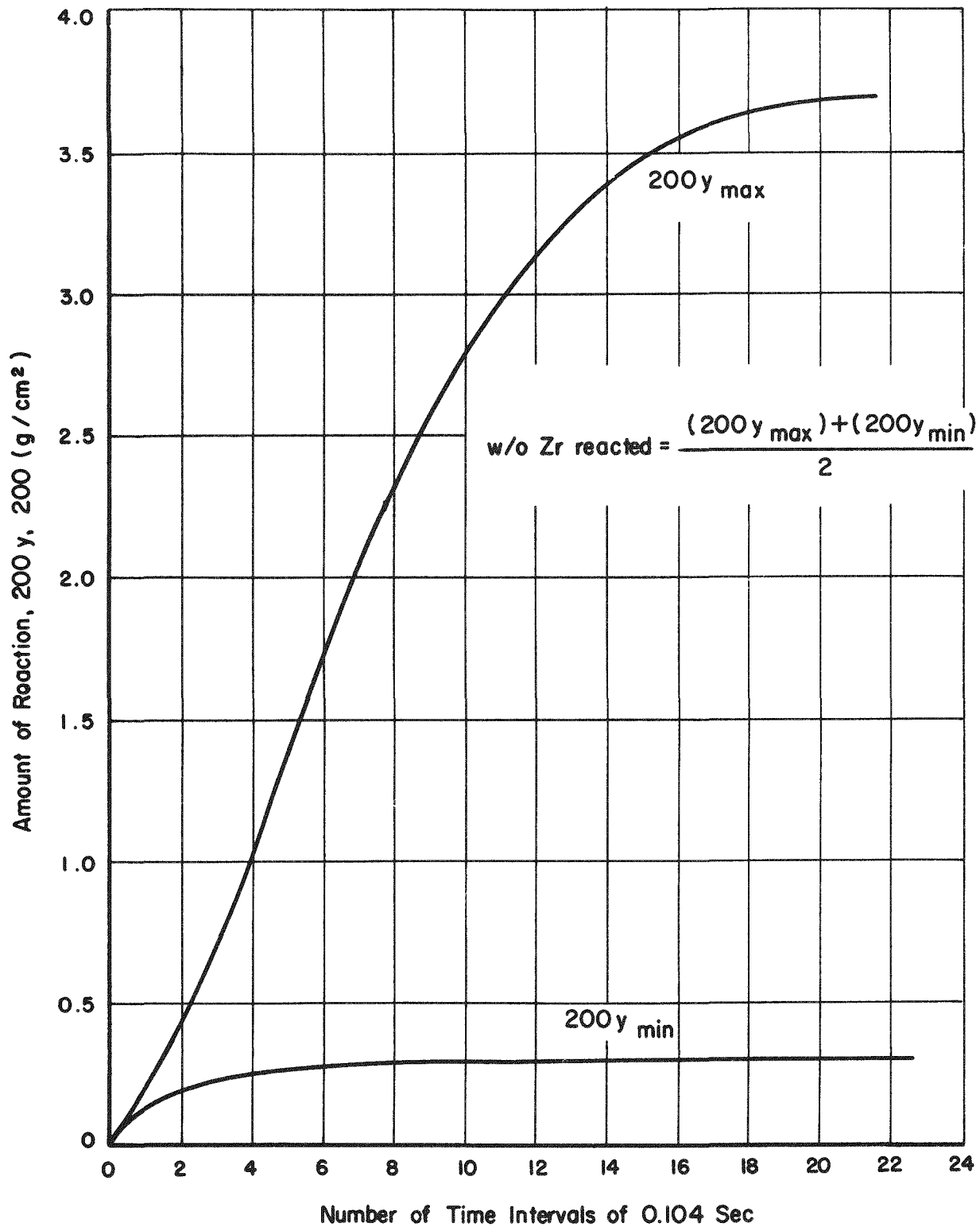


FIGURE D-8. REACTION-TIME CURVES FOR $r = 0.25$ CM,
 $T_0 = 2023$ K, $v_0 = 30$ CM PER SEC, $\epsilon = 0.8$,
 AND $y_0 = 0$

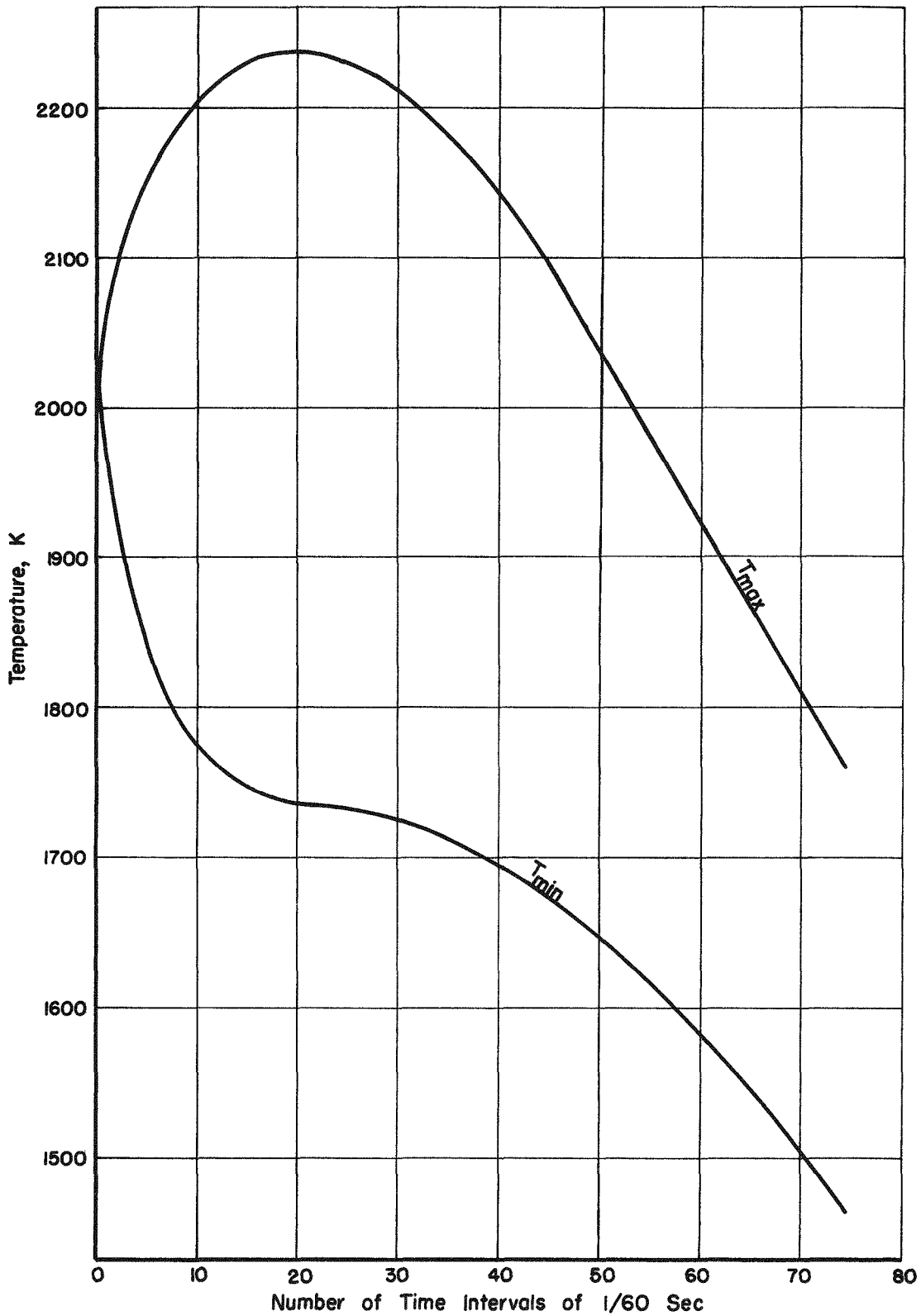


FIGURE D-9. TEMPERATURE-TIME CURVES FOR $r = 0.1$ CM,
 $T_0 = 2023$ K, $v_0 = 30$ CM PER SEC, $\epsilon = 0.4$,
AND $y_0 = 0$

109

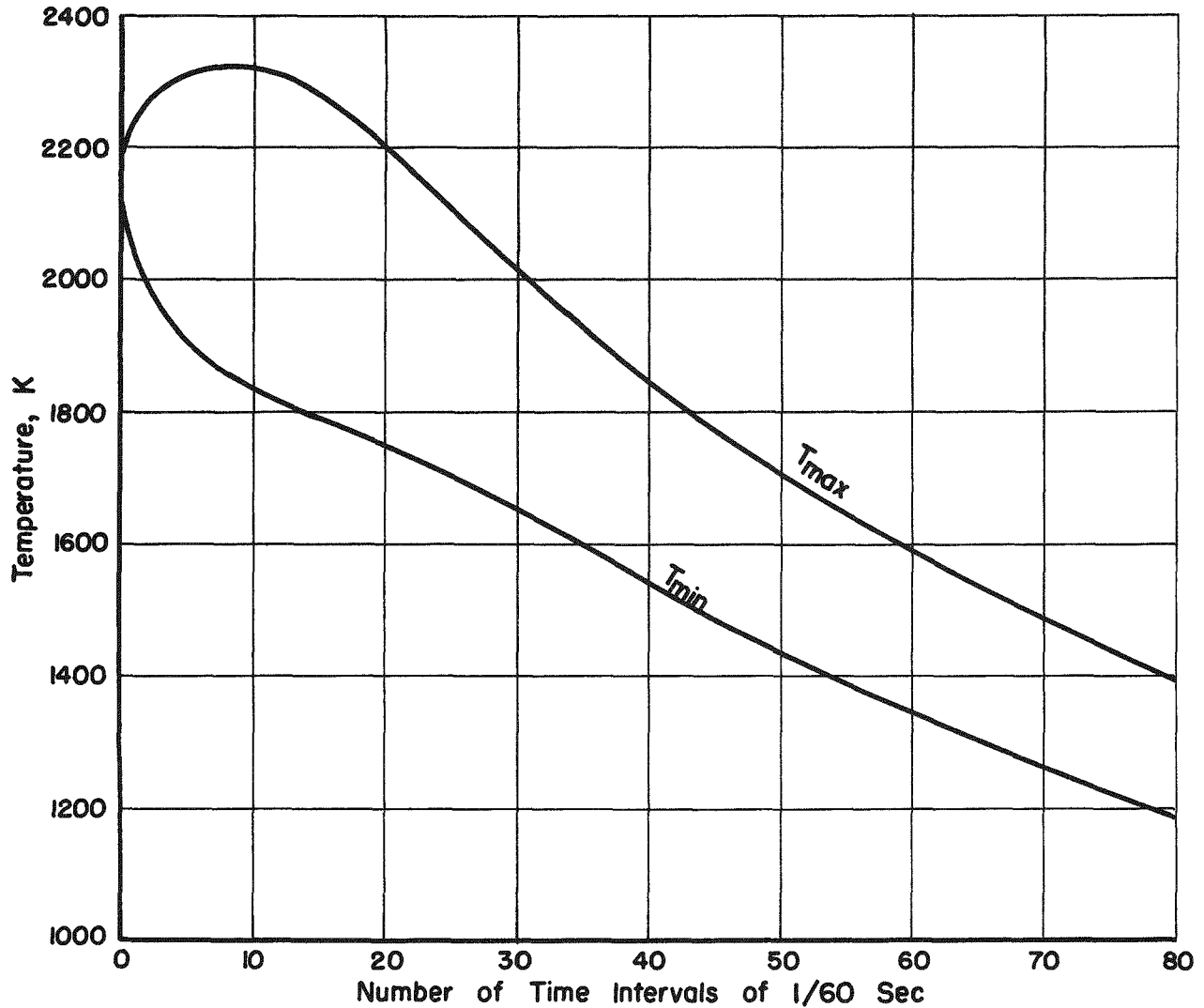


FIGURE D-10. TEMPERATURE-TIME CURVES FOR $r = 0.1$ CM,
 $T_0 = 2173$ K, $v_0 = 200$ CM PER SEC, $\epsilon = 0.8$,
AND $y_0 = 0.009$ G/CM²

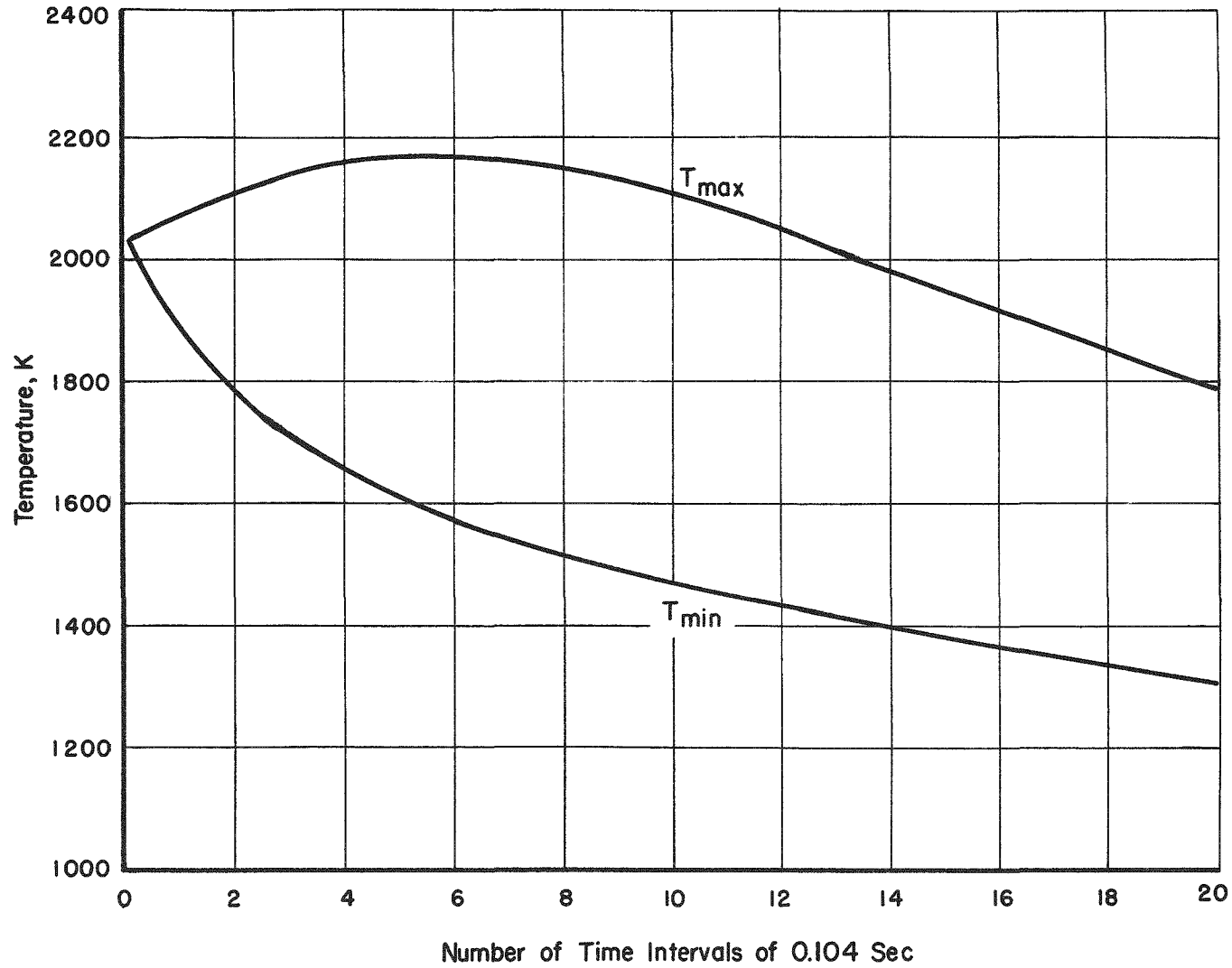


FIGURE D-11. TEMPERATURE-TIME CURVES FOR $r = 0.25$ CM, $T_0 = 2023$ K, $v_0 = 30$ CM PER SEC, $\epsilon = 0.8$, AND $\gamma_0 = 0$



TABLE D-1. SUMMARY OF CALCULATIONS FOR FIRST PROBLEM FORMULATED

Radius, cm	Initial Velocity ^(a) , cm/sec	Initial Tempera- ture, K	ϵ	Initial Amount of Oxidation, w/o	Final, w/o	Approximate Time to End of Reaction, sec
0.1	30	2023	0.25	0	Diverged	
0.1	30	2023	0.80	0	1.2	1
0.1	30	2023	0.60	0	1.7	1.1
0.1	30	2023	0.40	0	4.4	1.1
0.1	30	2173	0.25	4.5	Diverged	
0.1	30	2173	0.60	4.5	Diverged	
0.1	30	2173	0.80	4.5	7.5	1
0.1	200	2023	0.25	0	Diverged	
0.1	200	2023	0.60	0	1.7	1
0.1	200	2173	0.25	4.5	Diverged	
0.1	200	2173	0.80	4.5	7.8	1
0.25	30	2023	0.25	0	Diverged	
0.25	30	2023	0.80	0	2.3	2.6
0.25	30	2173	0.25	1.8	Diverged	
0.25	30	2173	0.80	1.8	Diverged	
0.25	200	2023	0.25	0	Diverged	
0.25	200	2173	0.25	1.8	Diverged	
0.25	87.4	2023	0.70	0	Diverged	
0.25	87.4	2023	0.80	0	2.3	2.6

(a) Terminal velocities are 56.3 cm/sec for $r = 0.1$ cm and 87.4 cm/sec for $r = 0.25$ cm.

112

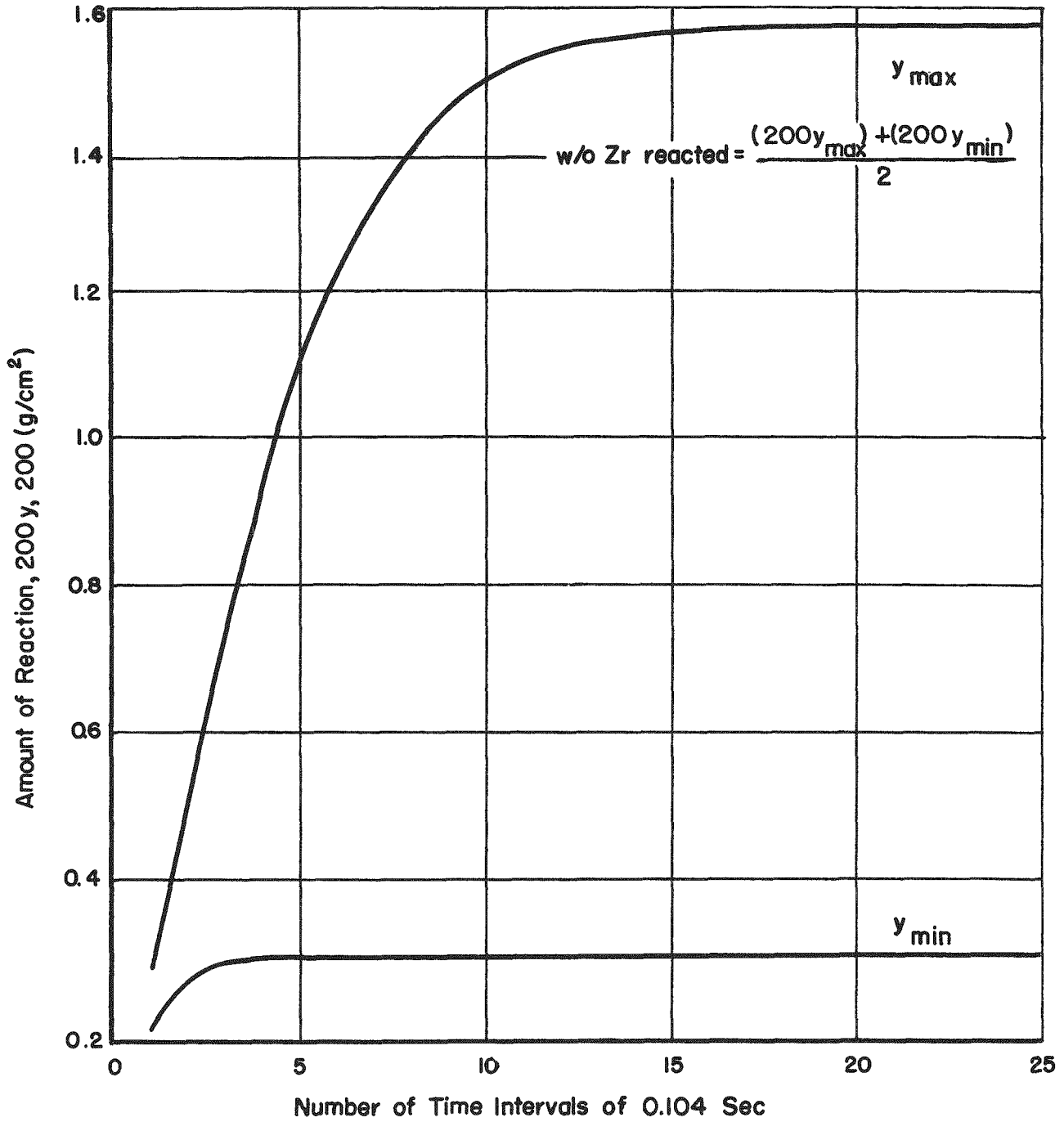


FIGURE D-12. REACTION-TIME CURVES FOR $T_0 = 2023\text{ K}$,
 $\epsilon = 0.8$, AND $a = 0.25\text{ CM}$

113

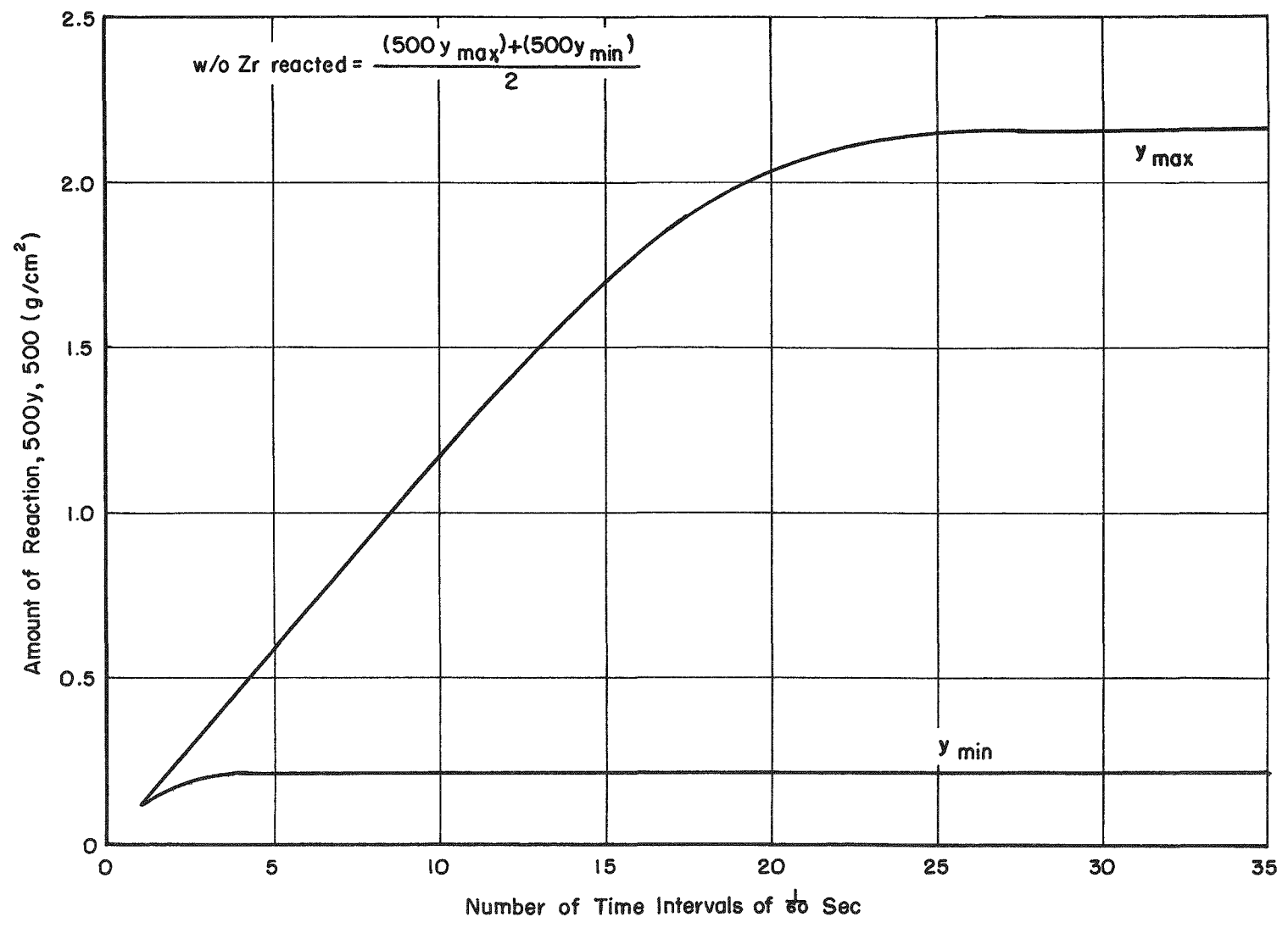


FIGURE D-13. REACTION-TIME CURVES FOR $T_0 = 2173\ K$, $\epsilon = 0.8$, AND $a = 0.10\ CM$

114

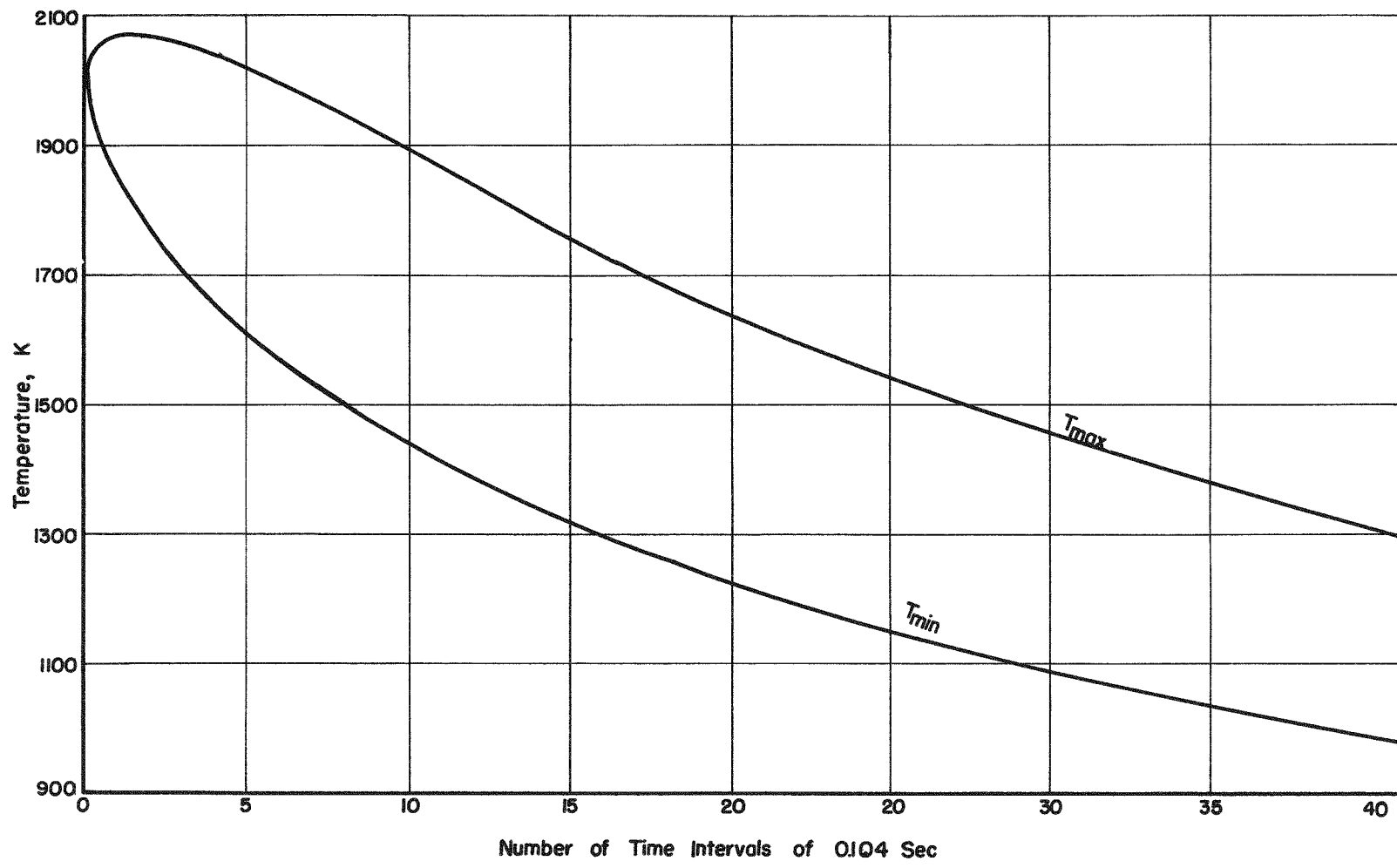


FIGURE D-14. TEMPERATURE-TIME CURVES FOR $T_0 = 2023$ K, $\epsilon = 0.8$, AND $a = 0.25$ CM

115

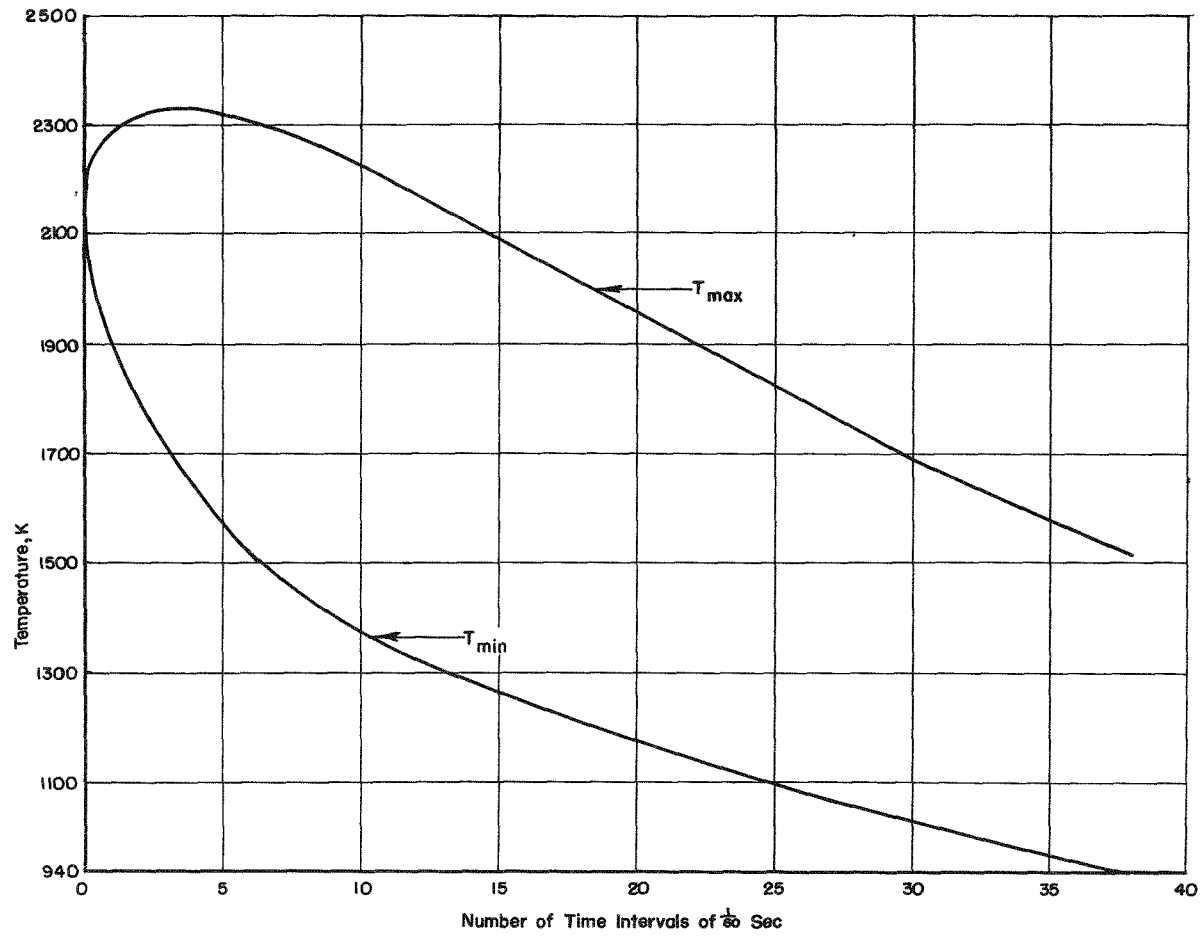


FIGURE D-15. TEMPERATURE-TIME CURVES FOR $T_0 = 2173$ K, $\epsilon = 0.8$, AND $a = 0.10$ CM

TABLE D-2. SUMMARY OF CALCULATIONS FOR SECOND PROBLEM FORMULATED

Radius, cm	Velocity, cm/sec	Initial Temperature	ϵ	Initial Amount of Oxidation, w/o	Zirconium Oxidized, w/o	
					Equation (D-3)	Equation (D-4)
0.1	56.3	2023	0.8	0	1.2	0.93
0.25	87.4	2023	0.8	0	2.3	0.93
0.25	87.4	2173	0.8	0	Diverged	1.4
0.25	87.4	2173	0.4	0	Diverged	2.5
0.1	56.3	2173	0.4	0	Diverged	1.5
0.1	56.3	2173	0.8	0	3.0	1.2
0.25	87.4	2173	0.25	0	Diverged	3.5

Results of the calculations for the third problem formulated are shown in Figure D-16.

Discussion of Results and Conclusions

The results given in Table D-1 indicate that larger diameter droplets react more completely than do smaller diameter droplets. This result does not agree with the result found by Lustman. The reason for the result found here lies in the asymmetry and in the change in convective heat transfer with droplet diameter. The asymmetry causes the larger droplet to react more than the smaller droplet since heat is conducted through the droplet from the hotter top side to the colder bottom side. The source of heat is proportional to the diameter squared, and the resistance to heat conduction is inversely proportional to the diameter. Thus, the temperature difference from top to bottom will tend to be larger for the larger droplet. Figures D-14 and D-15 illustrate this. Thus, if the reaction rate increases with temperature, the larger droplet tends to react more. Figure D-5 illustrates how the diameter influences the convective heat transfer. These effects were not present in the model considered by Lustman. With no θ dependence and if different size droplets had the same convective-heat-transfer coefficient, the smaller droplets would react more than the larger ones.

It may also be noted that the initial velocity has very little effect on the final amount of oxidation. This is because the droplets are very near terminal velocity (~ 57 cm per sec for the 0.2-cm-diameter droplet and ~ 87 cm per sec for the 0.5-cm-diameter droplet) after about 0.1 sec.

Another comparison may be made with Lustman's results regarding conditions for divergence. Lustman found that an emissivity of 0.293 was

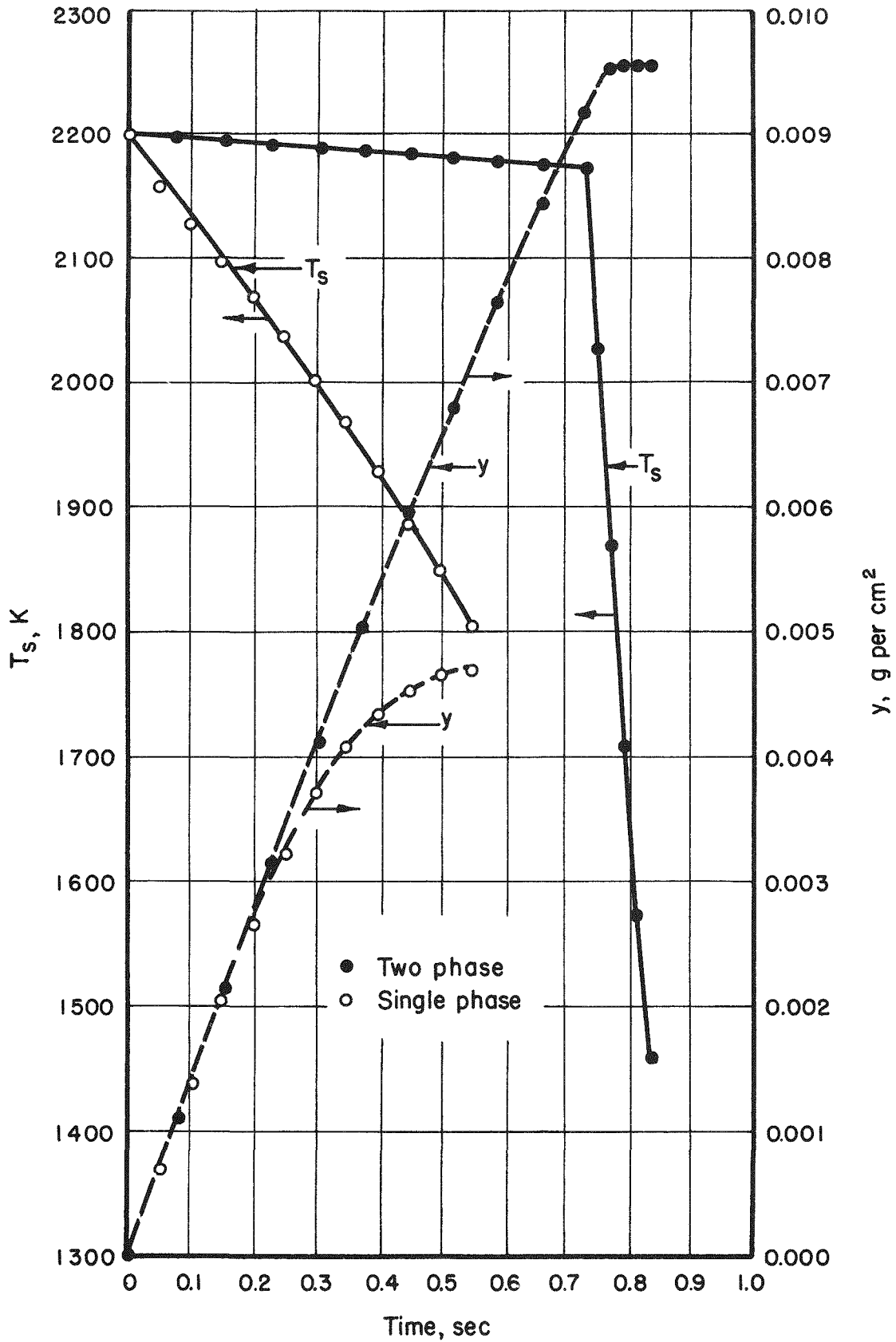


FIGURE D-16. TEMPERATURE AND OXIDATION HISTORIES SHOWING EFFECT OF PHASE CHANGE

critical for his conditions. Lower emissivity values led to complete reaction. Table D-1 indicates that the critical value of emissivity depends upon the initial conditions and the droplet size. It should also be pointed out that the critical condition depends upon the reaction kinetics and heat of reaction assumed.

The results of the calculations for the second problem formulated, given in Table D-2, also indicate the same diameter effect found in Table D-1 but it is not as pronounced. Also to be noted in Table D-2 is that the amounts of reaction are less for the second problem. No divergent cases were found, but this was to be expected since Equation (D-4) implies a maximum reaction rate, and the temperature dependence of the reaction kinetics is not realistically described by this equation outside the temperature range 2000 to 2200 K. The main value of the results of this problem was the better comparison with Lustman's results, since the choice of parameters is similar. As expected, the amounts of reaction were smaller than Lustman's values because convection heat transfer is now included. Also, as expected, where comparisons are possible the amounts of reaction for the second problem are less than those for the first problem. This is because of the differences in the reaction kinetics and the heat of reaction.

The results from the third problem, shown in Figure D-16, indicate the effect of the phase change. It will be noted that the amount of reaction was about doubled by including the phase change. Also to be noted is the sharp break in the surface-temperature curve at the time when the phase change is complete.

It would be interesting to have the results from a calculation combining the effects of the phase change and the asymmetry, but as noted earlier this problem is quite complex. On the other hand, some observations and predictions can be made about the results expected. First, since the bottom-side temperature would stay near the melting point longer, larger amounts of reaction there would be expected. Similarly, the top-side temperatures would be higher. However, if the reaction kinetics are temperature dependent, the asymmetry effect should still be in evidence, although the magnitude of the asymmetry may change.

Finally, an experiment described in more detail in Section C, Part 2 of this report was done to provide a check on the analysis reported here. Briefly, Zircaloy 2 droplets were melted from a 1/8-in. -diameter rod and allowed to fall through a column of water near 212 F. The droplets formed were about 0.5 cm in diameter. A weight-gain check on the droplets indicated some 40 per cent of the Zircaloy reacted, but a vacuum-fusion analysis indicated about 10 per cent of the Zircaloy reacted. The mathematical analysis of the first problem gave 2.3 per cent reaction for an emissivity of 0.8 and diverged for an emissivity of 0.7. The mathematical analysis of the second problem gave values of 1.4, 2.5, and 3.5 per cent for emissivity values of 0.8, 0.4, and 0.25, respectively. Even doubling these values to allow for the phase change does not bring the predicted values in line with

the experimental values. This, however, should not be surprising in view of the large uncertainty in the reaction kinetics and the sensitivity of the calculated values to parameter values under critical conditions.

Some observations regarding the droplet experiments referred to may be of interest in connection with the calculated results. During the first part of the droplet fall, the droplet appears to increase in brightness and then rather suddenly decreases in brightness. The increase in brightness can probably be ascribed to both an increase of emissivity and an increase of temperature. The emissivity is a strong function of the state of the droplet surface; i. e., the emissivity of the pure metal is low, but the emissivity of the oxide, is high. It seems reasonable that the emissivity would increase as surplus oxygen becomes available to the surface. The sudden decrease in brightness can be understood in terms of the curve in Figure D-16. It is noted that the effect of the phase change is to give a sharp break to the temperature curve.

Although some observers report that the top side of the droplet appears brighter than the bottom side, the photomicrographs of the reacted droplets do not indicate any variation of the thickness of the reactant layers around the droplet surface. However, the top side of the droplet does have a cavity which may be related to some asymmetry effect.

On the basis of the experimental evidence, the amount of reaction of the droplet is limited, and one can point to analytical results which support this view. On the other hand, there are analytical results which do not support this view; however, on either side the analytical results must be regarded as exploratory. The droplet problem is very complex, and a satisfactory analysis of the problem depends heavily upon adequate experimental data and an understanding of the phenomena taking place during those important first few seconds.

This work was done under subcontract to the Bettis Laboratory of the Atomic Energy Commission, operated by the Westinghouse Electric Corporation. Dr. Benjamin Lustman, of the Bettis Laboratory, was responsible for technical liaison, and the authors wish to express their gratitude to him for his interest and assistance during the conduct of this work.

References

- (D-1) Lustman, B., "Zirconium-Water Reactions", WAPD-137, Westinghouse Electric Corporation, Atomic Power Division, Pittsburgh, Pennsylvania (December 1, 1955).
- (D-2) Bostrom, W. A., "The High Temperature Oxidation of Zircaloy in Water", WAPD-104, Westinghouse Electric Corporation, Atomic

Power Division, Pittsburgh, Pennsylvania (March 19, 1954)
CONFIDENTIAL.

- (D-3) Jost, W., Diffusion, Academic Press, Inc., New York, New York (1952).
- (D-4) Bromley, L. A., LeRoy, N. R., and Robbers, J. A., "Heat Transfer in Forced Convection Film Boiling", UCRL-1894, University of California, Radiation Laboratory, Berkeley, California (August 1, 1952).
- (D-5) Dayton, R. W., Personal Communication.
- (D-6) Lemmon, A. W., Jr., et al., "Empirical Evaluation of the Properties of Steam at Elevated Temperatures and Pressures", BMI-858, Battelle Memorial Institute, Columbus, Ohio (August 25, 1953).
- (D-7) Keenan, J. H., and Keyes, F. G., Thermodynamic Properties of Steam, John Wiley and Sons, Inc., New York (1936).